



NTNU – Trondheim
Norwegian University of
Science and Technology

Small scale multiphase flow experiments on surge waves in horizontal pipes

Steinar Ingebrigtsen
Grødahl

Master of Energy and Environmental Engineering

Submission date: June 2014

Supervisor: Ole Jørgen Nydal, EPT

Norwegian University of Science and Technology
Department of Energy and Process Engineering

EPT-M-2014-40

MASTER THESIS

for

Student Steinar Ingebrigtsen Grødahl

Spring 2014

English title

Small scale multiphase flow experiments on surge waves in horizontal pipes

*Norwegian title**Småskala strømningsforsøk med tetthetsbølger i horisontal lagdelt flerfasestrøm***Background and objective**

Ramp up of production rates in wet gas pipelines can give long surge waves arriving at the receiving separator. Some experiments on the wave phenomenon will be attempted in the multiphase flow laboratory at NTNU with changes in gas flow rates, or liquid flow rates, in a test section with a dip. The two- and three phase flow phenomenon can be studied with available 1D dynamic flow models.

The following tasks are to be considered:

- 1 Modify and upgrade the existing facility at the multiphase flow laboratory at NTNU
- 2 Test setups and procedures to generate surge waves and measure the propagation along the line. Air-water flow first, and then air-water-oil flows.
- 3 Assess the capability of available 1D flow simulators to predict the surge wave experiments

Within 14 days of receiving the written text on the master thesis, the candidate shall submit a research plan for his project to the department.

When the thesis is evaluated, emphasis is put on processing of the results, and that they are presented in tabular and/or graphic form in a clear manner, and that they are analyzed carefully.

The thesis should be formulated as a research report with summary both in English and Norwegian, conclusion, literature references, table of contents etc. During the preparation of the text, the candidate should make an effort to produce a well-structured and easily readable report. In order to ease the evaluation of the thesis, it is important that the cross-references are correct. In the making of the report, strong emphasis should be placed on both a thorough discussion of the results and an orderly presentation.

The candidate is requested to initiate and keep close contact with his/her academic supervisor(s) throughout the working period. The candidate must follow the rules and regulations of NTNU as well as passive directions given by the Department of Energy and Process Engineering.


Risk assessment of the candidate's work shall be carried out according to the department's procedures. The risk assessment must be documented and included as part of the final report. Events related to the candidate's work adversely affecting the health, safety or security, must be documented and included as part of the final report. If the documentation on risk assessment represents a large number of pages, the full version is to be submitted electronically to the supervisor and an excerpt is included in the report.

Pursuant to "Regulations concerning the supplementary provisions to the technology study program/Master of Science" at NTNU §20, the Department reserves the permission to utilize all the results and data for teaching and research purposes as well as in future publications.

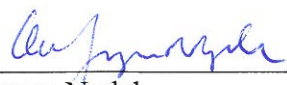
The final report is to be submitted digitally in DAIM. An executive summary of the thesis including title, student's name, supervisor's name, year, department name, and NTNU's logo and name, shall be submitted to the department as a separate pdf file. Based on an agreement with the supervisor, the final report and other material and documents may be given to the supervisor in digital format.

- Work to be done in lab (Multiphase Flow Lab)
 Field work

Department of Energy and Process Engineering, 14. January 2014



Olav Bolland
Department Head



Ole Jorgen Nydal
Academic Supervisor

Research Advisor: Zhilin Yang

Foreword

The purpose of this Master Thesis has been to see if long surge waves could be observed in the multiphase flow laboratory at NTNU. Then the capability of the transient multiphase flow simulators OLGA and LedaFlow to reproduce the lab observations was tested. Surge waves has been an interesting field to study and I have felt privileged because at I have got an opportunity to study a unique multiphase flow phenomenon that few people know anything about.

I would like to thank the research advisor Zhilin Yang for initiating the project. I would like to thank Mariana Diaz for the guidance at the multiphase flow lab. I would like to thank Martin Bustadmo for helping me setting up the lab, no experiments would have been conducted without his effort. I would like to thank Heiner Schumann and Milad Khatibi for help with the OLGA and LedaFlow simulations. I would like to thank Kristian Holmås for discussion and inputs. I would like to thank Ivar Brandt for simulation guidance and a PVT-file. Especially I would like to thank my supervisor Ole Jørgen Nydal for the guidance and for always having the door to his office open.

Steinar Ingebrigtsen Grødahl

Trondheim 12.6.2014

Abstract

Long surge waves are observed at the receiving separator after production ramp up on several gas-condensate fields. Surge waves are observed as long and slow oscillations in the liquid flow rate at the outlet of the pipeline, occurring in stratified three-phase flow. One single surge wave can have a duration of one hour and propagate over a distance of 100 km. The presence of surge waves can last for a couple of days, after production ramp up, before the flow is stabilized.

Surge waves are caused by liquid accumulation in the pipeline. Liquid will accumulate in low spots in the pipeline during production shut down and at low gas flow rates, because the interfacial drag between the gas and the liquid is not strong enough to drag all the liquid along with the gas at low gas flow rates. When the gas flow rates are ramped up the accumulated liquid is eventually swept along with the gas, and finally the liquid arrives at the receiving facility in surge waves. Surge waves can cause operational problems. Unplanned production shut-in can be the consequence if the total liquid volume in the surge waves exceeds the liquid handling capacity at the receiving facility. Three-phase surge waves are often divided into a condensate surge followed by a water/MEG surge. Such cases can lead to hydrate formation in periods without MEG return. Surge waves have been difficult to predict by the available commercial transient multiphase flow simulators, and as they can cause severe operational problems, it is important to be able to predict, control and handle the presence of surge waves. Surge waves represent the main flow assurance challenge on the Ormen Lange field.

Laboratory experiments on surge waves have been conducted in the multiphase flow lab at NTNU. The purpose of the lab experiments was to find out if it is possible to reproduce surge waves in the lab at NTNU. A 57,84 meter long test pipeline was configured with a dip geometry in the start. The lab experiments were conducted in two-phase with water and air as test fluids. Steady state stratified flow, with fixed gas and liquid flow rates, was established through the entire pipeline before the gas flow was choked and then ramped up again. This caused liquid to accumulate in the dip during the gas downtime. The liquid was then expelled through the pipeline in a wave when the gas flow was turned up again. Except for the very long wave duration and occurrence in three-phase flow, the result was waves with the

characteristics of surge waves: Occurrence in the stratified flow regime, initiated because of liquid accumulation in a low spot during a change in the gas flow rate, a relatively smooth front, a low peak holdup between 7 and 17 % and ability to travel through the entire pipeline without getting totally smeared out. The wave duration was up to around 20 seconds at the end of the pipeline, which is relatively long for the relatively short and narrow (60 mm inner diameter) pipeline.

The lab observations have been attempted simulated in OLGA and LedaFlow. OLGA is generally capable of reproducing the lab observations very well. OLGA predicted waves with very similar behavior as the observations for all the eight analyzed cases. The general trend was that OLGA predicted a slightly higher wave peak amplitude and a slightly lower wave velocity than what is seen in the lab observations. LedaFlow showed a much more poor performance than OLGA to simulate the lab observations. LedaFlow is only capable of reproducing a solution similar to the observations for two of the eight analyzed cases, which were the cases with highest U_{sg} and lowest U_{sl} .

Sammenheng

Lange tetthetsbølger, “surge waves”, blir observert ved mottaksseparatoren etter oppstart av produksjon ved flere gass-kondensatfelt. Tetthetsbølgene blir observert som lange og trege svingninger i hastigheta til væskestrømninga ved utløpet av rørledninga i trefasestrømning. En enkelt tetthetsbølge kan vare i en time og forplante seg over en avstand på 100 km. Etter gjenoppstart av produksjon kan det ta flere dager før tetthetsbølgene slutter å komme og stasjonær strømning blir oppnådd.

Tetthetsbølger forårsakes av at væske akkumulerer i rørledninga. Væske akkumulerer i rørledninga under produksjonsstans og ved lave strømningsrater, fordi drakraften mellom gassen og væska ikke er sterk nok til at gassen klarer å dra med seg all væska gjennom hele rørledninga ved lav gass strømningsrate. Når gassstrømningsraten økes vil etterhvert den akkumulerte væska bli blåst ut gjennom røret og væska ankommer som lange tetthetsbølger. Tetthetsbølgene kan forårsake operasjonelle problemer. Hvis det totale væskevolumet i

tetthetsbølgene overstiger kapasiteten til mottaksseparatoren kan det forårsake uplanlagt nedstengelse av produksjon. Tetthetsbølgene er et fenomen som inntreffer i trefasestrømning og de er ofte delt i en kondensatbølge fulgt av en vann/MEG bølge. Den typen tilfeller kan forårsake formasjon av hydrater i perioder uten MEG strømning. De tilgjengelige kommersielle flerfasesimuleringsprogrammene har hatt problemer med å predikere denne typen lange tetthetsbølger. På grunn av problemene tetthetsbølgene kan forårsake er det viktig å kunne predikere, kontrollere og håndtere tilstedeværelsen av lange tetthetsbølger. Lange tetthetsbølger er hoved flow assurance utfordringa på Ormen Langefeltet.

Laboratorieeksperimenter på tetthetsbølger har blitt gjennomført i flerfaselaboratoriet på NTNU. Formålet med labeksperimentene var å finne ut om det er mulig å reproducere tetthetsbølger i labben på NTNU. Ei 57,84 meter lang testrørledning var satt opp med en knekk i starten. Eksperimentene ble gjennomført i tofase, med vann og luft som test fluider. Stasjonær lagdelt strømning ble satt opp gjennom hele røret, med fastsatte strømningsrater på gass og væske, før gasstrømninga ble strupt ei lita stund og trappet opp igjen. Dette fikk væske til å akkumulere i knekken på røret mens gassen ble strupt. Væska ble så blåst ut gjennom røret i en tetthetsbølge når gassraten igjen ble trappet opp. Bortsett fra veldig lang varighet og forekomst i trefasestrømning var resultatet bølger med karakteristikkene til lange tetthetsbølger: Forekomst i lagdelt strømning, initiert på grunn av væskeakkumulering i et lavt punkt i løpet av endring i strømningsrate, relativt jevn front, lav amplitude og evne til å forplante seg hele veien gjennom røret uten å bli smurt ut totalt. Varigheta var rundt 20 sekunder ved slutten av røret, noe som er relativt lenge for ei relativt kort og trang rørledning med 60 mm indre diameter.

Observasjonene fra laboratoriet har blitt forsøkt simulert i programmene OLGA og LedaFlow. OLGA reproduserte generelt observasjonene bra. OLGA predikerte bølger som oppførte seg veldig likt de observerte bølgene for alle de åtte analyserte tilfellene. Den generelle trenden var at OLGA predikerte bølger med en litt høyere amplitude og litt lavere hastighet enn observert. LedaFlow predikerte observasjonene mye dårligere enn OLGA. LedaFlow klarte bare å reproducere ei løsning omtrent lik observasjonene for to av de åtte analyserte tilfellene, de to tilfellene med høyest U_{sg} og lavest U_{sl} .

Table of Contents

Foreword	i
Abstract	ii
Sammendrag	iii
1. Introduction	8
2. Objectives	8
3. Surge wave phenomenon	9
3.1. Definition	9
3.2. Mechanism	10
3.3. Simulator performance	14
3.4. Surge waves in gas-condensate pipelines	15
3.4.1. Åsgard B	15
3.4.2. Huldra – Heimdal	21
3.4.3. Ormen Lange	22
3.4.4. Snøhvit	23
3.5. Earlier conducted laboratory experiments at IFE	23
3.5.1. IFE’s experimental work, facility and test fluids	23
3.5.2. Propagation of long liquid surges	24
3.5.3. Dip generated surges of finite length	27
3.5.4. Pump generated surges of finite length	29
3.5.5. Two surges in sequence	29
3.6. Project work experiments	30
4. Laboratory experiments	32
4.1. Experimental facility at NTNU	32
4.1.1. The multiphase flow loop	32
4.1.2. Experimental setup	34
4.1.3. Holdup measurement instrumentation, calibration and calculation	37
4.1.4. Curve smoothing	38
4.1.5. Wave velocity calculation	39
4.1.6. Camera recording	40
4.2. Performed experiments, result analysis and discussion	40
4.2.1. Performed experiments	40
4.2.2. Test procedure	41

4.2.3. Lab result analysis and discussion	41
5. Computational simulation	49
5.1. Simulation programs	49
5.1.1. OLGA.....	49
5.1.2. LedaFlow.....	52
5.2. OLGA simulation setup.....	56
5.2.1. Simulation setup and boundary conditions	56
5.2.2. Mesh.....	57
5.2.3. Mass equation discretization	60
5.2.4. The OLGA HD model.....	60
5.3. LedaFlow simulation setup	61
5.3.1. Simulation setup and boundary conditions	61
5.3.2. Mesh.....	62
5.3.3. Slug capturing and discretization	64
5.4. Simulation result analysis and discussion	65
6. Conclusion.....	75
7. Suggestions for further work.....	76
References	77
Appendix A: Lab and simulation results	80
Case 1: $U_{sg} = 13,4$ m/s, $U_{sl} = 0,0113$ m/s	80
Case 2: $U_{sg} = 10,9$ m/s, $U_{sl} = 0,0113$ m/s	84
Case 3: $U_{sg} = 8,5$ m/s, $U_{sl} = 0,0113$ m/s	88
Case 4: $U_{sg} = 7,6$ m/s, $U_{sl} = 0,0113$ m/s	92
Case 5: $U_{sg} = 13,4$ m/s, $U_{sl} = 0,0264$ m/s	97
Case 6: $U_{sg} = 10,9$ m/s, $U_{sl} = 0,0264$ m/s	102
Case 7: $U_{sg} = 8,5$ m/s, $U_{sl} = 0,0264$ m/s	106
Case 8: $U_{sg} = 7,4$ m/s, $U_{sl} = 0,0264$ m/s	111
Appendix B: Camera screenshots	116
Case 1: $U_{sg} = 13,4$ m/s, $U_{sl} = 0,0113$ m/s	116
Case 2: $U_{sg} = 10,9$ m/s, $U_{sl} = 0,0113$ m/s	118
Case 3: $U_{sg} = 8,5$ m/s, $U_{sl} = 0,0113$ m/s	121
Case 4: $U_{sg} = 7,6$ m/s, $U_{sl} = 0,0113$ m/s	123
Case 5: $U_{sg} = 13,4$ m/s, $U_{sl} = 0,0264$ m/s	126
Case 6: $U_{sg} = 10,9$ m/s, $U_{sl} = 0,0264$ m/s	128
Case 7: $U_{sg} = 8,5$ m/s, $U_{sl} = 0,0264$ m/s	131
Case 8: $U_{sg} = 7,4$ m/s, $U_{sl} = 0,0264$ m/s	133

Appendix C: Risk Assessment Report 136

1. Introduction

Ramp up of production rates in wet gas pipelines can give long surge waves arriving at the receiving separator. This phenomenon causes flow assurance challenges on several gas-condensate fields and this phenomenon is described in the first part of this Master Thesis. Experiments have been conducted in the multiphase flow laboratory at NTNU to see if long surge waves could be observed in the lab. Computational simulations have been performed in OLGA and LedaFlow to test the simulation programs capability of reproducing the lab observations.

2. Objectives

The main objective in this Master Thesis was to modify and upgrade the multiphase flow lab to find out if long surge waves could be observed in a test section with a dip, considering the possibility for further research work on surge waves at NTNU. The possibility of creating long surge waves that are able to propagate through the entire pipe length of 57,84 meters has been investigated.

The capability of the simulation programs OLGA and LedaFlow to reproduce the lab observations has also been tested. The question was mainly if the programs were able to predict a long wave with small holdup to propagate through the entire pipe length or if the wave eventually would get smeared out totally due to numerical diffusion.

3. Surge wave phenomenon

3.1. Definition

Liquid surge waves can be explained as isolated liquid film segments that propagate through a pipeline [1, p. 5]. Surge waves occur in three-phase gas dominated pipelines where they are observed as oscillations in liquid flow at the outlet of the pipeline. The oscillations are very slow, with a typical period of about 1 hour and they can last for a couple of days. Surge waves can propagate over a distance of 100 km [2, p. 13]. The surge waves represent an increase in holdup, but they do not block the entire pipe cross section area, hence gas is transported along with the surge waves. The total liquid volume carried in the surge waves is significant due to the long wavelength [3, p. 8]. The surge waves are therefore a phenomenon that occurs in the stratified flow regime. A schematic outline of a surge wave is shown in figure 1 below.

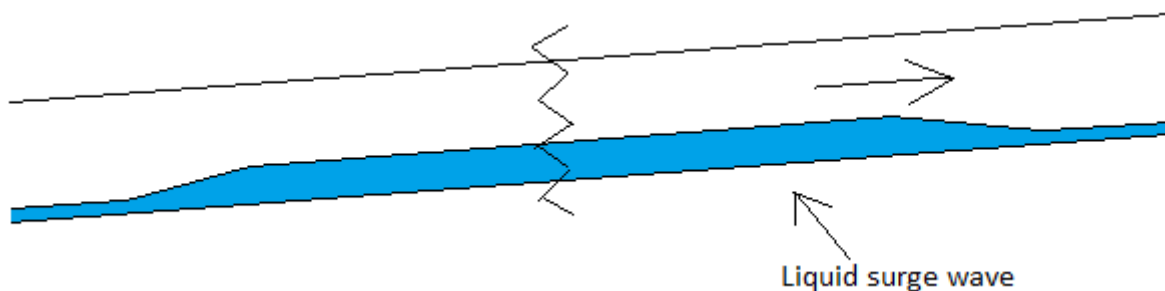


Figure 1: Illustration of a surge wave in a stratified gas- liquid pipe flow.

Institute for Energy Technology (IFE) has earlier conducted laboratory experiments on surge waves to get a better understanding of the phenomenon. IFE use the notations positive and negative surges when studying an isolated liquid film segment in the lab. If the holdup increases with time in a surge wave at a fixed observation point it is denoted as a positive surge. If the holdup decreases it is denoted as a negative surge. The velocity is denoted U_+ for a positive surge and U_- for a negative surge. This is illustrated in figure 2 below [1, p. 5].

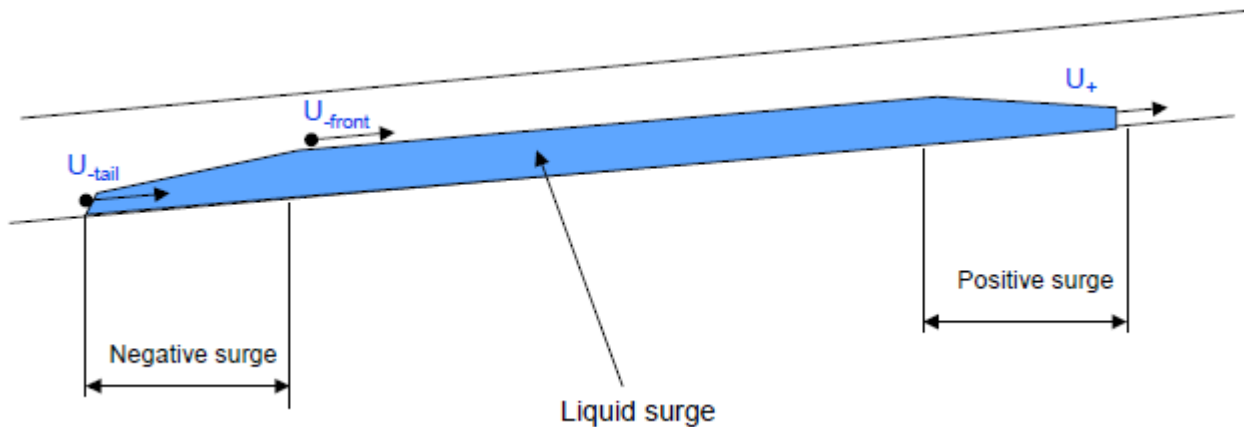


Figure 2: IFE's surge wave notation. [1, p. 5]

3.2. Mechanism

Surge waves are mainly a transient phenomenon that is initiated by a change from one steady state to another. In gas- condensate pipelines the surge waves are initiated by a change in the production rate. The oscillations in the liquid flow are caused by liquid mass waves propagating down the pipeline with a velocity close to the liquid transport velocity [2, p. 13]. Surge waves normally occur during production at low flow rates, typically during production ramp up [3, p. 8] and sometimes also during ramp down [4, p. 10]. When the production rate is increased the pipeline will move from a state with a large liquid content to a state with less liquid content. When this excess liquid is expelled out of the pipeline, it is seen as a long surge wave at the outlet [3, p. 8]. Liquid will accumulate in the low spots along the flowline during a production shut down. The liquid will then propagate through the flowline as surge waves when the production is ramped up again.

Unstable surge waves can also occur at low flow rates in flowlines with high liquid content at a constant production rate [3, p. 8]. When the reservoir pressure goes down the production rate will fall by itself, the interfacial drag force between the gas phase and the liquid phase is decreased and liquid will accumulate in the pipeline. The liquid then arrives in surge waves at the outlet of the pipeline at the receiving facility [3, p. 7]. The liquid content in the pipeline will increase steeply when the production is decreased, as liquid accumulation in a pipeline is a function of gas flow rate [5, p. 9]. This defines a minimum production flow rate in order to

avoid instabilities in the flow that leads to the presence of surge waves. The typical minimum production flow rate is illustrated in figure 3 below. Even small changes in the production flow rates for a pipeline operating in this region can cause large surge waves [3, p. 8]. The ability to produce at low flow rates at low reservoir pressure is important in order to maximize the field recovery [3, p. 7]. The flowlines are dimensioned for a large production at high flow rates and are consequently exposed to liquid accumulation, leading to surge waves at falling flow rates during field tail-end production. It is therefore important to be able to handle the presence of surge waves in order to squeeze down the technical production flow rate cut off limit, as the production rate where surge waves start to occur is much higher than the economical cut off limit [6, p. 1].

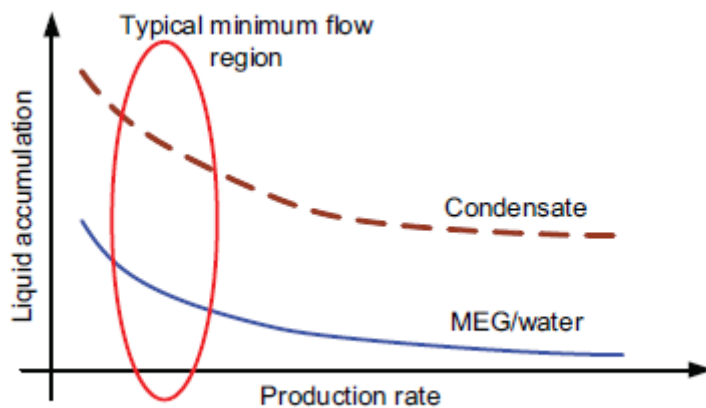


Figure 3: Conceptual relationship between production rate and liquid content of condensate and MEG/water. [3, p. 8]

Surge waves are a unique multiphase flow phenomenon. The surge waves differ from both slug flow and roll waves. While riser slugging is a problem in oil dominated flow, surge waves are a problem in gas dominated flow [7, p. 303]. The presence of ramp up surge waves is not as severe as the presence of startup slugs, as startup slugs can initiate severe slugging [7, p. 297]. Slug flow blocks the entire cross section area of the pipeline, while surge waves only occupy a fraction. Surge waves can propagate over a distance of 100 km and last for an hour, while slugs are typically less than 500 pipe inner diameters long [8, p. 8]. Slug flow is therefore easier to reproduce in a lab.

Roll waves or large waves are the largest waves occurring in the two-phase stratified flow regime [9, p. 3]. Surge waves must not be confused with roll waves. Roll waves are characterized by a steep wave front [2, p. 7], and they are the waves with the largest amplitude that occurs in two-phase pipe flow. The peak of the roll wave front tends to roll over and create a breaking wave [9, p. 2]. Roll waves are therefore the complete opposite type of wave phenomena compared to a surge wave which is characterized by slow oscillations, long duration, low amplitude and a smooth wave front. The formation of roll waves must therefore be avoided during attempts of creating surge waves in the lab. An image of a typical roll wave observed in a two-phase air-water flow in the multiphase flow lab is seen in figure 4 below.

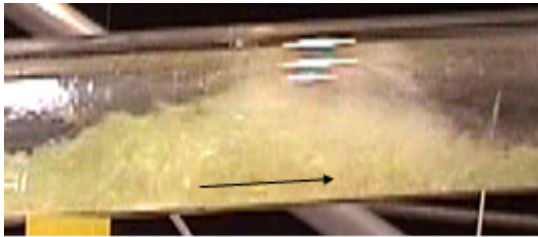


Figure 4: Roll wave observed in the lab. [10]

Surge waves are easiest studied in laboratories in the term of two-phase flow, where the surge wave consist of a single liquid phase that is expelled through the pipeline by the interfacial drag force between the gas- and liquid phases. In this Master Thesis, two-phase surge waves are primarily studied as a laboratory phenomenon with the purpose getting a better understanding of the pipeline surge wave phenomenon and to investigate whether or not surge waves can be observed in the multiphase flow lab, regarding the possibilities for further research work on this special flow regime. Similar surge wave instabilities as in three-phase flow are not reported for two-phase field flowlines [4, p. 1], and it might therefore not be possible to reproduce this exact phenomena in two-phase in the lab.

In gas-condensate flowlines the surge waves appear in the term of three-phase flow. This represents very complex multiphase flow. The different phases in the flow are gas, condensate and a mixture of water and mono ethylene glycol (MEG). MEG is injected into the flow at the wellhead in order to avoid the formation of hydrates [3, p. 9]. The MEG is then transported through the flowline along with the well stream, back to the platform where it is regenerated. The surge waves propagate through the pipeline as a condensate surge followed by a mixed

water/MEG surge [3, p. 10]. The condensate phase and the water/MEG phase can also be mixed into each other, depending on the conditions in the flowline. In those cases the surge waves will not be characterized by two different liquid phases arriving in sequence. This is the situation at Ormen Lange [11].

The main problem caused by surge waves is the large unpredicted liquid volumes arriving at the receiving separator. As the surge waves are difficult to predict, and contain a significant amount of liquid, they can cause unplanned production shutdown if the liquid volume arriving in the surge waves exceeds the liquid handling capacity at the receiving facility [3, p. 12]. The importance of the ability to predict the surge waves is therefore the motivation behind research on surge waves. Surge waves are mainly a greater issue at offshore platforms than at large onshore plants. As space and weight offshore is limited and desired to be kept low, it is requested to use as compact equipment as feasible. This results in smaller receiving separators and less capability to handle surge waves [3, p. 7]. Onshore plants can be equipped with large slugcatchers with large capacity to handle surge waves [12, p. 2]. It is still necessary to have control over the presence of surge waves, as too large surge waves potentially can flood the slug catchers, even at onshore plants [13, p. 4]. Surge waves divided into a condensate surge followed by a water/MEG surge can also lead to hydrate formation, as there are periods with little or no MEG flow through the pipeline [4, p. 1].

Control over the occurrence of surge waves represents a crucial flow assurance challenge in order to avoid the problems described above and ensure stable field operation. Different techniques can be applied to handle surge waves. If a reliable flow assurance system is installed, the production ramp up can be monitored to ensure that the liquid volume of the incoming surge waves is within the capacity of the slug catcher. Production choke back is another strategy to handle surge waves at an offshore installation with limited liquid handling capacity. The choke opening at the arrival at the platform is reduced when a surge wave arrives, the liquid inflow is reduced and overflowing of the liquid handling facility is avoided. This is described in section 3.4.1. Surge waves can also be avoided by a reduction of the receiving pressure. If the receiving pressure is reduced, the gas speed will be higher through the flowline, the interfacial drag between the gas and the liquid will increase and there will be less liquid accumulation in the pipeline, resulting in less surge waves [4, p. 2].

3.3. Simulator performance

“The physics behind these very long waves has not been well understood.” [2, p. 13]

The commercial transient multiphase flow simulators have not been able to predict surge waves in gas-condensate systems satisfactorily [2, p. 13]. There have been large deviations between the observed surge waves and the flow predicted by the oil and gas simulator (OLGA). There are examples of OLGA not being able to reproduce flow instabilities caused by surge waves [4, p. 7]. Surge waves not found in simulations have been observed at Heimdal [12, p. 1]. FMC Technologies has developed a code, FlowManager, that can be tuned against field data and predict surge waves satisfactorily for a specific system, illustrated in figure 5 below. This system is implemented at the Ormen Lange field, which is described in section 3.4.3. As the surge waves appear in the stratified flow regime it is the stratified flow model that is applied when surge waves are being predicted by FlowManager. The slug model is not applied [11]. FlowManager treats the surge waves kinematic waves [2, p. 13]. Further development of the simulation tools to predict surge waves more accurately is very important as many old gas-condensate fields are reaching tail-end production, the flow gets gas dominated, liquid will accumulate in low spots and surge waves will appear.

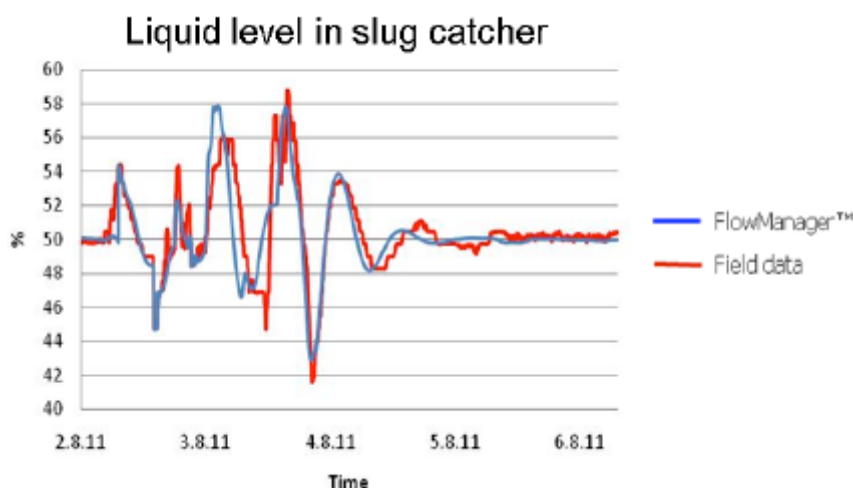


Figure 5: FlowManager prediction compared to field data from Ormen Lange. [5, p. 12]

3.4. Surge waves in gas-condensate pipelines

“Surge waves is something that eventually will occur in all gas-condensate pipelines.”

– Zhilin Yang, Statoil.

3.4.1. Åsgard B

The Mikkel and Midgard fields are gas and condensate fields tied back to the Åsgard B platform. The distance to Åsgard B is 40 km for Midgard and 80 km for Mikkel, the field layout is illustrated in figure 6 below. Two 20 inch flowlines are connected to Åsgard B through a 300 meter high S- riser [4, p. 2]. The production rates at the Mikkel and Midgard fields are expected to fall as the reservoir is emptied. Field tests have been conducted in order to identify the flow rates where liquid surge waves starts to appear [3, p. 7].

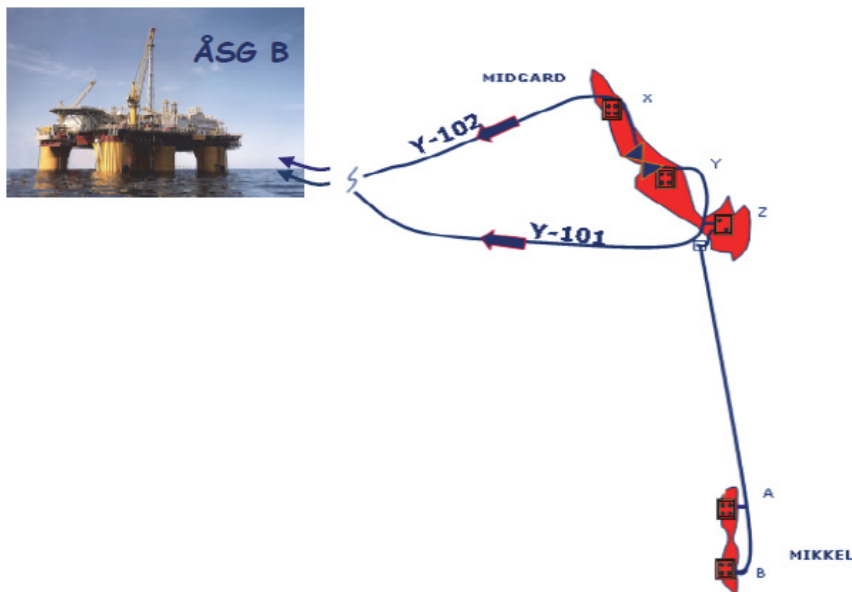


Figure 6: Mikkel – Midgard field layout. [4, p. 3]

At reduced flow rates liquid starts to accumulate in the flowlines and long surge waves are experienced at Åsgard B. The liquid surge waves are separated in a condensate surge followed a water/MEG surge. The flow rate of gas is reduced slightly when the surge waves arrive at the platform. The surge waves are unstable, with varying duration and frequency [4, p. 1]. At Åsgard B the surge waves represent a challenge due to the water/MEG handling capacity. If the rate of MEG exceeds the regeneration capacity, the MEG surge drum will eventually get

overfilled. Such a situation may result in production shut down [3, p. 9]. At the peak rate of the surge waves the liquid volumes exceed the water/MEG handling capacity. This happens at low flow rates and the water/MEG handling capacity at the platform defines the minimum production flow rate. Another concern is hydrate formation in periods with little or no MEG return [4, p. 2]. To identify the flow rates where surge waves started to occur the production rate was reduced gradually until the point where surge waves started to appear was reached; this is seen in figure 7 below.

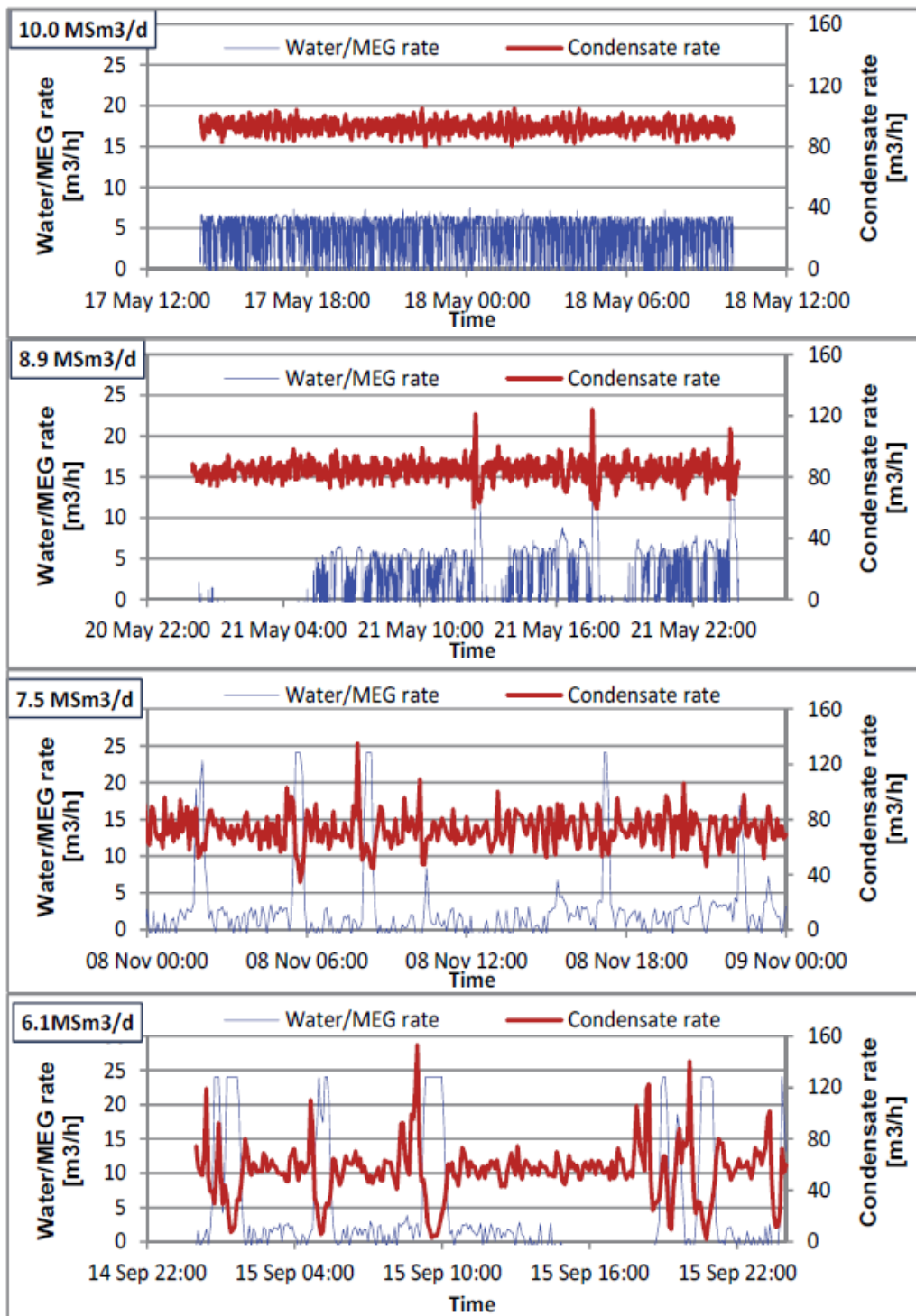


Figure 7: MEG/water and condensate rates from Y-102 at Åsgard for different production rates. [4, p. 5]

As seen in figure 7, the flow rates are quite stable for a production rate of 10 Msm³/d. There are small fluctuations in water/MEG and condensate flow rates [4, p. 5]. At 7,5 MSm³/d regular surge waves appears. The liquid phases are separated in a condensate surge arriving first, followed by a water/MEG surge. The condensate surge waves have flow rates up to 160 – 180 m³/h. The water/MEG surge waves are larger than 24 m³/h, which is the maximum reading of the meter. The condensate flow rate is very low during the arrival of the water/MEG surges. The surge wave frequency varies between ½ hour to many hours, with a duration less than ½ hour. At 6,1 Msm³/h the water/MEG flow rates are estimated about 50 m³/h. The duration is up to 1 hour. The condensate surges are smaller, with flow rates up to 130 – 140 m³/h. The water/MEG surges get larger with a reduction of production flow rate [4, p. 6]. This defines the minimum flow rate, as the water/MEG handling capacity is reached [4, p. 12].

As seen in figure 8 below, there is about 10 % reduction in the gas flow rate during the arrival of the liquid surge waves [4, p. 6]. This illustrates that the surge wave holdup in the pipeline is small and that surge waves differ from slug flow that block the pipeline cross section area. As seen in the figure, the duration of a single surge wave can exceed a couple of hours. At Åsgard B the duration of the surge waves observed can vary significantly. The duration of the water/MEG surges varies between 15 and 105 minutes, with a period of ½ to 11 hours between each water/MEG surge wave. There is little or no MEG returned to Åsgard B between the surge waves. The surge waves get longer the longer the period between each surge wave. The condensate surge waves last from zero to 75 minutes, with a period similar to the water/MEG surges [3, p. 10].

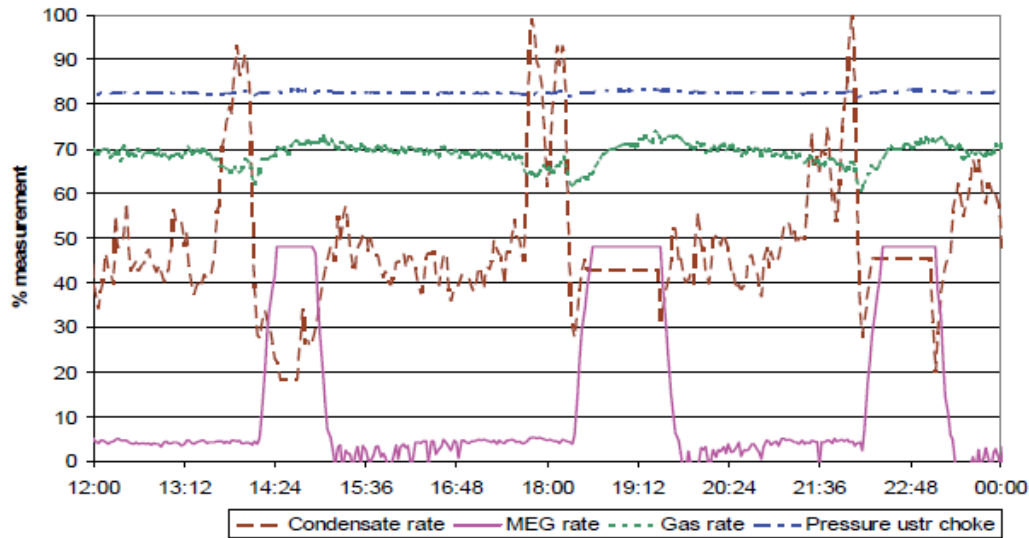


Figure 8: The three phase surge waves phenomenon, 6,1 Msm³/d. The condensate phase is followed by the water/MEG phase. [4, p. 6]

Actions to control the surge waves arriving at Åsgard B have been implemented to prevent the surge drum from getting overfilled, leading to process shut down [3, p. 9]. Instead of measuring liquid flow at the outlet of the first or second separators, multiphase metering has been installed at the inlet of the production unit. The surge waves are detected when they arrive without any delay when the liquid flow is measured at the inlet. Then the flow is choked back when a surge wave arrives, and overfilling of the MEG surge drum is avoided [3, pp. 12 - 13]. As seen in figure 9 below, flooding of the MEG surge drum is avoided when the flow is choked.

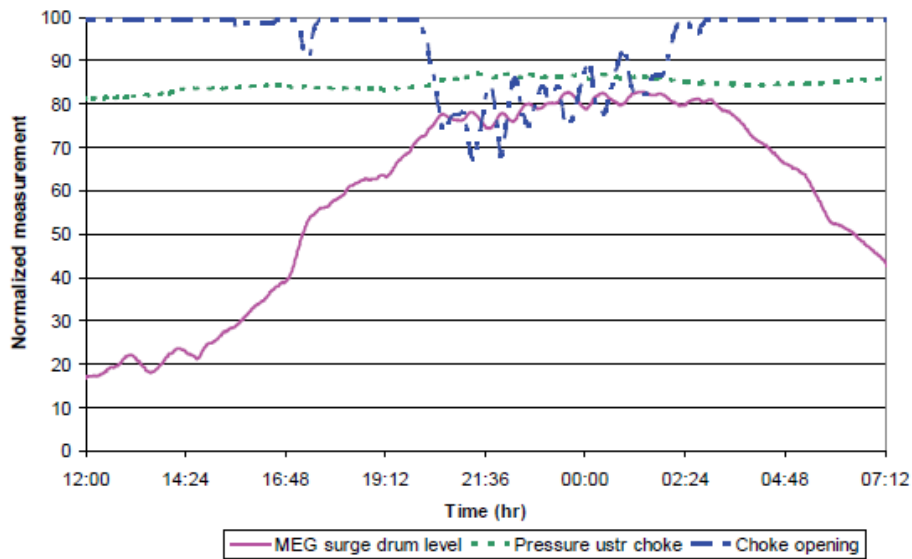


Figure 9: Avoiding overfilling of the MEG surge drum by choking back production. [3, p. 15]

Another observation is that the impact on the liquid flow rate is greater than the impact on the gas flow rate when the choke opening is reduced. The flow rate of gas is not reduced as much as the flow rate of liquid. The gas production can therefore be kept relatively high while the surge waves are choked, and the surge wave handling does not need to be very expensive due to fairly high gas production. This effect is illustrated in figure 10 below [3, p. 15].

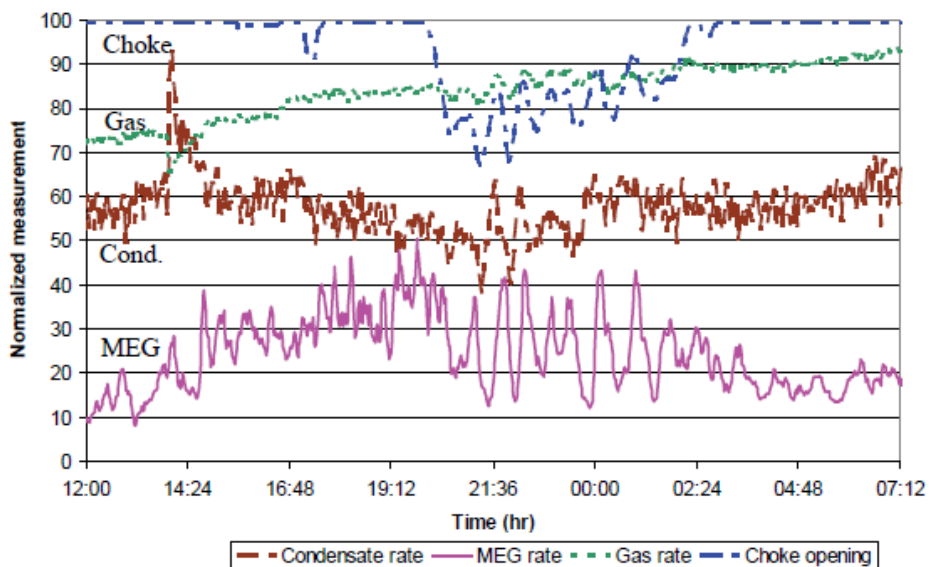


Figure 10: Impact of choking on the gas-, condensate- and MEG rates. [3, p. 15]

3.4.2. Huldra – Heimdal

Huldra is a gas and condensate field connected to the Heimdal platform through a 150 km long, 22 inch multiphase flowline, as illustrated in figure 11 below. At the Heimdal platform, the production from Huldra is processed and exported. The multiphase flow arriving at Heimdal contains gas, condensate and a mixture of water/MEG [6, p. 1].

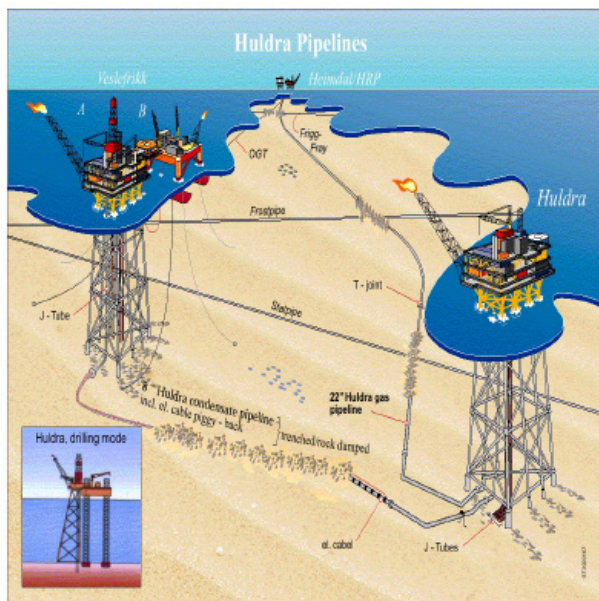


Figure 11: The Huldra – Heimdal pipeline system. [6, p. 9]

Inaccurately predicted liquid surge waves, received from Huldra, have been a challenge at Heimdal. These surge waves are experienced during the first days of production after a startup or after a flow rate increase. The liquid flow rate varies significantly with a one hour period. The formation of surge waves is caused by liquid accumulated in the low spots in the pipeline during shut-in. After startup the liquid travels as surge waves through the pipeline. These surge waves are a challenge at Heimdal because the receiving separator is very small, with a volume of only 7 m³. The surge waves arriving at Heimdal are relatively small and only noticed because of the small liquid receiving capacity, they would probably not have been noticed at a facility with a larger receiving separator [12, p. 7]. It takes about 12 hours before the liquid flow reaches steady state after startup. OLGA predicts steady state to be reached much faster [1, p. 2].

3.4.3. Ormen Lange

Ormen Lange is a gas and condensate field that has a 120 km long subsea to shore tie-back multiphase transport of unprocessed well stream [14, p. 45]. The transport flowline goes up the steep Storegga hill, with an inclination up to 35 degrees [14, p. 47]. The field layout is illustrated in figure 12 below.

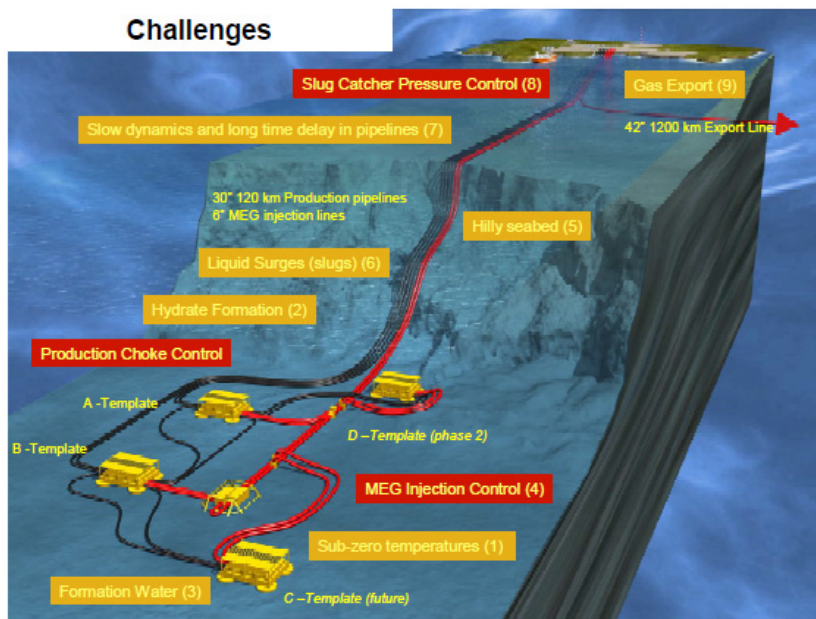


Figure 12: The Ormen Lange field layout and flow assurance challenges. [13, p. 4]

Large surge waves are experienced during production ramp up, and the liquid surge waves represent the main flow assurance challenge at Ormen Lange [14, p. 45]. If the production is ramped up too quickly, large surge waves can flood the slug catchers and the receiving facility may experience unplanned shutdowns. The surge waves at Ormen Lange have very slow oscillations. The duration of a surge wave is typically around one hour and surge waves continue to arrive for one or two days after production ramp up, before the flow is stabilized [2, p. 13]. A flow assurance system has been installed to control the multiphase flow behavior, and to ensure that the production is ramped up in a manner that not causes surge waves that are large enough to flood the slugcatcher [5, p. 1]. FlowManager is applied and tuned with the field data for Ormen Lange, and it is able to predict the surge waves arriving at Ormen Lange satisfactorily [5, p. 12], illustrated in figure 5. All transient pipeline operations are simulated in advance, to ensure safe and optimized operation of the production system [14, p. 45].

3.4.4. Snøhvit

Snøhvit is a gas and condensate field that has a 143 km long, 28 inch subsea to shore tie-back multiphase transport of unprocessed well stream. The flow includes gas, condensate and water/MEG. Due to the harsh ambient conditions, very long pipeline distances and rough seabed, it was the most complex gas-condensate development ever done when it was set in operation in 2007 [12, p. 2]. There is a large potential for severe liquid accumulation in the pipeline [15, p. 396]. Liquid surge waves have not been a major concern at Snøhvit, as the slug catcher of 3000 m³ provides a large liquid handling capacity [12, p. 2]. After shutdown the production has been ramped up to the same level as before shutdown, before large amounts of liquid have accumulated in the pipeline. In special cases, condensate has been able to accumulate in the pipeline creating surge waves. The liquid accumulation in the pipeline has been monitored carefully to ensure that the surge waves have been within the capacity of the slug catcher in those situations [15, p. 401].

3.5. Earlier conducted laboratory experiments at IFE

3.5.1. IFE's experimental work, facility and test fluids

IFE has earlier done lab experiments on two-phase surge waves. They published the report “Surge waves in gas-liquid pipe flow – Experiments and analysis” in 2004 [1]. The objective of the work was to get a better understanding of the behavior of surge waves in order to improve the models, as there were deviation between observed field data and simulations done in OLGA for the Huldra – Heimdal pipeline. OLGA predicted steady state liquid flow after startup of the pipeline to be reached much faster than the actual 12 hours [1, pp. 2 - 3]. The experiments were carried out at IFE's Well Flow Loop, which is a closed multiphase loop with a 25 meter long test section. The pipeline in the test section has an inner diameter of 10 cm and consists of both steel and transparent PVC pipes. Holdup and pressure is measured with gamma densitometers and differential pressure transducers along the pipeline test section, illustrated in figure 13 below [1, p. 6].

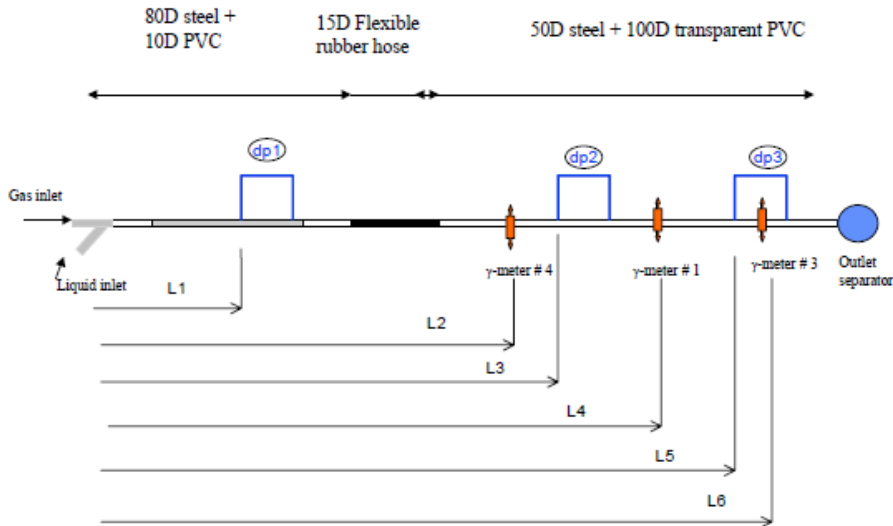


Figure 13: Distribution of gamma densitometers and differential pressure transducers along the 25 meter long test section. [1, p. 8]

The experiments were conducted in two-phase with a gas phase and a single liquid phase. The gas phase applied was sulphur hexafluoride (SF_6). SF_6 has about five times the molecular weight of air. This enables a high gas density at moderate pressures, and transparent pipes can be applied for visual observations of flow conditions that are similar to the conditions found in gas-condensate pipelines. Three different liquids were tested in combination with SF_6 ; tap water, the oil Exxol D80 and the oil Marcol [1, p. 8]. The water density is not influenced by the high gas density. The dynamic viscosity of the water at 20°C and atmospheric conditions is 1,0 cP. Exxol D80 is light, solvent oil. At test conditions the density gets higher when the oil is saturated with the SF_6 gas. The dynamic viscosity is 1.7 cP at atmospheric conditions at 20°C [1, p. 9]. The Marcol oil has a significantly higher dynamic viscosity than the other test fluids, 12 cP at atmospheric conditions at 20°C . The Marcol oil density increases when it is SF_6 saturated [1, p. 10]. Surge waves were initiated in four different ways at IFE and are described in the sections 3.5.2 – 3.5.5.

3.5.2. Propagation of long liquid surges

Long liquid surge waves, illustrated in figure 14 below, were studied in order to get an understanding of the velocities of the front and tail of long surge waves with a given gas flow rate and with initially dry pipe wall ahead of the surge wave. Different experiments were conducted on all three liquids with varying pressure, surface tension, gas density and pipeline

inclination. The pipeline was set up with the straight geometry seen in figure 13, with an inclination of -1° to 4° [1, p. 12].

The following mechanism was used to initiate the long surge waves [1, p. 12]:

- The gas compressor was run for 4-5 minutes in order to create a dry pipe and single phase gas flow in the pipeline.
- The gas flow rate was then adjusted to the predefined value and a long surge wave was initiated by a sudden start of the liquid pump.
- Liquid then entered upstream in the pipeline, and propagated as a positive surge wave through the pipeline.
- After a while, the holdup increase stopped creating a steady state two-phase flow through the pipeline.
- The liquid pump was switched of, and a negative surge was initiated as the holdup decreased. The whole surge wave was eventually expelled out of the pipeline.

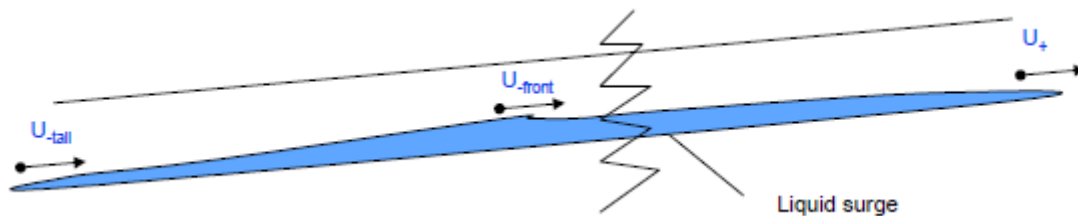


Figure 14: Schematic layout of the front and tail of long liquid surges. [1, p. 12]

The following observations were noticed for long liquid surges:

- The front of the positive surge moves faster for water than for Marcol [1, p. 14].
- The front velocity of the positive surge increases with increasing superficial liquid velocity (U_{sl}) and with decreasing pipe inclination [1, p. 14].
- The tail velocity of the negative surge moves slower than the front [1, p. 19].
- The velocity increases with increasing gas velocity, it does not show any dependency on the liquid flow rate [1, p. 19].
- The tail velocity is independent on the pipeline inclination [1, p. 19].

- The tail velocity is lower for the liquid with highest viscosity [1, p. 19].

In a narrow range of gas flow rates the tail of the long liquid surges ends in an end shock/hydraulic jump. The gas flow rates where this phenomenon occurred was close to the minimum gas flow rate required to expel the liquid out through the pipe, after the liquid pump was switched off. In this situation the interfacial drag from the gas phase on the liquid film is very close to the gravity force [1, p. 20]. An outline of a surge wave with an end shock is illustrated in figure 15 below.

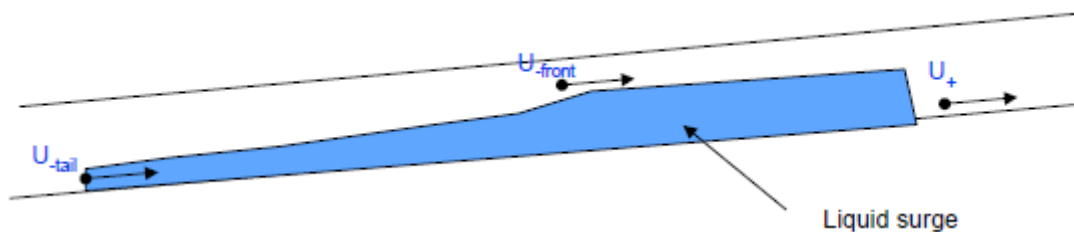


Figure 15: Schematic outline of the liquid surges in experiment with an end shock. [1, p. 21]

The following observations were noticed for surges with an end shock [1, p. 21]:

- There is a small range of gas velocities where end shocks occur.
- The tail velocity with an end shock seems to be independent of the fluid viscosity.
- The gas velocity where an end shock occur increases with increasing pipe inclination. Explained by the balance between interfacial friction and weight being moved towards higher superficial gas velocity (U_{sg}) when the pipe inclination increases.
- The gas velocity where an end shock occurs increases with decreasing gas density, explained by the balance between interfacial friction and weight being moved towards higher U_{sg} when the gas density decreases.

3.5.3. Dip generated surges of finite length

The experiments conducted on dip generated surge waves are the most realistic experiments compared to field conditions. When the production is shut down in gas-condensate pipelines, liquid will accumulate in the low spots of the pipeline. When the production is ramped up again, the liquid accumulated in the low points will start to travel downstream by the impact of the increasing interfacial drag of the gas [1, p. 23].

The lab test section was configured with a dip in the flexible hose, with 10 meters downwards inclined pipe followed by 15 meters upwards inclined pipe, illustrated in figure 16 below. The upwards inclinations tested varied between $0,5^\circ$ and 2° . After drying the test section, surge waves were initiated by pumping a known liquid volume in the dip and then starting the gas compressor, blowing the liquid out of the pipeline by the gas-liquid interfacial drag [1, p. 23]. The dip generated surge waves are initially characterized by a distinct front, a holdup peak value and a long tail, illustrated in the figures 17 and 18 below [1, p. 24].

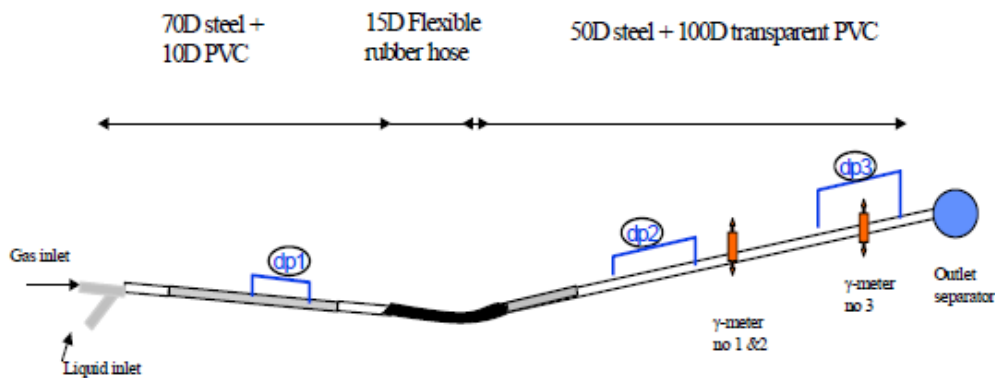


Figure 16: Schematic layout of the experimental setup for the study of dip generated liquid film segments of finite length. [1, p. 24]

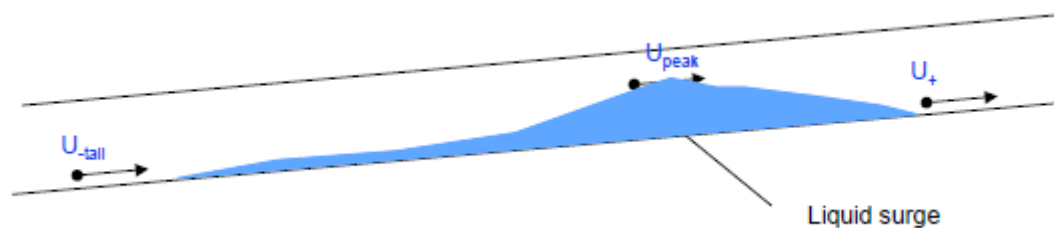


Figure 17: Schematic outline of the dip generated liquid surges. [1, p. 24]

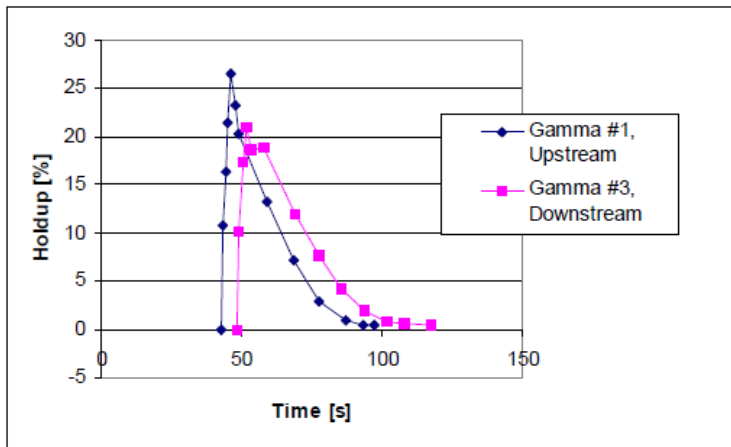


Figure 18: Holdup profile in dip generated surge waves. [1, p. 26]

The following observations were noticed for the dip generated surge waves [1, p. 25]:

- The front and peak velocities are very close; the tail velocity is significantly lower.
- Equal amount of liquid accumulated in the low point of the dip is expelled through the pipeline faster for water than for Marcol.
- The experiment duration time, and the front and peak velocities increases with increasing liquid volume accumulated in the dip.
- The peak holdup increases slightly with an increase in gas velocity.
- The peak holdup increases with increasing liquid volume accumulated in the dip.
- The peak holdup decreases with increasing pipe inclination.

The shape of the dip generated surge waves changed all the way through the pipeline and they did not reach a steady state condition. It is not clear if these dip generated surge waves eventually will reach a steady state condition, or if they will be stretched out as very long and thin liquid films in a sufficient long pipeline [1, p. 25].

3.5.4. Pump generated surges of finite length

With a straight pipe geometry, as in figure 13, pump generated surge waves were initiated in a 4° pipe inclination. The experiments on pump generated surge waves were carried out because the dip generated surge waves did not reach a steady state. These surge waves were initiated by first running the gas compressor at a fixed, predefined flow rate. The liquid pump was then started, initiating a positive surge wave. The liquid pump was shut off, and the surge wave was expelled through the test section of the pipe [1, p. 28].

The following observations were noticed on pump generated surge waves [1, p. 29]:

- There was no systematic difference in the front- and tail velocities of these pump generated surges. This indicates that they travel as lumps through the pipeline and do not change shape.
- The peak holdup and the shape of the holdup curve does not change significantly along the pipeline with time and position. The shape of these surge waves is fairly symmetric.

3.5.5. Two surges in sequence

For all the surge wave experiments described above, the pipe wall was initially dry before the liquid surges were initiated. Experiments were conducted on two surges in sequence, in order to find out whether the thin liquid film from the first surge wave influence the velocities of the following surge wave. The experiments on two surges in sequence were conducted with the same pipe geometry as the pump generated surges. The liquid pump was turned on, initiating a positive surge wave. After 60 – 100 seconds it was turned off and on again, introducing two surge waves in sequence [1, p. 31]. The holdup and front velocity of the positive- and negative surges for the first surge in the sequence behaves as the long surge waves described in section 3.5.2. The velocity at the front of the following surge was slightly lower than for the first surge. This difference seemed to be systematic, but is within the measurement uncertainty. The conclusion on the following surge is therefore that it does not seem to be significantly influenced by whether the pipe wall in front of the surge is wet or dry [1, p. 32].

3.6. Project work experiments

Laboratory experiments on surge waves were conducted during the Master Thesis pre-project work. The experiments were carried out in a 16,95 meter long test pipeline with a dip geometry; see figure 19 below. The pipe inner diameter was 60 mm. The idea was to see if surge waves could be observed in a two-phase air-water flow with changes in the gas flow rate. Steady state stratified flow was established through the pipeline before the gas flow was choked for a few seconds and ramped up again. The liquid that accumulated in the dip during the gas down time was then blown through the pipeline in a wave, when the gas flow was ramped up again.

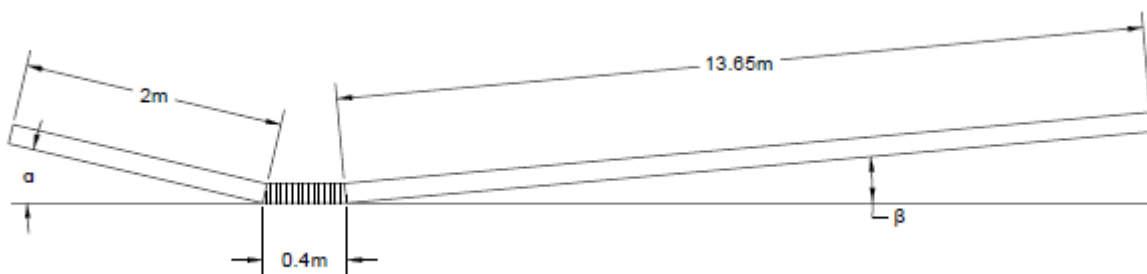


Figure 19: Schematic outline of the geometry of the test pipeline applied in the project work. Measurements of the waves were recorded at 5,3 and 11,8 meters downstream the dip.

The results from the project work experiments was initiation of waves that share several similarities with surge waves: The waves were initiated as a result of a flow rate ramp up, where liquid accumulated in a low spot during a low gas flow rate propagated through the pipeline when the gas flow rate was ramped up. The peak holdup was up to 30 %, thus the waves did only occupy a fraction of the pipe cross section area, and the waves had a smooth, non breaking front. The very long wavelength that characterizes surge waves in gas-condensate pipelines was not observed during the project work as the typical duration of the waves initiated in the project work was only a couple of seconds. Hence, surge waves were concluded to not be successfully reproduced in the lab during the Master Thesis pre-project. The short wavelength was probably a result of the combination of a short pipeline with a small inner diameter, and a small liquid amount accumulated during the short gas down time. A longer wave is expected to be observed in a longer test pipeline. A plot of the typical shape of the waves initiated in the project work is seen in figure 20 below.

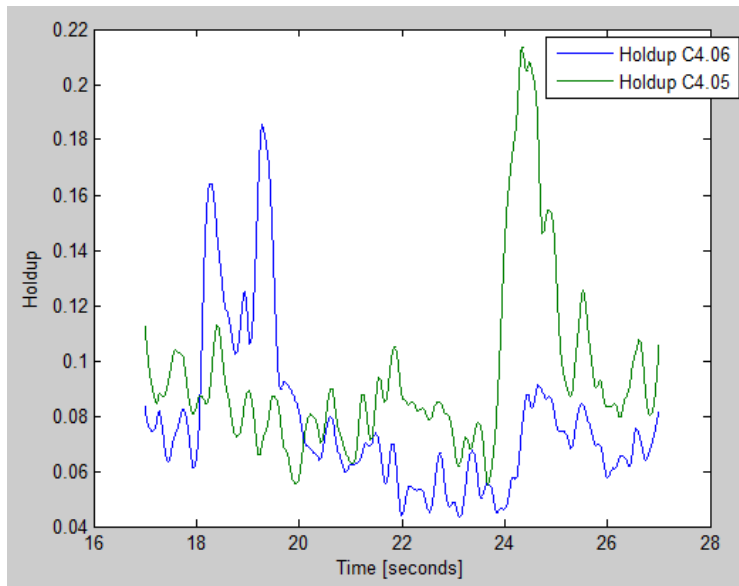


Figure 20: Wave propagation from 5,3 to 11,8 meters downstream the dip. The angles denoted in figure 19 were $\alpha = 0,86$ and $\beta = 0,80$. $U_{sl} = 0,026$ m/s and $U_{sg} = 7,6$ m/s.

The waves were characterized by being split into two parts at 5,3 meters downstream the dip, growing into a single wave at 11,8 meters. It seemed like some of the liquid got carried away immediately when the gas flow ramp up started, and that the rest of the liquid followed right after when the gas flow was ramped up completely.

4. Laboratory experiments

Laboratory experiments on surge waves have been conducted during this Master Thesis work in the multiphase flow laboratory at the Department of Energy and Process Engineering at NTNU. The idea of the lab experiments was to see if long surge waves could be observed in a stratified gas-liquid flow in a test section with a dip. The waves were going to be initiated by choking the gas flow, resulting in liquid accumulation in the dip, and then ramp up the gas flow to its initial rate to blow the accumulated liquid through the pipeline as a surge wave. The behavior of the surge waves through the test pipeline was then going to be studied.

The earlier experiments described in the previous sections have been conducted in fairly short pipelines. IFE's well flow loop has a test section with a total length of 25 meters, and a 16,95 meters long pipeline was used for the pre-project experiments. As surge waves arriving at field installations can propagate over a distance of 100 kilometers, the idea of these Master Thesis lab experiments was to set up a much longer pipeline than what has been applied in earlier laboratory experiments on surge waves, in order to study the propagation of the surge waves over a much longer distance than what has been studied in earlier lab experiments. A pipeline with a total length of 57,84 meters was therefore set up in the multiphase flow lab. Similar lab experiments on surge waves as the experiments performed in this Master Thesis have, to our knowledge, not been conducted before. The results of these experiments might therefore be interesting for the understanding of the surge wave phenomenon.

4.1. Experimental facility at NTNU

4.1.1. The multiphase flow loop

The multiphase flow lab at NTNU consists of three main loops; one for air, illustrated in figure 21, one for water, illustrated in figure 22, and one for oil. They can be connected to an S-riser test section and a horizontal test section. The horizontal test section can be tilted to create different angles, and different pipes with different inner diameter can be used. The test fluids are tap water, atmospheric air and a given oil at ambient room temperature.

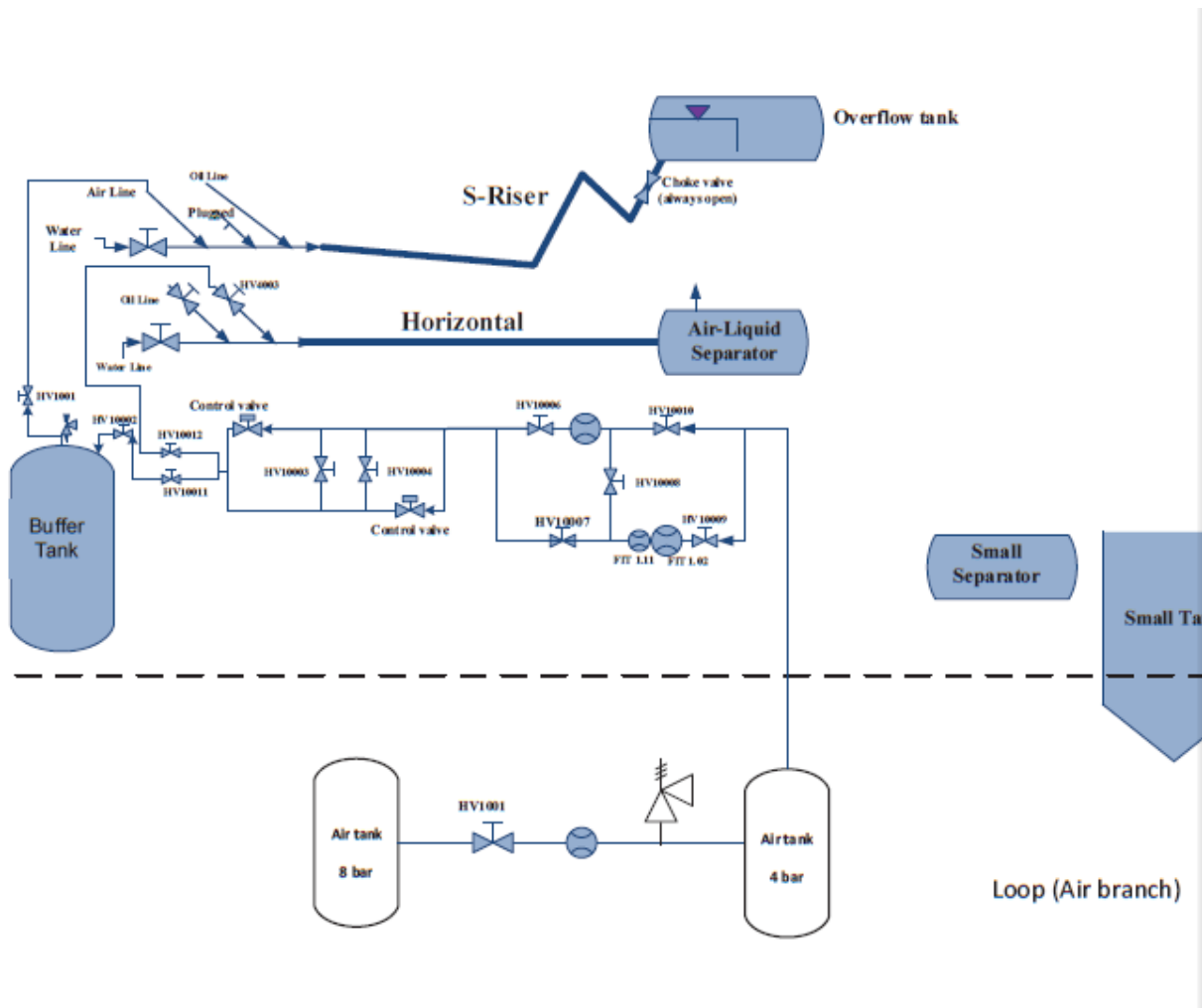


Figure 21: Schematic outline of the air loop at the multiphase flow laboratory at NTNU. The dotted line represents the floor between the first floor and the basement. The test sections are shown as the Horizontal and the S-riser flowlines. [Provided by NTNU]

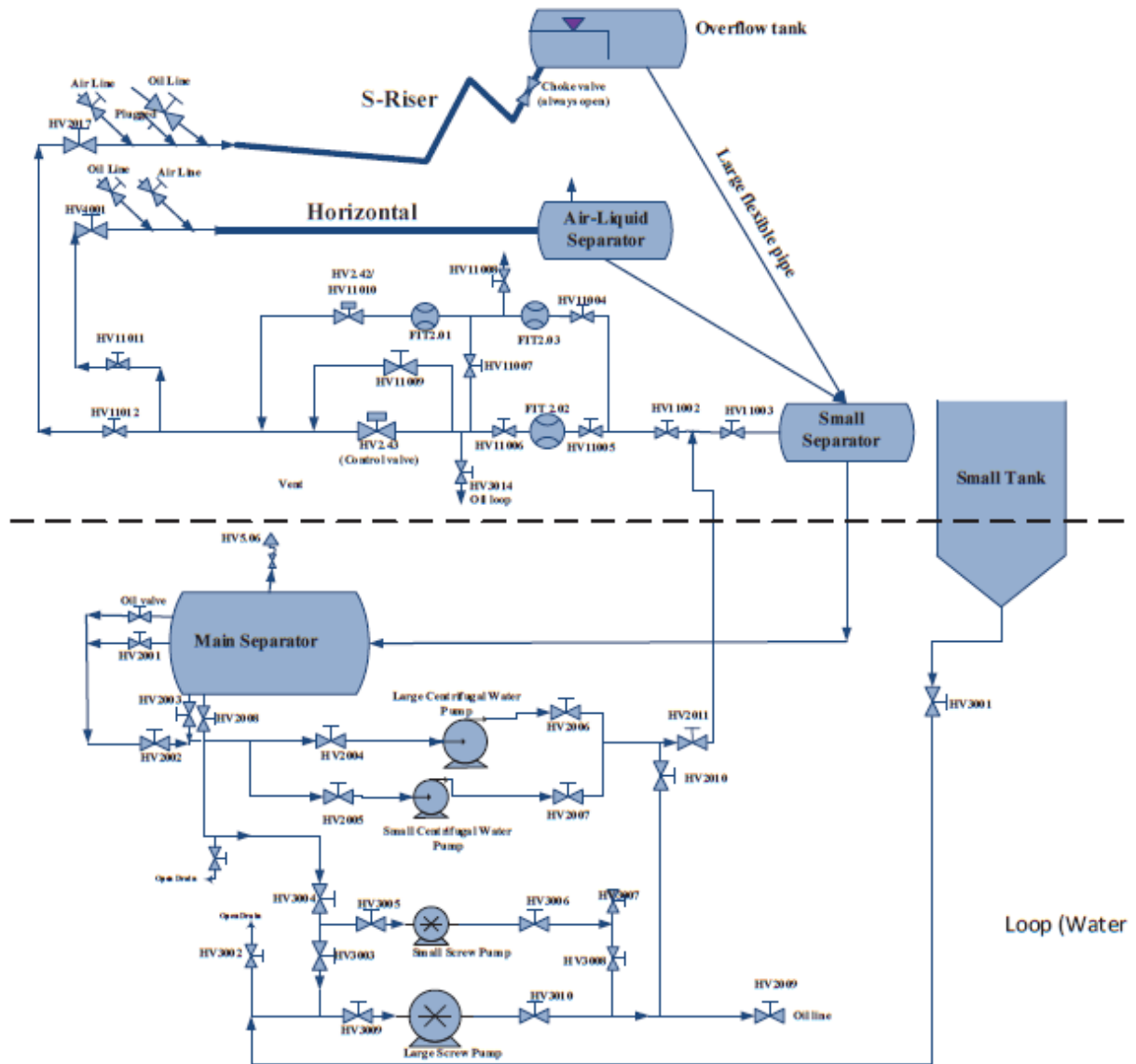


Figure 22: Schematic outline of the water loop at the multiphase flow laboratory at NTNU. The dotted line represents the floor between the first floor and the basement. The test sections are shown as the Horizontal and the S-riser flowlines. [Provided by NTNU]

4.1.2. Experimental setup

The inner diameter of the flowline applied was 60 mm. The lab setup applied in this Master Thesis work was a combination of the S-riser- and the horizontal test sections. The S-riser nozzle, seen in figure 23 below, was connected to a plexi pipe connected to a flexible hose, creating a 1 meter downwards inclined flowline, with a 4 cm drop and with an angle of $2,3^\circ$. The hose was then horizontal for 0,5 meters before it was directed upwards, creating a dip, see figure 24 below. The hose was upwards inclined with an angle of $1,4^\circ$ for 4,6 meters,

before it was connected to a horizontal plexi pipeline after an 11 cm elevation.

The rest of the flowline was horizontal and connected to the existing 60 mm inner diameter pipeline on the horizontal test section after the last 180° turn. Finally the flowline ended in the air-liquid separator, seen in figure 22, after a total length of 57,84 meters. A schematic outline of the test flowline is shown in figure 25 below. It has to be taken into consideration when analyzing the results, that the behavior of the waves probably are affected by the two 180° turns. An image of the last 180° turn is shown in figure 26 below. The plexi pipe roughness is 0,05 mm; a slightly different pipe roughness must be expected to apply for the flexible hoses that were applied to make the turns.

The large air valve was applied to get sufficient high air flow rate to create stable, stratified flow through the entire pipeline. The large air flowmeter was applied for best possible measurements of relatively high air flow rates. The small centrifugal water pump was applied and the small water valve was applied for best possible regulation of the small water flow rates.



Figure 23: The S-riser nozzle was attached to a downwards inclined rail and connected to a short plexi pipe that was connected to a flexible hose. The construction created a one meter downwards inclined flowline, with a four cm drop. Then the flexible hose was approximately horizontal for 50 cm, before it was inclined upwards again to create the dip geometry outlined in figure 25.



Figure 24: Liquid accumulated in the bottom of the dip when the gas flow was choked.

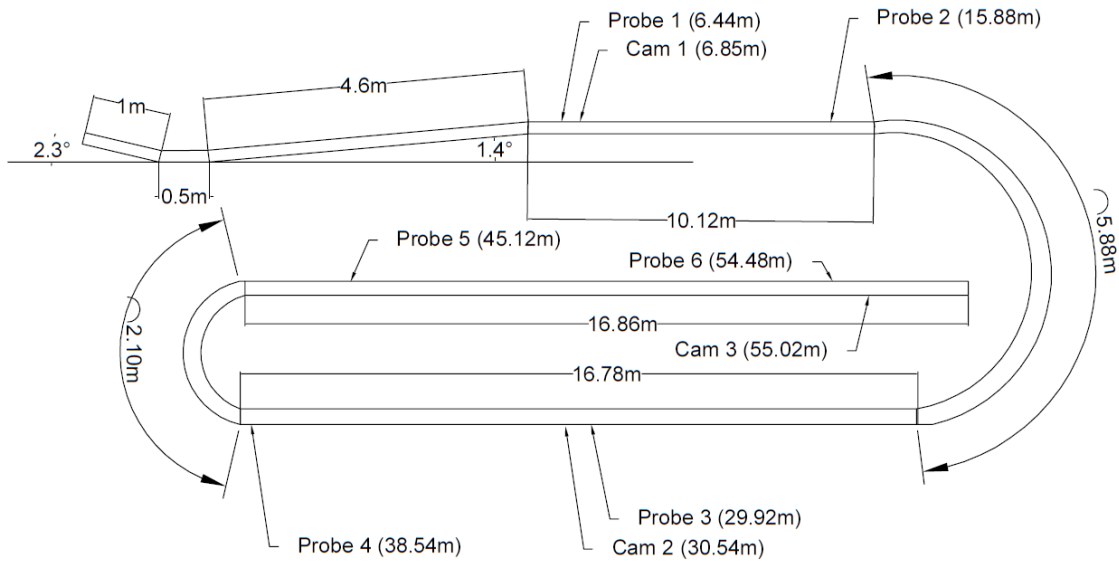


Figure 25: Schematic outline of the test geometry with a dip. The total length is 57,84 meters. The flowline after the dip is approximately horizontal. The drawing is not in scale.

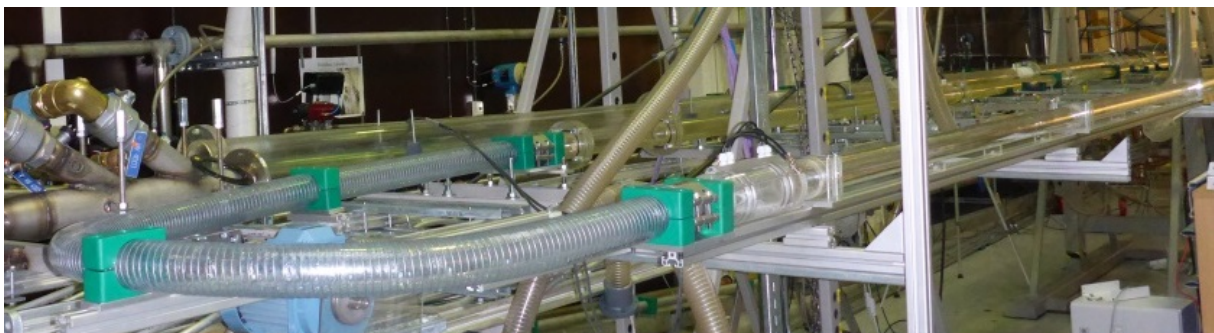


Figure 26: The last and narrowest turn on the flowline. It must be assumed that the two 180° turns on the flowline influenced the behavior of the waves.

Two flow regimes had to be avoided during the attempts to create surge waves; slug flow and roll waves. Slug flow is easily created in small systems with a dip at low gas flow rates. Total cross section liquid blockage and upstream pressure buildup leading to slug flow happens if

the gas flow rate is low. Slug flow was avoided by creating stratified flow at a high gas flow rate. Roll waves, with a steep, breaking front, occurred if the gas downtime was too long, creating a fierce, short wave with a sharp, breaking front.

4.1.3. Holdup measurement instrumentation, calibration and calculation

Six probes were placed out along the pipeline to measure the water volume fraction. The probes were positioned at 6,44 m, 15,88 m, 29,92 m, 38,54 m, 45,12 m and 54,02 m downstream the inlet nozzle. All the probes were positioned downstream the dip, see figure 25. The probes measure the conductance through the pipe cross section, and logs the values continuously.

The log files from the lab comes as large excel files and the conductance values have to be converted into holdup, to make Matlab plots of the waves. The instrumentation has to be calibrated before the experiments are carried out. The calibration was done by logging the conductance along the pipeline when the pipeline was completely filled with water and when it was completely dry, in order to obtain an average value for both completely filled pipeline, C_f , and completely dry pipeline, C_e . Then the desired experiments were conducted. Each individual conductance value, C , was then normalized into C_n by applying equation 1. The holdup, H , was then calculated by equation 2. Equation 2 is a regression polynomial that calculates the holdup within an error of $\pm 5\%$ [16].

$$C_n = \frac{C - C_e}{C_f - C_e} \quad (1)$$

$$H = -0.7509 * C_n^4 + 0.3204 * C_n^3 + 0.6645 * C_n^2 + 0.7626 * C_n \quad (2)$$

4.1.4. Curve smoothing

The surface of the stratified flow is not completely smooth as small waves are created in the gas-liquid interface when the liquid is dragged through the pipeline by the gas. The lab plots therefore contains a lot of short term fluctuations, so Matlab curve smoothing filters have to be applied on the lab plots to smooth out most of the short term fluctuations, in order to highlight the characteristic trend of the waves. The excel log of each prope has to be read by Matlab and Matlab creates a vector of the excel log. Then a moving average filter is applied on the vector, creating a smoother plot.

[17].

The results from the lab are presented with both raw and smooth holdup plots in Appendix A. Three examples of moving average curve smoothing are shown in figure 27 below. The plot in the upper left corner in the figure shows the raw holdup plot of a wave. The plot in the upper right corner shows the wave smoothed with the moving average function $yy = \text{smooth}(y,0.005, 'moving')$. This wave still has some noise, but it is showing a clear trend. The lower left corner shows the function $yy = \text{smooth}(y,0.01, 'moving')$. Here almost all of the noise is removed from the plot, but the high values are kept fairly good. This function has been applied to show the trend of all the lab results presented in Appendix A. The lower right corner shows the function $yy = \text{smooth}(y,0.05, 'moving')$ applied on the wave. Here all the noise is removed, showing only the large term trend. This function has a very large impact on the plot, smearing out the wave peak in such a way that the peak value read out from the plot is obviously cut lower than than the actual value. This function is therefore unsuitable to use because the peak value of the wave is important to know when the lab results are being compared against the simulation results. The curve smoothing might be an error source when reading the maximum wave peak amplitude out of the plots, as the maximum amplitude might be cut too much because of the curve smoothing.

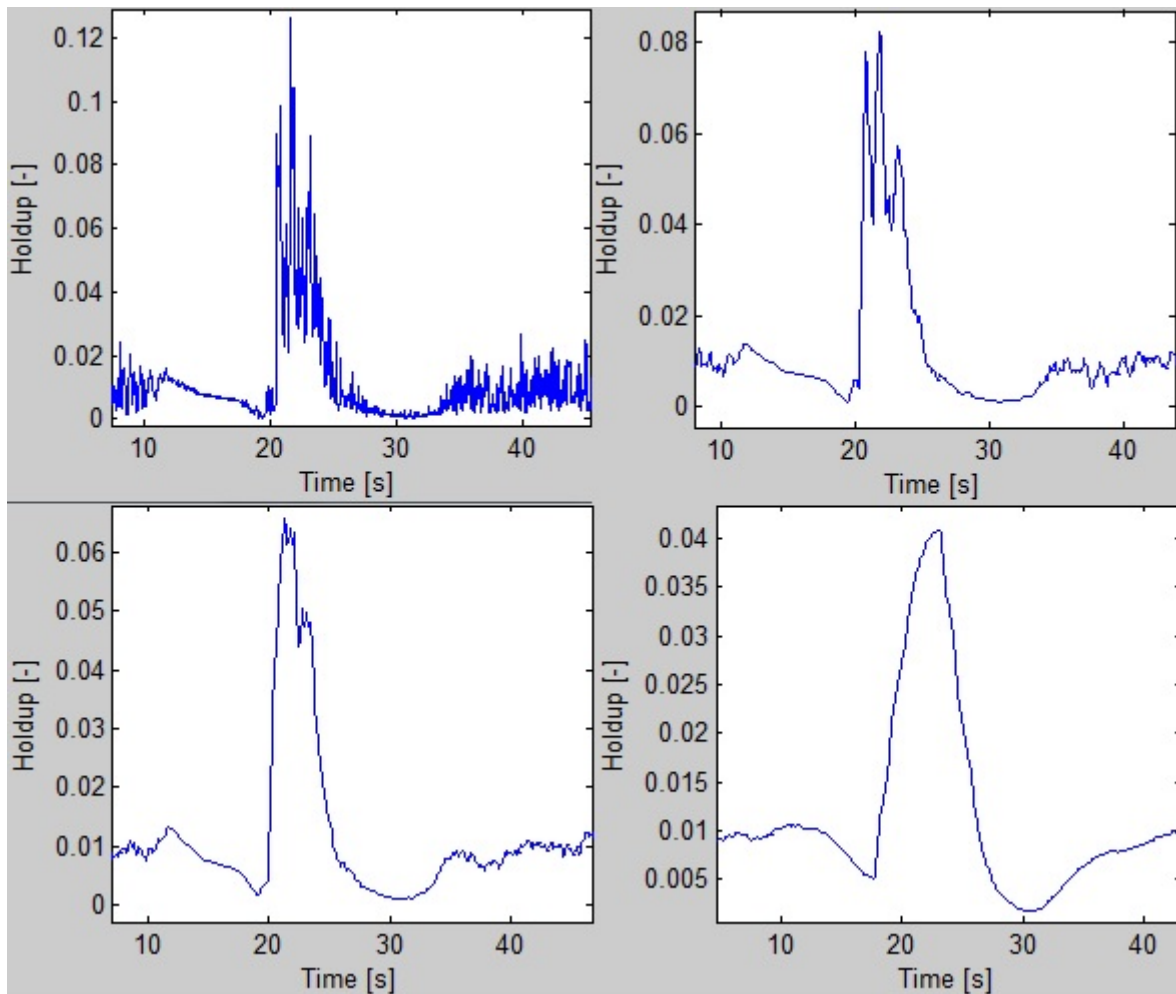


Figure 27: Curve smoothing impact on a wave. Raw holdup plot in the upper left corner. The moving average function $yy = \text{smooth}(y, 0.005, 'moving')$ applied in the upper right corner. The moving average function $yy = \text{smooth}(y, 0.01, 'moving')$ applied in the lower left corner. This is the function that is applied on the waves presented in Appendix A, containing the lab results. The moving average function $yy = \text{smooth}(y, 0.05, 'moving')$ applied in the lower right corner.

4.1.5. Wave velocity calculation

The wave velocities have been calculated as the average velocity for a wave moving from one probe to the next probe. It was not possible to configure the lab instrumentation in a way that would enable the calculation of instantaneous velocity at each of the measurement probes. Only six channels were intact on the box that receives the signals from the probes, hence the cables to all the six channels had to be distributed to the six probes shown in figure 25 in order to measure the wave shape along the entire pipeline. An approximate instantaneous wave velocity could have been calculated for each probe if 12 channels had been available, configuring each probe with two measurement spots and calculate the average wave velocity

between the two spots on each probe.

4.1.6. Camera recording

Three cameras were positioned along the pipeline, at 6,85 m, 30,54 m and 55,02 m downstream the inlet nozzle, to record the waves at each of the long sides of the flowline, see figure 25. Screenshots from the camera records of each waves are presented in Appendix B.

4.2. Performed experiments, result analysis and discussion

4.2.1. Performed experiments

Eight lab cases have been analyzed. An overview over the flow rates in the different cases are presented in the test matrix in table 1 below. Four different initial gas flow rates were applied on two different, constant water flow rates. All the experiments have been performed in the same, fixed pipeline geometry.

Table 1: Test matrix

Case:	Initial air flow rate		Initial air valve opening [% of full opening]	Water flow rate	
	U_{sg} [m/s]	\dot{m} [kg/s]		U_{sl} [m/s]	\dot{m} [kg/s]
1	13,4	0,045	27	0,0113	0,032
2	10,9	0,037	25	0,0113	0,032
3	8,5	0,029	23	0,0113	0,032
4	7,6	0,026	22	0,0113	0,032
5	13,4	0,045	27	0,0264	0,075
6	10,9	0,037	25	0,0264	0,075
7	8,5	0,029	23	0,0264	0,075
8	7,4	0,025	22	0,0264	0,075

Only two-phase air-water experiments have been performed. Three-phase experiments have not been conducted during this project. The laboratory was not equipped with instrumentation to measure the holdup properly for flows containing both water and oil. Oil with fluid properties suitable for surge wave experiments was not available. The oil tank was filled with a highly viscous NEXBASE oil which is considered to be unsuitable for surge wave experiments, oil with properties more like condensate is considered to be more suitable to apply for surge wave experiments. The Exxol oil applied in the IFE experiments would be preferable.

4.2.2. Test procedure

The following test procedure was applied to initiate surge waves:

1. The test section geometry was set up.
2. Steady state stratified flow was established through the entire pipeline, with fixed air- and water flow rates.
3. The data logger and cameras were turned on.
4. The air valve was choked down to 17 percent of total opening, $U_{sg} = 3,9$ m/s ($\dot{m} = 0,013$ kg/s), and ramped up to its initial value after 10 seconds.
5. The water volume accumulated in the dip, during the choking of the air flow, was expelled through the pipeline in a surge wave and steady state stratified flow was reestablished through the entire pipeline.

4.2.3. Lab result analysis and discussion

Raw and smoothed holdup trend plots and inlet gas flow rate plots of all the eight analyzed cases are presented in Appendix A. Screenshots of each wave at the three different cameras are presented in Appendix B. The analysis of the observed waves is limited to analysis of the wave shape change and change in wave peak amplitude in the smoothed holdup plots and change in velocity compared to change in U_{sg} and U_{sl} . Other factors such as changes in pressure and rate of liquid accumulation in the dip have not been analyzed in this project.

The results shows that it is possible to initiate relatively long waves with a relatively low holdup and a smooth wave front that moves through the entire pipe length, with changes in the air flow rate in the applied lab setup geometry. Figure 28 below shows what the wave initiated in case 2 with $U_{sg} = 10,9$ m/s and $U_{sl} = 0,0113$ m/s looks like at the passing of camera 1. The wave has the same shape as the surge wave outlined in figure 1, it does not look anything like the roll wave seen in figure 4. Figure 29 below, shows how the wave develops through the pipeline. The wave peak amplitude is falling rapidly between probe 1 and 3, where further amplitude reduction stops, or slows down dramatically. The reason for slightly lower amplitude at probe 3 than at the following probes is likely that the test pipeline might not have been completely horizontal. The wave is, systematically in all eight cases, getting longer and longer at the passing of each probe, the wave length is doubled between probe 1 and 6, seen in all the holdup trend plot figures in Appendix A. This means that the peak amplitude eventually will get reduced slowly as the wavelength increases. However, the reduction of holdup appears to stop, the increase in wavelength slows down and it can be assumed that this wave would be able to travel a very long distance in a much longer pipeline before it eventually would get smeared out completely. It is a question whether a steady state condition is about to be reached as the change in shape slows down the further the wave propagates, this can not be concluded based on the present results. If an almost steady state condition could be achieved in a longer pipeline, the waves will be able to travel over a very long distance, very alike field observed surge waves.

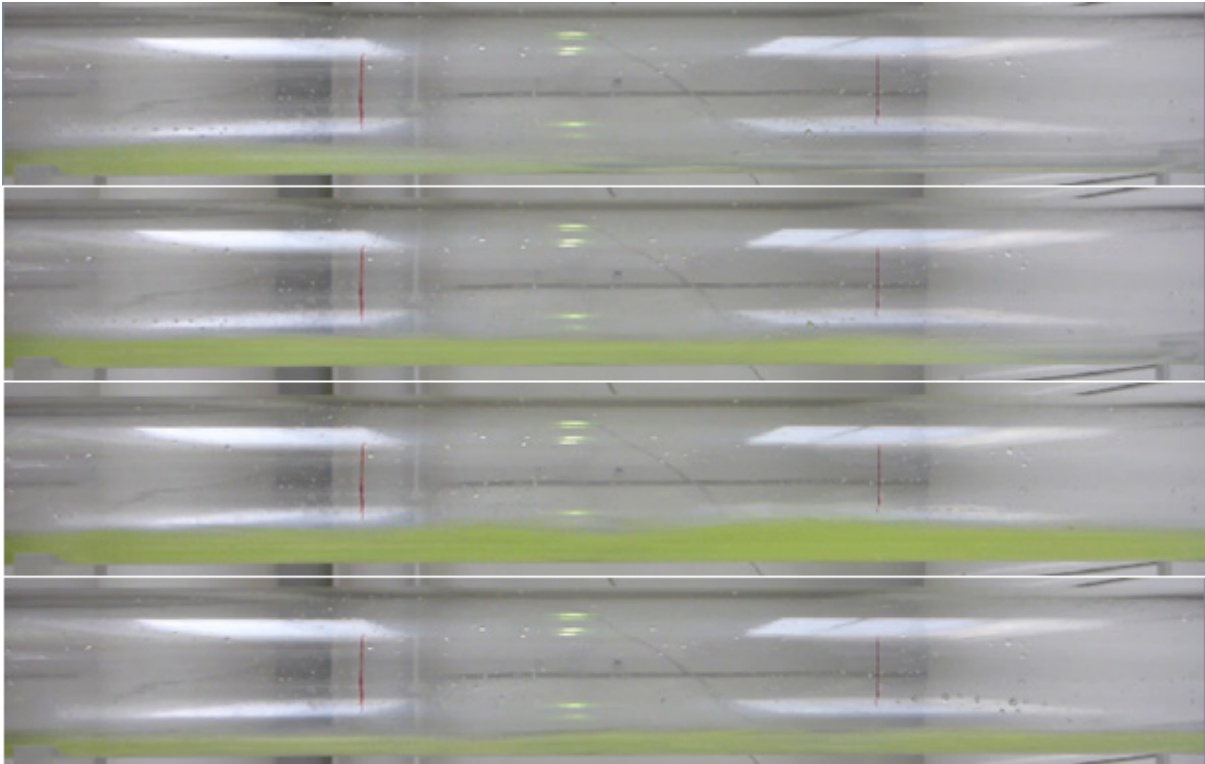


Figure 28: Screenshots of the wave in case 2 at cam 1. The passing of the wave front is seen in the two images at the top and the passing of the wave peak in the second lowest image. The lowest image shows that steady state stratified flow is reestablished after the wave has passed.

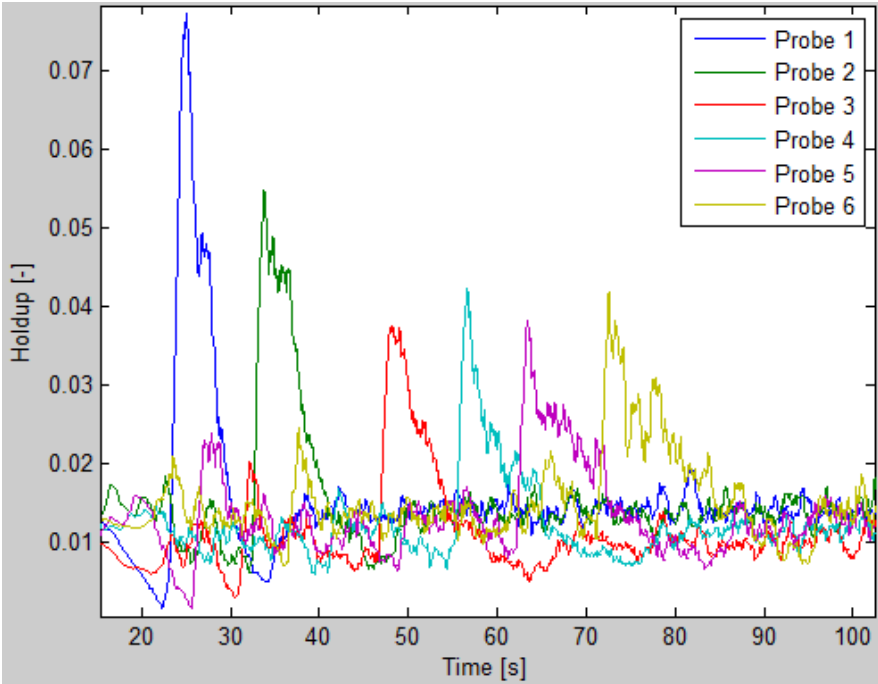


Figure 29: Holdup trend plot of the wave observed in case 2. $U_{sg} = 10,9$ m/s, $U_{sl} = 0,0113$ m/s.

Figure 30 below, shows the holdup trend plot of wave initiated in case 4 with $U_{sg} = 7,6$ m/s and $U_{sl} = 0,0113$ m/s. The wave has initially a much higher peak amplitude than in the wave seen in figure 29. The holdup falls dramatically from probe 1 to 3. The wave almost seemed to “died out” when observed in the lab, but the plot shows that the wave still can be observed at probe 6, just before the pipeline outlet. The wave shape at probe 3 is almost alike the shape at probe 6, and the wave does not seem to be smeared out much from probe 3 to 6. The wave is therefore expected to be able to propagate over an even longer distance than the test pipeline. As the wave holdup and the steady state holdup before and after the wave is systematically lower at probe 3 than at the other probes, it seems that there is a small slope in the pipeline past probe 3, causing a lower holdup at probe 3 than at the rest of the pipeline which also is observed in figure 29.

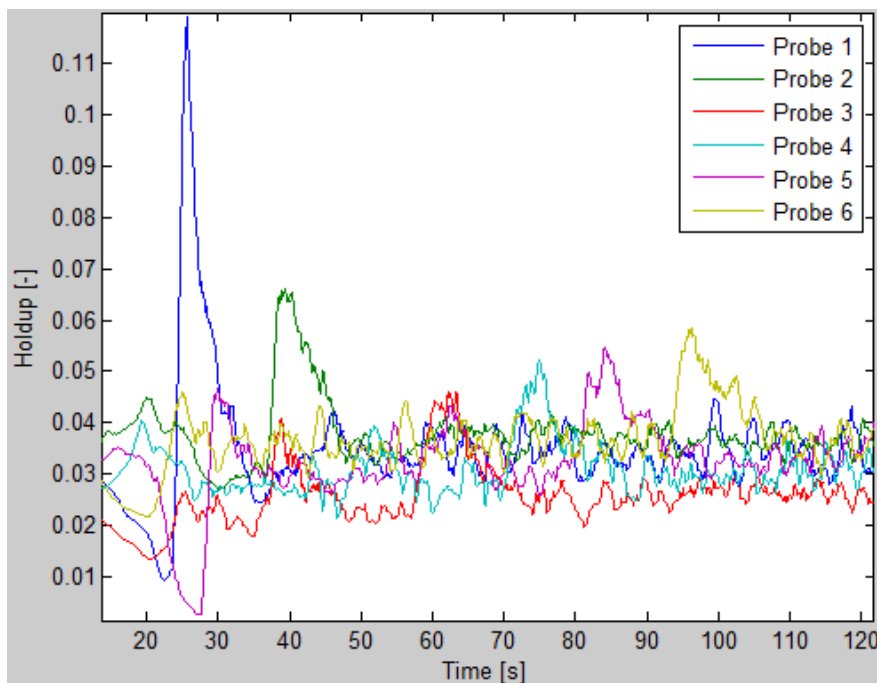


Figure 30: Holdup trend plot of the wave propagation observed in case 4, $U_{sg} = 7,6$ m/s, $U_{sl} = 0,0113$ m/s.

Figure 31 below, shows profile plots of the wave peak holdup from probe 1 to 6 for all the eight analyzed cases. The trend is clear; the wave peak amplitude increases with increasing U_{sl} and decreasing U_{sg} . The fall in wave peak amplitude from probe 1 – 3 is larger the lower U_{sg} that is applied. The fall in peak amplitude seems to stop after probe 3 for nearly all the cases, indicating that the pipeline has not been completely horizontal. For most of the waves

the holdup actually grows slightly after probe 3. This indicates that the waves are capable of propagating over an even longer distance than the test pipeline.

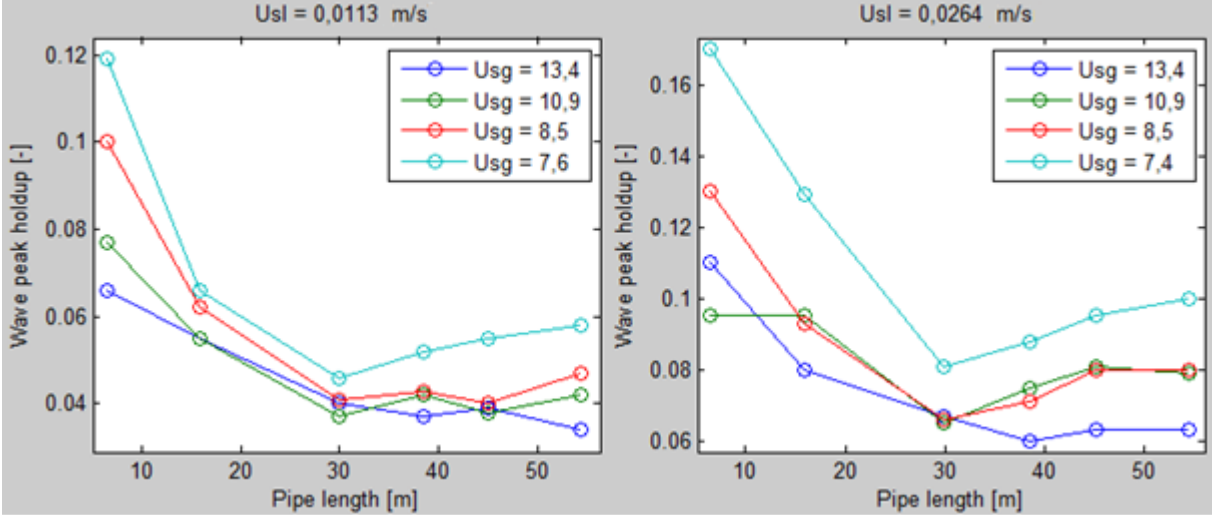


Figure 31: The wave peak holdup along the pipeline for all the 8 analyzed cases.

Figure 32 below, shows plots of the velocities of the waves. The velocity clearly increases with increasing U_{sg} and increasing U_{sl} . The velocity falls slightly along the flowline for the highest U_{sl} values, seen in the right of the figure. This trend is not clear for the highest U_{sg} values and the lowest U_{sl} values, seen in the left in the figure. The start and end velocity does not change for $U_{sg} = 10,9$ m/s and $U_{sl} = 0,0113$ m/s. The velocity increases slightly towards the end of the pipeline for $U_{sg} = 13,4$ m/s and $U_{sl} = 0,0113$ m/s. There are fluctuations in the velocity along the pipeline for $U_{sg} = 13,4$ m/s. This might be explained by that the highest velocities being more influenced by the change in direction and pipeline roughness in the flexible hoses in the turns than the lower velocities, causing fluctuations in the wave propagation velocity.

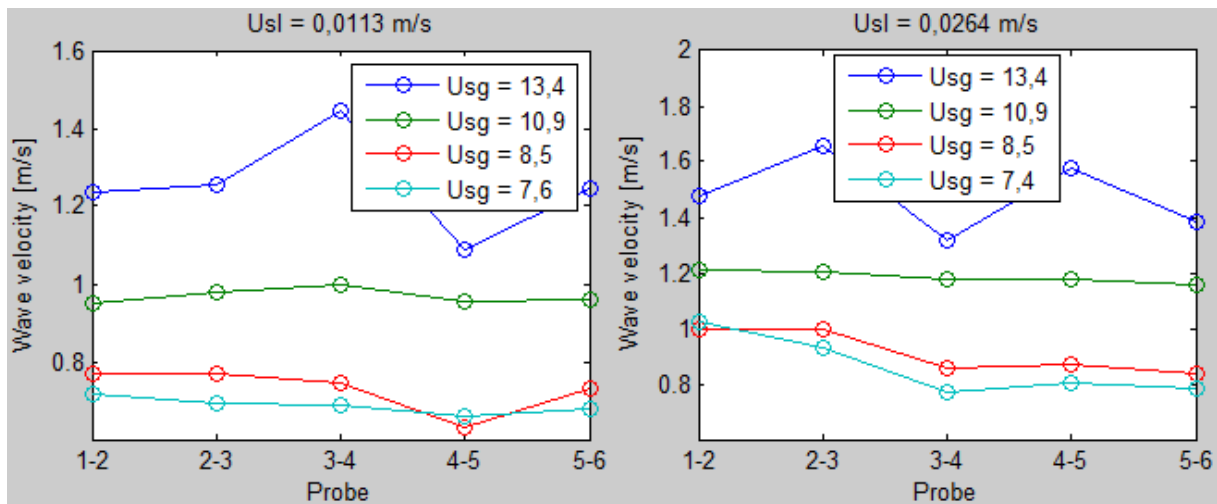


Figure 32: The wave propagation velocity between the probes along the pipeline for all the 8 analyzed cases.

Most of the waves observed in the project work were split in two parts when measured at 5,3 meters downstream the dip, growing into a single wave before they reached the next probe at 11,8 meters downstream the dip, see figure 20. This effect was not observed for any of the waves in these Master Thesis experiments, as most of the waves came in one peak. The waves that differs are the waves with $U_{sl} = 0,0264$ m/s in case 7 with $U_{sg} = 8,5$ m/s and 8 with $U_{sg} = 7,4$ m/s. The wave in case 7 is characterized by two sequencing peaks during the entire propagation through the pipeline, almost growing into one peak right before the outlet of the pipeline. The wave in case 8 is characterized by a second and smaller sequencing wave following after 15 seconds at probe 1 and 25 seconds at probe 6. This is seen in figure 33 below. The explanation for this effect might be that some of the liquid gets carried away immediately when the gas flow ramp up starts, and that the rest of the liquid follows right after when the gas flow is ramped up completely. This effect seems to apply when a relatively small gas flow has to drag a relatively large water flow through the pipeline. This might also be related to the mechanism creating surge waves on fields at tail-end production, where the gas flow rate is too small to avoid liquid accumulation in low spots, resulting in surge waves when a large liquid volume has accumulated.

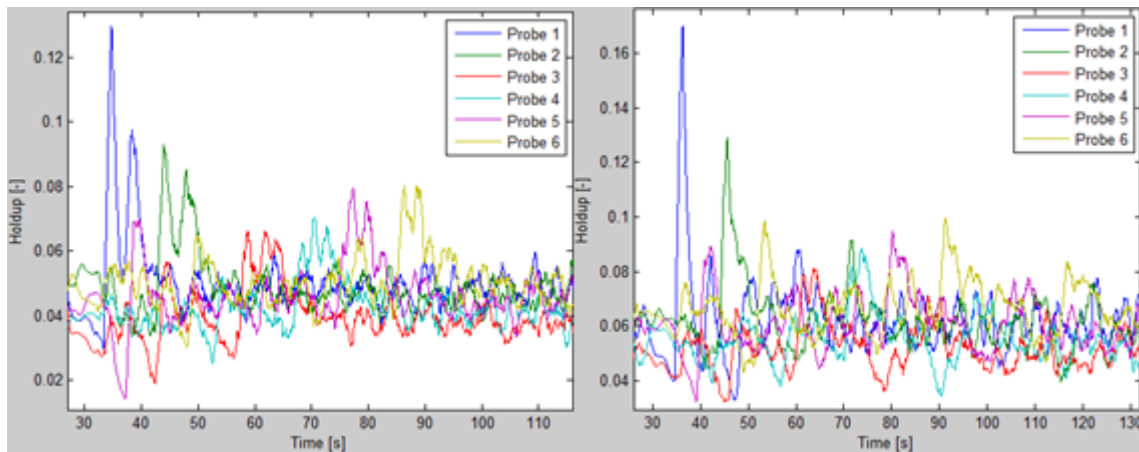


Figure 33: Holdup trend plot of the wave propagation observed in case 7, $U_{sg} = 8,5$ m/s, $U_{sl} = 0,0264$ m/s to the left and case 8, $U_{sg} = 7,4$ m/s, $U_{sl} = 0,0264$ m/s to the right. The wave in case 7 is characterized by two, sequencing peaks. The wave in case 8 is characterized by a second and smaller wave following after 15 seconds at probe 1 and 25 seconds at probe 6.

The waves in the project work were shorter, with a duration around a couple of seconds and they had a higher peak holdup amplitude, up to 30 %, than the waves in the Master Thesis. The wave peak amplitude at probe 1 on the waves observed in this Master Thesis work varied between 17 and 6,6 %, see figure 31. The wave duration was around 7 – 9 seconds at probe 1 and up to around 20 seconds at probe 6, seen in the figures 29, 30 and 33. Hence, much longer waves than observed in the pre-project have been observed in this Master Thesis project. If the case is that the duration of the waves increases linearly with the pipelength, it can be assumed that waves equivalent to real surge waves have been observed and that the duration would be even longer in a longer pipeline.

The observed waves shows several similarities with the surge waves observed in the field; Low holdup, relatively long duration, and they are initiated by a change in flow rates in a gas dominated flow. The question is therefore whether or not proper surge waves have been successfully reproduced. The answer is probably both yes and no. The waves observed in the lab are probably the most surge wave like waves that are possible to initialize in a two-phase air-water flow in the low pressure system in the multiphase flow loop at NTNU with the current pipeline geometry. However, surge waves creating severe flow assurance challenges in the field all occur in three-phase, representing much more complex fluid mechanics than the two-phase surge waves observed in the lab. Field observed surge waves can arrive in a condensate surge, followed by a water/MEG surge. It would be interesting to see if such a situation is possible to create in the lab at NTNU. Field observed surge waves has a very

much longer duration than the waves observed in the lab. This is probably due to the much larger liquid accumulation potential in a very long and wider pipeline. The system pressure and the gas density are also factors that definitely influences the surge waves, and those factors are very different in a field pipeline with high pressure and much more dense gas than the approximately atmospheric conditions in the lab.

One question is if it is possible to accumulate large enough amounts of liquid in the test pipeline to generate very long surge waves and avoid transition into slug flow at the same time, with air as gas phase. It is not obvious whether that is possible or not in the small low pressure system at the lab. There is a large compressibility potential upstream the low liquid accumulation point when low pressure air is used as test fluid, which easily results in full pipe cross section liquid blockage, leading to slug flow. Another question is whether a prezzurized and more dense gas phase, like the SF₆ applied at IFE, would allow larger liquid volumes to accumulate in the dip, without leading to full cross section blockage and following transition into slug flow. If a larger liquid volume was allowed to accumulate it would probably lead to an even longer surge wave.

5. Computational simulation

All the eight cases from the lab, presented in the test matrix in table 1, have been attempted simulated in the simulation programs OLGA and LedaFlow, in order to determine the capability of the simulation programs to reproduce the lab observations.

5.1. Simulation programs

5.1.1. OLGA

OLGA has been developed since 1979, in order to simulate multiphase transport of oil, gas and water. The motivation behind the development of the multiphase transport technology is much better field economy than traditional offshore oil-gas-water separation and single phase transport [18]. The development of the multiphase transport technology is considered to be the most important Norwegian invention since 1980 [19].

The physical model applied in OLGA is called a three-fluid model. The three-fluid model applies three separate continuity equations, for the gas-, water- and oil/condensate phase respectively. Mass can also be transferred between the phases, interphasial mass transfer. The model operates with three separate momentum equations, one for each of the the continuous water- and oil/condensate fields, and a mixture momentum equation for gas and liquid droplets. The velocity of the liquid droplets in the gas field is calculated by a slip relation. A single mixture energy equation is applied for the entire multiphase mixture, hence all phases are assumed to be at the same temperature. Consequently, seven conservation equations are solved; three for mass, three for momentum and one for energy, one equation is solved for pressure. [20, pp. 3-4] The general formulation of the equations is seen in the equations 3 – 9 below: [21, pp. 1-3]

Mass conservation equations:

For the gas phase:

$$\frac{\partial}{\partial t}(V_g \rho_g) = -\frac{1}{A} \frac{\partial}{\partial z}(AV_g \rho_g v_g) + \psi_g + G_g \quad (3)$$

For the liquid at the wall:

$$\frac{\partial}{\partial t}(V_L \rho_L) = -\frac{1}{A} \frac{\partial}{\partial z}(AV_L \rho_L v_L) - \psi_g \frac{V_L}{V_L + V_D} - \psi_e + \psi_d + G_L \quad (4)$$

For liquid droplets:

$$\frac{\partial}{\partial t}(V_D \rho_L) = -\frac{1}{A} \frac{\partial}{\partial z}(AV_D \rho_L v_D) - \psi_g \frac{V_D}{V_L + V_D} - \psi_e + \psi_d + G_D \quad (5)$$

Where:

- V_g, V_L, V_D = gas, liquid film and liquid droplet volume fraction
- ρ = density
- v = velocity
- p = pressure
- A = pipe cross section area
- ψ_e, ψ_d = entrainment deposition rates
- G_f = possible mass source of phase f. f = g (gas), L (liquid), i (interface), D (droplets)

Momentum conservation equations:

Combined momentum equation for gas and liquid droplets:

$$\begin{aligned} \frac{\partial}{\partial t}(V_g \rho_g v_g + V_D \rho_L v_D) &= -(V_g + V_D) \left(\frac{\partial p}{\partial z} \right) - \frac{1}{A} \frac{\partial}{\partial z} (A V_g \rho_g v_g^2 + A V_D \rho_L v_D^2) \\ -\lambda_g \frac{1}{2} \rho_g |v_g| v_g \frac{S_g}{4A} - \lambda_i \frac{1}{2} \rho_g |v_r| v_r \frac{S_i}{4A} + (V_g \rho_g + V_D \rho_L) g \cos \alpha & \\ + \psi_g \frac{V_L}{V_L + V_D} v_a + \psi_e v_i - \psi_d v_D & \end{aligned} \quad (6)$$

For the continuous liquid phases:

$$\begin{aligned} \frac{\partial}{\partial t}(V_L \rho_L v_L) &= -V_L \left(\frac{\partial p}{\partial z} \right) - \frac{1}{A} \frac{\partial}{\partial z} (A V_L \rho_L v_L^2) - \lambda_L \frac{1}{2} \rho_L |v_L| v_L \frac{S_L}{4A} \\ + \lambda_i \frac{1}{2} \rho_g |v_r| v_r \frac{S_i}{4A} + V_L \rho_L g \cos \alpha - \psi_g \frac{V_L}{V_L + V_D} v_a - \psi_e v_i + \psi_d v_D & \\ -V_L d(\rho_L - \rho_g) g \frac{\partial V_L}{\partial z} \sin \alpha & \end{aligned} \quad (7)$$

Where:

- A = pipe inclination angle
- S_g, S_L, S_i = wetted perimeters of the gas, liquid and interface
- G_f = internal source, assumed to enter at a 90 degree angle to the pipe wall and not carry net momentum

Mixture energy conservation equation:

$$\begin{aligned} \frac{\partial}{\partial t} \left[m_g \left(E_g + \frac{1}{2} v_g^2 + gh \right) + m_L \left(E_L + \frac{1}{2} v_L^2 + gh \right) + m_D \left(E_D + \frac{1}{2} v_D^2 + gh \right) \right] &= \\ - \frac{\partial}{\partial z} \left[m_g v_g \left(H_g + \frac{1}{2} v_g^2 + gh \right) + m_L v_L \left(H_L + \frac{1}{2} v_L^2 + gh \right) + m_D v_D \left(H_D + \frac{1}{2} v_D^2 + gh \right) \right] + H_s + U & \end{aligned} \quad (8)$$

Where:

- E = internal energy per unit mass
- h = elevation
- H_S = enthalpy from mass sources
- U = heat transfer from pipe walls

Pressure equation:

$$\begin{aligned}
 & \left[\frac{V_g}{\rho_g} \left(\frac{\partial \rho_g}{\partial p} \right)_{T,R_S} + \frac{1-V_g}{\rho_L} \left(\frac{\partial \rho_L}{\partial p} \right)_{T,R_S} \right] \frac{\partial p}{\partial t} = - \frac{1}{A \rho_g} \frac{\partial (A V_g \rho_g v_g)}{\partial z} \\
 & - \frac{1}{A \rho_L} \frac{\partial (A V_L \rho_L v_L)}{\partial z} - \frac{1}{A \rho_L} \frac{\partial (A V_D \rho_L v_D)}{\partial z} + \psi_g \left(\frac{1}{\rho_g} - \frac{1}{\rho_L} \right) \\
 & + G_g \frac{1}{\rho_g} + G_L \frac{1}{\rho_L} + G_D \frac{1}{\rho_L}
 \end{aligned} \tag{9}$$

Closure models

A set of empirical closure models are provided to solve the conservation equations. For separated gas-liquid flow, closure laws for wall friction, interphasial friction, droplet entrainment/deposition, gas bubbles in liquid film and liquid/liquid dispersion must be provided. [22, p. 9]

5.1.2. LedaFlow

LedaFlow is a transient multiphase flow simulation program developed since 2001. LedaFlow was developed to improve the accuracy and increase the detail of information in multiphase flow simulations. This was done in order to overcome the challenges the industry was going to meet during new field developments in deeper, harsher, more remote and longer tie-backs than previous projects [23]. OLGA was only a 1D simulator; the goal was therefore to develop a full 3D simulator. As 3D simulations are extremely time consuming and computer power demanding, a quasi 3D simulator was developed. The LedaFlow Q3 is basically a 2D

model with 3D effects. [24, p. 9] The LedaFlow simulations done in this Master Thesis have only been carried out in the LedaFlow 1D model.

LedaFlow 1D is a mechanistic [25, p. 1] three-fluid-nine-field model. It consists of three continuous phases of gas, water and oil, and all the phases can be mixed into each other in the form of droplets and bubbles, creating totally nine different fields. See figure 34 below.

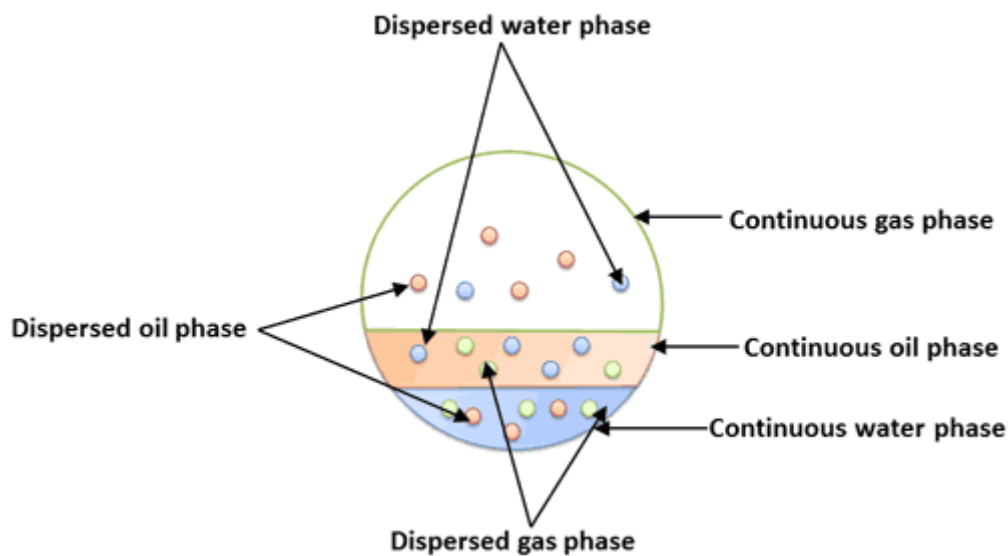


Figure 34: The LedaFlow nine field approach. [26]

All together 15 conservation equations are solved in the LedaFlow three-phase model. Three momentum and three energy equations are solved, one for each of the continuous phases. And nine mass equations, one for each of the nine fields. [27, p. 1] The general formulation of the conservation equations applied in LedaFlow is seen in equations 10 – 12 below: [25, p. 3]

Mass conservation equations:

$$\frac{\partial \alpha_k \rho_k}{\partial t} + \frac{\partial}{\partial x} (\alpha_k \rho_k u_k) = \sum_{i \neq k} \Gamma_{ki} + \Gamma_{kext} \quad (10)$$

Momentum conservation equations:

$$\begin{aligned} \frac{\partial}{\partial t}(\alpha_k \rho_k u_k) + \frac{\partial}{\partial x}(\alpha_k \rho_k u_k u_k) = & -\frac{\partial \alpha_k P_k}{\partial x} - \alpha_k \rho_k g \sin \theta + \frac{\partial \alpha_k \tau_k}{\partial x} \\ + P_{\text{int}} \frac{\partial \alpha_k}{\partial x} + \sum_{i \neq k} F_{ki} - F_{kw} + \sum_{i \neq k} \Gamma_{ki} u_{ki} + \Gamma_{k\text{ext}} u_{k\text{ext}} \end{aligned} \quad (11)$$

Energy conservation equations:

$$\frac{\partial}{\partial t}(\alpha_k \rho_k h_k) + \frac{\partial}{\partial x}(\alpha_k \rho_k u_k h_k) = \frac{\partial}{\partial x}(\alpha_k \kappa_k \frac{\partial T}{\partial x}) + \alpha_k \frac{DP}{Dt} + Q_{kw} + \sum_{i \neq k} Q_{ki} + \Gamma_{k\text{ext}} h_{k\text{ext}} \quad (12)$$

Where:

- k = field index
- u = average field velocity
- t = time
- x = coordinate along the pipe
- α = field volume fraction
- ρ = field density
- $\Gamma_{k\text{ext}}$ = net external mass source (system mass extraction and injection)
- Γ_{ki} = net mass flow rate obtained by field k from field i
- τ_k = shear stress of field k in axial direction
- P_k = field pressure
- P_{int} = pressure at large scale interface (only for stratified flow)
- g = gravity
- θ = pipe inclination angle
- F_{ki} = interfacial friction between field k and other fields
- F_{kw} = wall friction
- $u_{k\text{ext}}$ = velocity of external mass source
- h_k = enthalpy of field k
- κ_k = effective thermal conductivity of field k
- T_k = temperature of field k

- P = system pressure (average pressure $P = \sum \alpha_k P_k$)
- Q_{ki} = interfacial heat transfer rate of field k with other fields
- Q_{kw} = heat transfer rate of field k at pipe wall
- $h_{k\text{ext}}$ = enthalpy of external mass source

Closure models

A set of physical models, closure models, are required to solve the conservation equations. The closure models describes the mass, momentum and energy exchange between the different fields and between a field and the pipe wall. Closure models are required for [25, p. 4]:

- Flow geometry; in order to identify different flow regimes.
- Interphasial mass transfer; to describe droplets of liquids and bubbles of gas that are transferred between the continuous phases and interphasial mass transfer because of phase change.
- Momentum exchanges; wall friction, interphasial friction and momentum exchange because of mass transfer.
- Energy exchange; heat transfer between the fluids and the wall and between the different phases and relationship between temperatures and enthalpy.

Slug capturing

LedaFlow offers a special feature for the simulation of hydrodynamic slug flow called slug capturing. Slug capturing is a more detailed way of simulating hydrodynamic slug flow than the use of the unit cell model. While the unit cell model is good for predicting average holdups and pressure fall in a pipeline with a coarse mesh, it does not contain information about individual slugs and is therefore not very good for simulating the interaction between hydrodynamic slug flow and terrain induced slugs. The slug capturing mode requires a fixed, fine mesh; the size of the cells have to be shorter than the length of a slug in order to calculate the formation of a slug. The solution is exposed to numerical diffusion and higher order discretization in time and space is applied to avoid the slugs to be smeared out due to numerical diffusion. [27, pp. 1-2]

5.2. OLGA simulation setup

The simulations have been performed in OLGA 7.1.

5.2.1. Simulation setup and boundary conditions

A basic OLGA case was started and the pipeline geometry was configured with the dimensions shown in table 2 below. Two mass sources, one for air and one for water, were set on section one on pipe one.

Table 2: The OLGA setup geometry.

Pipe	x [m]	y [m]	Length [m]	Elevation [m]	Diameter [m]
Start Point	0	0			
PIPE-1	0,9992	-0,04	1	-0,04	0,06
PIPE-2	1,4992	-0,04	0,5	0	0,06
PIPE-3	6,09788	0,07	4,6	0,11	0,06
PIPE-4	57,8379	0,07	51,74	0	0,06

The following assumptions and boundary conditions were applied:

- Aadiabatic model without any temperature calculations.
- All temperatures were set to 20° C.
- Outlet node prezzure boundary set to 1 atm.
- A straight pipeline without any turns was assumed.
- A constant pipeline roughness of 0,05 mm was assumed for the entire pipeline.
- An air-water PVT-file obtained from Ivar Brandt, a multiphase flow expert in Schlumberger was applied [28].
- Max dt = 1 sec.

- Min dt = 0,00001 sec.
- Slugvoid Sintef.
- 1 st. order mass equation discretization.

The OLGA simulations initially stabilized at a slightly higher steady state holdup after the waves than before the waves. This is shown in figure 35 below. To avoid this effect, OLGA was run twice on each simulation of the lab waves: First, a simulation with the built in steady-state-pre-processor, and then an additional simulation with a restart file based on the results from the first simulation. The result was then equal steady state holdup before and after the waves passed, seen in all the holdup plots of the OLGA solutions presented in Appendix A.

5.2.2. Mesh

It is necessary to run the same case with different meshes in order to detect how fine mesh that is required to apply on the pipeline to get the numerical solution to converge, and eliminate numerical diffusion. A too fine mesh can potentially result in instabilities or cause the simulation to crash. The flow rates applied to initiate the test wave are presented in table 3 below. The test wave is an attempt of simulating the wave in case 2 presented in the test matrix in table 1.

Table 3: The flow rates applied to initiate the wave seen in figure 35. The air flow is choked after 10 seconds.

Time [s]	Air flow rate [kg/s]	Water flow rate [kg/s]
0	0,037	0,032
10	0,037	0,032
11	0,013	0,032
22	0,013	0,032
23	0,037	0,032

Six different cases were run with meshes from 0,25 – 10 pipe inner diameters ($\Delta x = 0,25D - 10D$). Figure 35 below shows the plot of a wave at probe 1, 3 and 6 with $\Delta x = 0,25D$ at the top, 1D in the middle and 10D at the bottom. The effect of numerical diffusion on the coarsest mesh is obvious when compared to the finer meshes, hence the solution is not reached at $\Delta x = 10D$. The difference in peak amplitude is not very large for probe 1 for the case with $\Delta x = 1D$ compared to $\Delta x = 0,25D$. The difference in amplitude is slightly larger for probe 3 and 6. The wave front is clearly sharper for probe 3 and 6 at $\Delta x = 0,25D$ compared to $\Delta x = 1D$. This means that numerical diffusion is decreased from $\Delta x = 1D$ to $0,25D$.

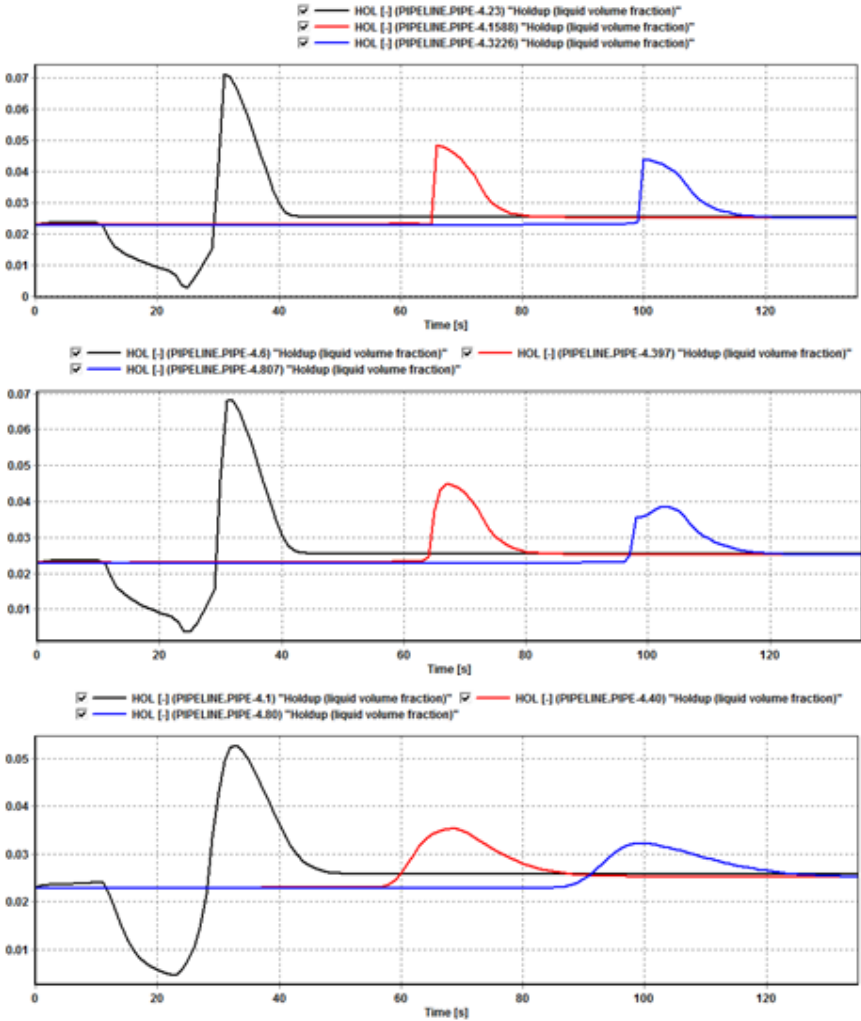


Figure 35: The influence of different meshes on a wave. $\Delta x = 0,25$ pipe inner diameters in the plot at the top, $\Delta x = 1$ in the middle and $\Delta x = 10$ at the lowest plot.

The image to the left in figure 36 below shows the peak holdup at the three probes for the six different cases run. The curve for probe 1 is starting to flatten out after $\Delta x = 2D$, indicating that a convergent solution is approaching. The curve for probe 3 is starting to flatten out after $\Delta x = 1D$, but from $0,5 - 0,25D$ it is rising again. The curve from probe 6 continues to grow linearly the finer the mesh gets. This means that the wave is more exposed to numerical diffusion the further down the pipeline it moves. This is as expected because the equations have been solved very many times between the propagation from probe 1 to probe 6 and earlier numerical error will influence the wave further down the pipeline. This means that the numerical diffusion is continuously eliminated the finer the applied mesh is, as additional instabilities or simulation crash did not appear in the simulations with $\Delta x = 0,25D$. The image to the right shows the wave velocity for the same cases. The curves do not flatten completely out and numerical diffusion is removed the finer the applied mesh is, but the growth in all the curves is slowing down when the mesh gets finer than $\Delta x = 2D$.

As the simulations for $\Delta x < 1$ are very time consuming, they lasts for up to 1,5 hours, and the curve flattens out after $\Delta x = 1D$ for probe 1 and flattens slightly out for probe 3, it was decided together with the supervisor that all the eight cases from the lab were going to be run in OLGA with a $\Delta x = 1D$ mesh.

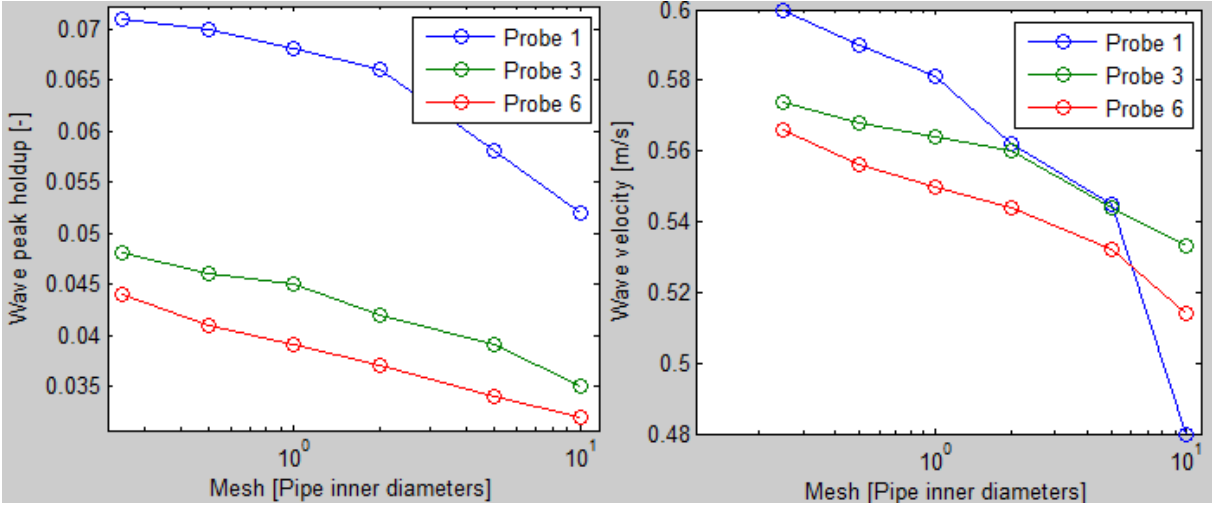


Figure 36: Wave peak holdup and velocity at $\Delta x = 0,25D - 10D$

5.2.3. Mass equation discretization

The wave seen in figure 35 has also been simulated with second order mass equation discretization at a mesh $\Delta x = 1D$. Second order mass equation discretization creates a slightly sharper front and slightly higher wave peak holdup than first order discretization, see figure 37 below. Second order discretization generates approximately the same solution for $\Delta x = 1D$ as first order generates for $\Delta x = 0,25D$, see figure 35. All the simulations of the lab observations are done with first order discretization because it is more robust and it is the recommended default setting by OLGA to be used for most situations. [20, p. 24] It was therefore desired to investigate the capability of this default setting, even though second order discretization is specially designed to maintain sharp fronts.

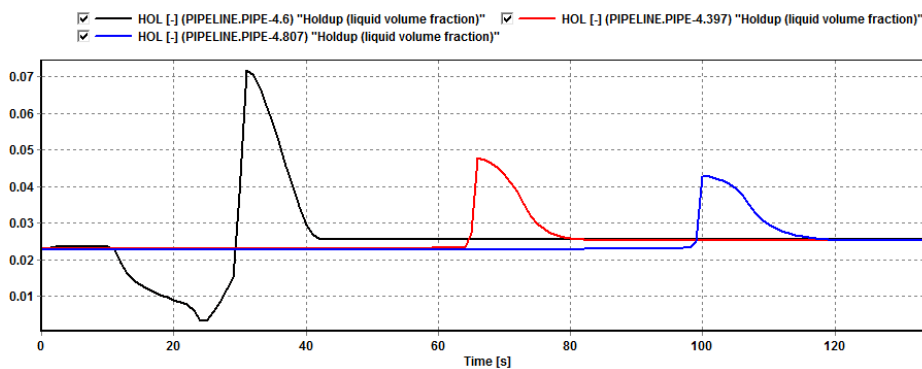


Figure 37: Second order mass equation discretization applied on the wave shown in figure 35, $\Delta x = 1D$. The solution is almost identical to the first order solution with $\Delta x = 0,25D$. A second order scheme maintains sharp fronts better than first order, as second order is less exposed to numerical diffusion.

5.2.4. The OLGA HD model

One can choose a model called OLG AHD in addition to the normal OLGA model when running an OLGA simulation. The OLG AHD model was tested on the wave seen in figure 35 with a mesh $\Delta x = 1D$ and first order mass equation discretization. The result is shown in figure 38 below. The wave gets dragged out, eventually creating a very long wavelength, much longer than the lab observations seen in figure 29. As the result of the OLGA model seen in figure 35 fits much better to the observations in figure 29 than the OLG AHD model in figure 35, the OLG AHD model was rejected and not applied to simulate all the lab

observations.

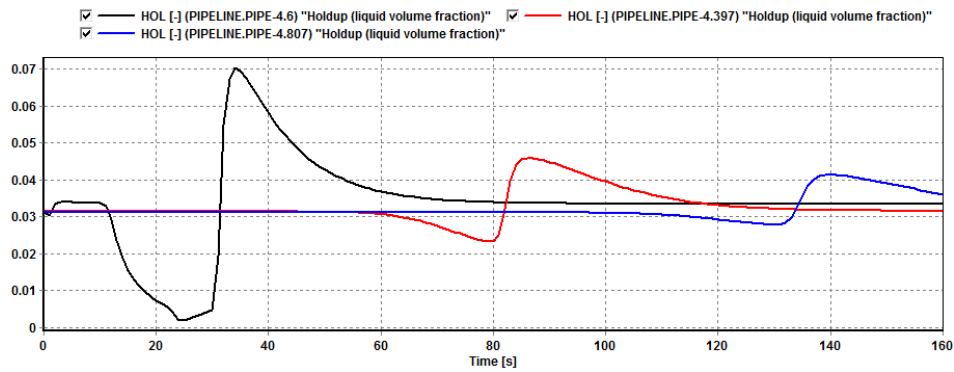


Figure 38: The OLGABD model applied on the wave shown in figure 35, $\Delta x = 1D$.

5.3. LedaFlow simulation setup

The LedaFlow simulations have been performed in the version v1.4.242.619.

5.3.1. Simulation setup and boundary conditions

The lab pipeline geometry was configured with the dimensions shown in table 4 below. Two mass sources, one for air and one for water, were placed in section one.

Table 4: The LedaFlow setup geometry

x [m]	y [m]	z [m]	Diameter [mm]	T _{out} [K]
0,00	0	0	60	293
1,00	0	-0,04	60	293
1,50	0	-0,04	60	293
6,10	0	0,11	60	293
57,84	0	0,11		293

The following assumptions and boundary conditions were applied to the model:

- A 3-phase case was created for the program to accept the use of water. All oil mass fractions were set to zero and the air-water PVT-file obtained from Brandt was applied [28].
- A constant pipeline roughness of 0,05 mm was assumed for the entire pipeline.
- All temperatures were set to 20° C.
- An adiabatic model without any temperature calculations was assumed.
- Outlet node pressure boundary set to 1 atm.
- The CFL time step was set to 0,1 after some testing.
- Max dt = 1 sec.

The LedaFlow simulations initially stabilized at a slightly lower steady state holdup after the waves, than before the waves. This is seen in figure 39 below. To avoid this effect, LedaFlow was run twice on each simulation of the lab waves: First, a simulation with the built in steady-state-pre-processor, and then an additional simulation with a restart file based on the results from the first simulation. The result was then equal steady state holdup before and after the waves passed, seen in all the holdup plots of the LedaFlow solutions presented in Appendix A.

5.3.2. Mesh

The flow rates applied to initiate the test wave are presented in table 3 above. LedaFlow behaves different than OLGA. LedaFlow is not able to simulate the lab waves at as fine meshes as OLGA. The solution shows additional instabilities initiated after the wave at $\Delta x = 5D$, see figure 39 below. It was therefore clear that a much more coarse mesh had to be applied in LedaFlow than in OLGA. Figure 40 shows how the numerical diffusion is eliminated and the solution stabilizes when Δx is approaching 10D, for the wave at probe 3 and 6. At Probe 1, the holdup and wave velocity increases the finer the applied mesh is. This indicates that the initiation of the wave is more mesh dependent than the wave propagation further down the pipeline. It was decided to apply a $\Delta x = 10D$ mesh for the entire pipeline to simulate the waves observed in the lab. This is the mesh where the solution for both holdup

and velocity converges for probe 3 and 6 and this it is the first mesh that has higher velocity for probe 1 than for the sequencing probes, which correlates with the OLGA solution seen in figure 36.

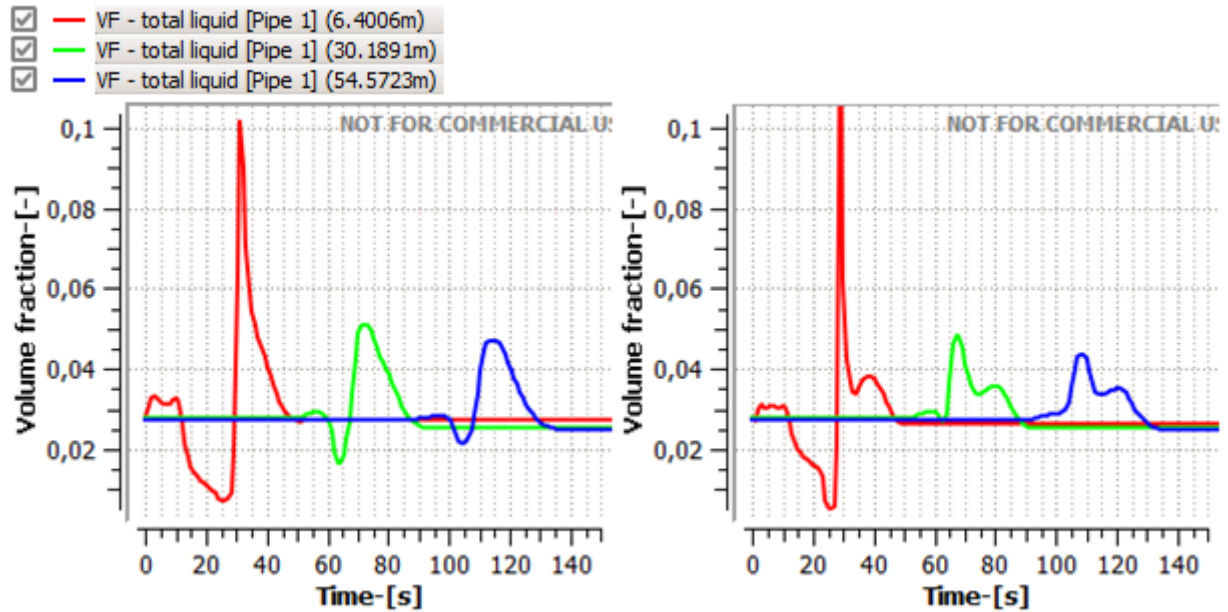


Figure 39: $\Delta x = 10D$ in the plot to the left and $5D$ in the plot to the right. An additional instability is generated behind the wave at $\Delta x = 5$.

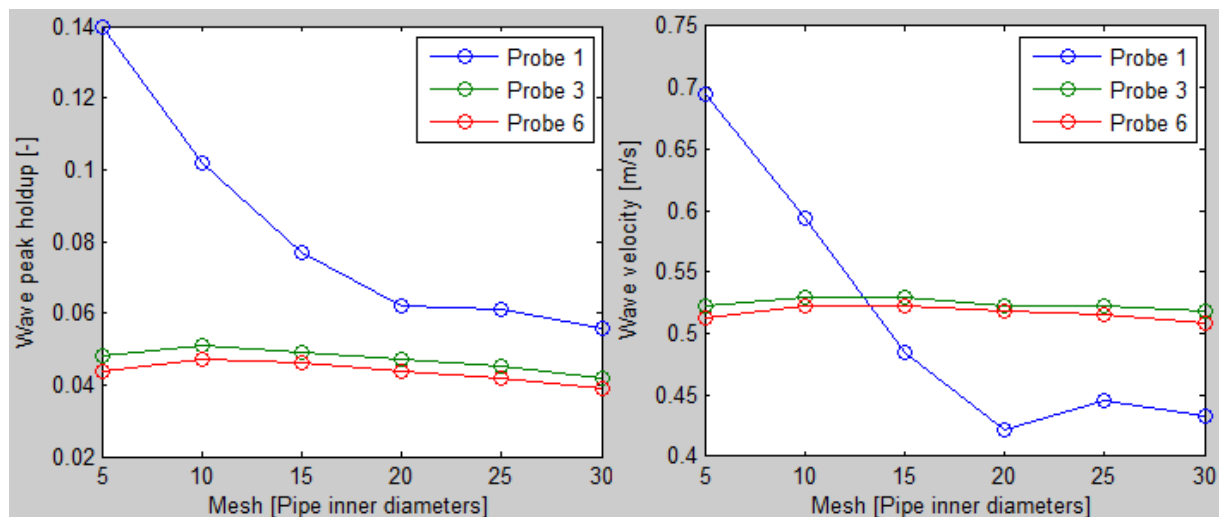


Figure 40: Wave peak holdup and wave speed at different meshes.

5.3.3. Slug capturing and discretization

The results obtained in LedaFlow are completely different with slug capturing activated than without. As there is no slug capturing in OLGA, the thought was first to make the LedaFlow simulations without slug capturing, in order to compare the difference in the results derived from similar settings in both programs. This turned out to be impractical, as the results obtained in LedaFlow with the same settings as OLGA did not look anything like the lab observations. Consequently the LedaFlow results were calculated with the settings that showed best accordance compared to the lab observations. The LedaFlow results are therefore presented with higher order discretization in time and space and slug capturing activated. In figure 39, slug capturing is activated. In figure 41 below, the same wave is seen without slug capturing. The plot to the left is with lower order discretization and the plot to the right is with higher order discretization. These waves do not look anything like the observed wave shown in figure 29, which is attempted reproduced.

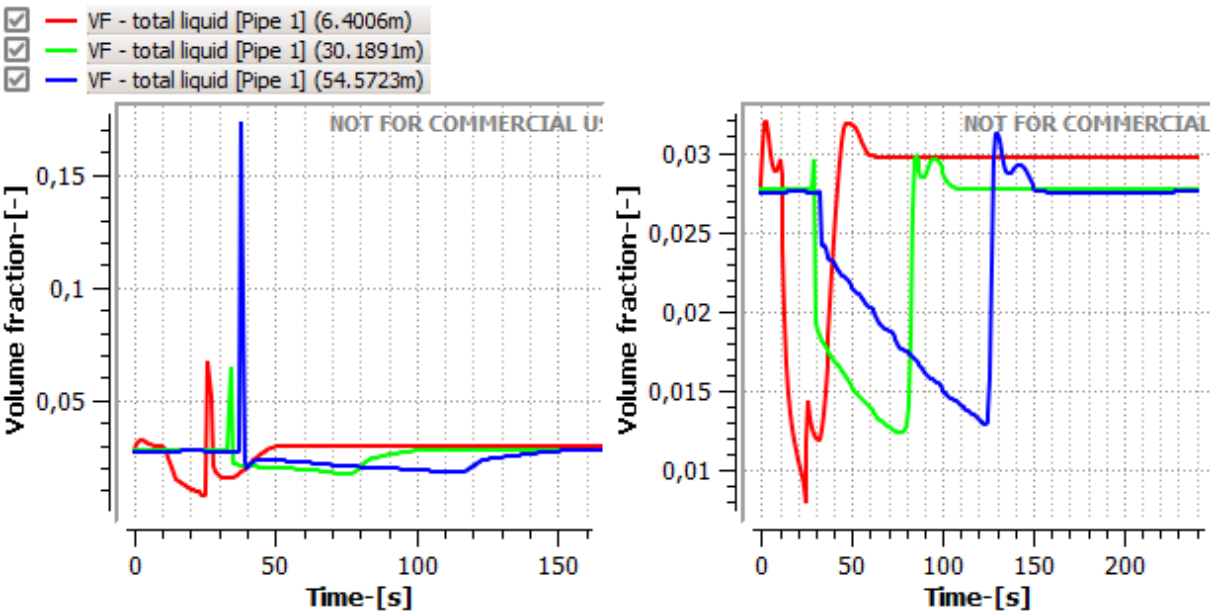


Figure 41: Lower order discretization to the left and higher order discretization without slug capturing to the right. $\Delta x = 10D$

5.4. Simulation result analysis and discussion

The entire OLGA and LedaFlow simulation results are presented in Appendix A.

The simulation results shows that both programs are capable of initiating waves similar to the lab observations. Figure 42 below shows the wave in case 1, with $U_{sg} = 13,4$ m/s and $U_{sl} = 0,0113$ m/s, compared to the OLGA and LedaFlow simulations. Both OLGA and LedaFlow shows an almost equal solution regarding the wave peak holdup through the entire pipeline. LedaFlow shows a gradually smoother wave front than OLGA, and the OLGA solution correlates better with the observations than the LedaFlow solution regarding the wave front. This is the case where the OLGA and LedaFlow solutions are closest to each other and this is the LedaFlow solution that is closest to the lab observations; see figure 43 below. The gas velocity, U_g , is also plotted for probe 1 to show how the gas flow is choked and that the wave is coming when the gas flow has been ramped up again.

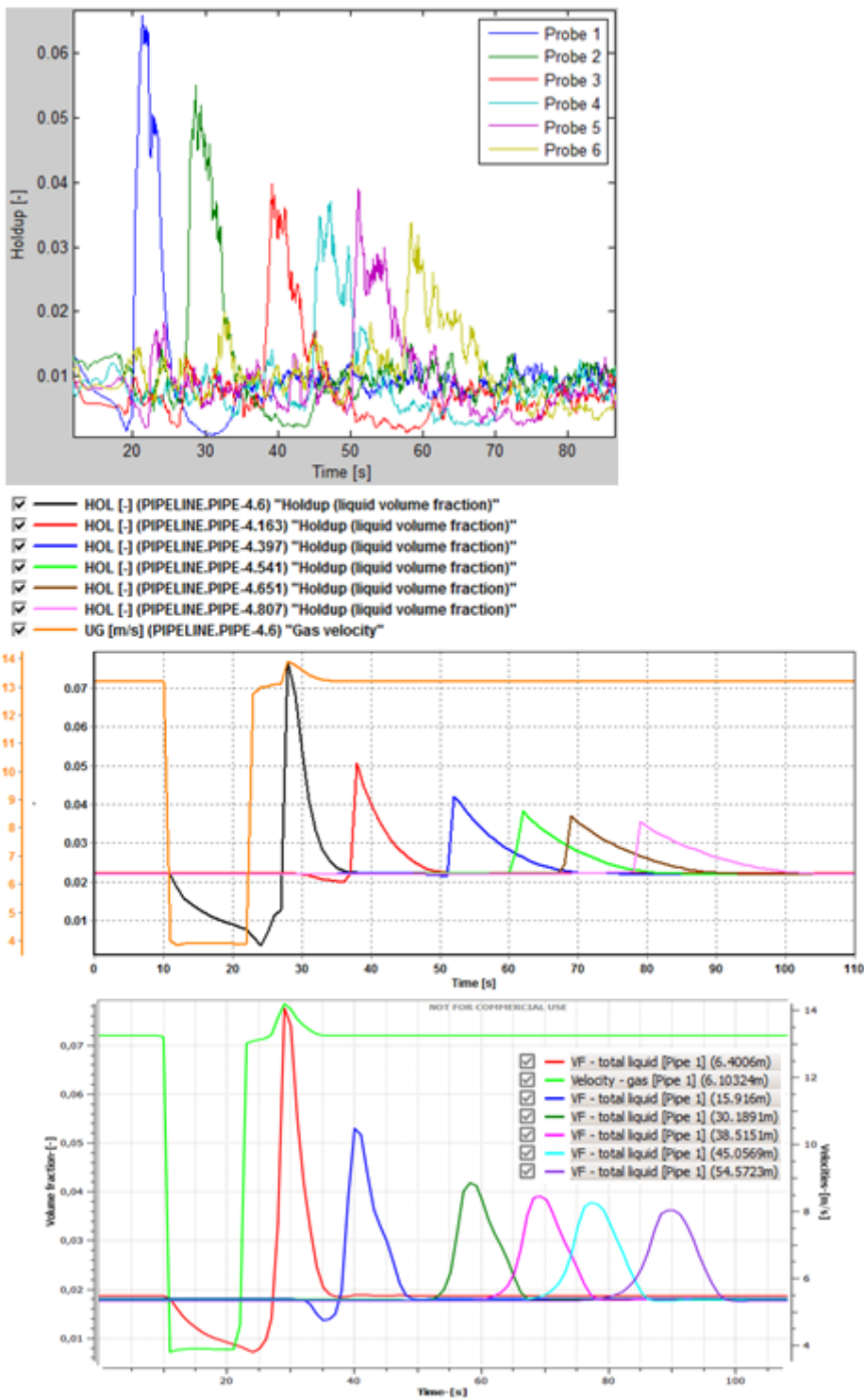


Figure 42: Holdup trend plot of the lab observation (top) OLGA simulation (middle) and LedaFlow simulation (bottom) simulation of the wave in case 1, $U_{sg} = 13,4$ m/s, $U_{sl} = 0,0113$ m/s.

The figures 43 and 44 below shows that the OLGA solution generally follows the lab observations well. OLGA consistently predicts a wave that behaves very similar to the observed waves. OLGA generally predicts a slightly higher wave peak holdup than what is observed. The lab observation results can be affected by the moving average filter that has been applied to smooth the plots, thus the OLGA simulations showing a systematically slightly higher wave peak holdup than the observation plot therefore can be concluded to correlate very well with the lab observations, despite the use of first order mass equation discretization. LedaFlow shows a holdup solution that correlates well with the lab results only for case 1 and 2, see figure 43 and 44. The LedaFlow solution for case 3 – 8 does not look anything like the lab observations. The LedaFlow solution for the wave peak holdup is much higher than for the lab observations. The waves created have a very short wave length, very sharp front and a very high amplitude compared to the lab observations. A systematic fall in amplitude is not seen. Figure 45 below, shows trend plots of how the LedaFlow holdup solution looks like for case 3 to the left and case 6 the right. The LedaFlow solutions for case 4 and 8 do not generate a wave that can be compared to the lab observations, see figure 46 below, and they are therefore excluded from the figures 43 and 44.

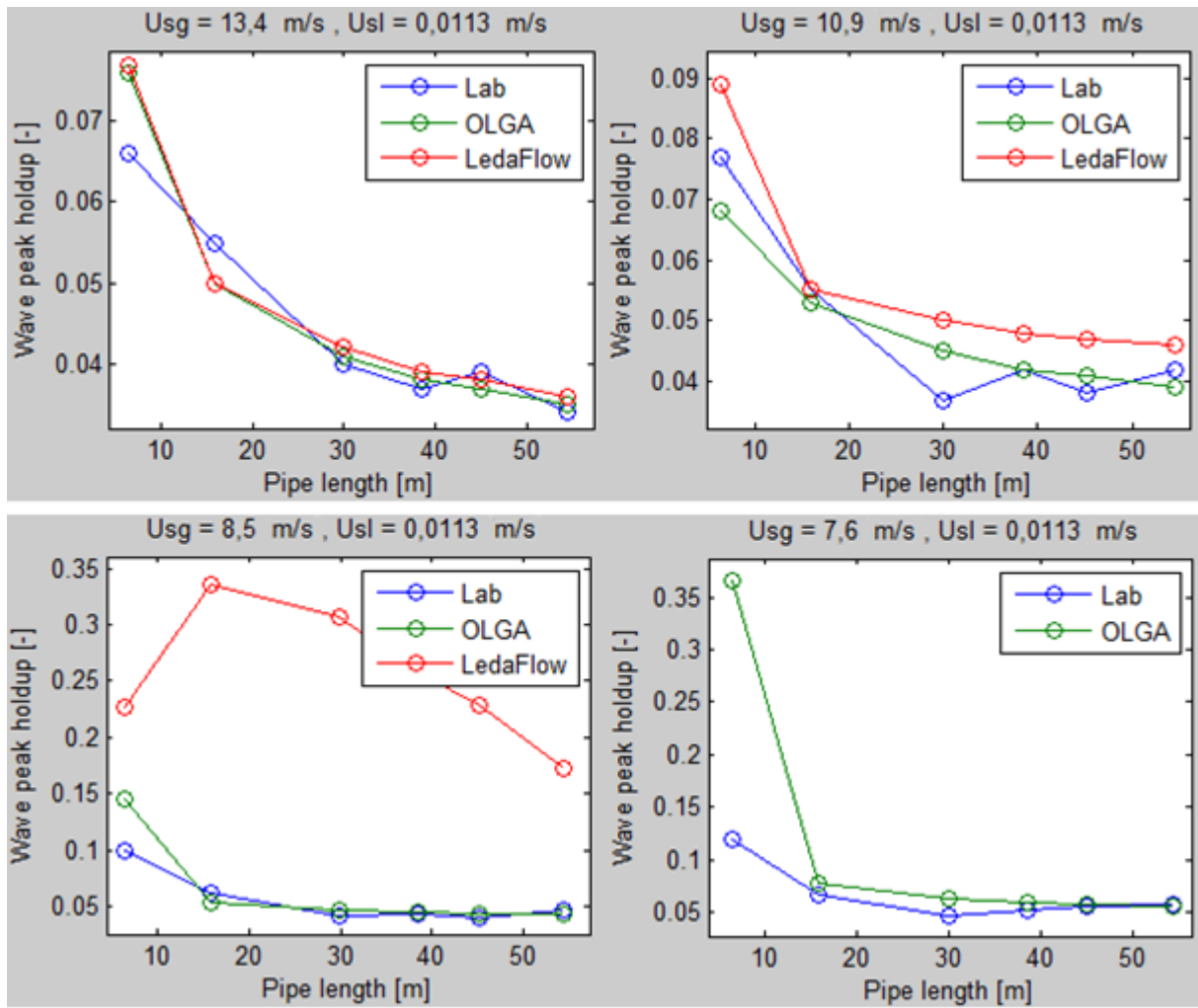


Figure 43: The lab observations of the wave peak holdup compared to the OLGA and LedaFlow simulations for case 1 - 4.

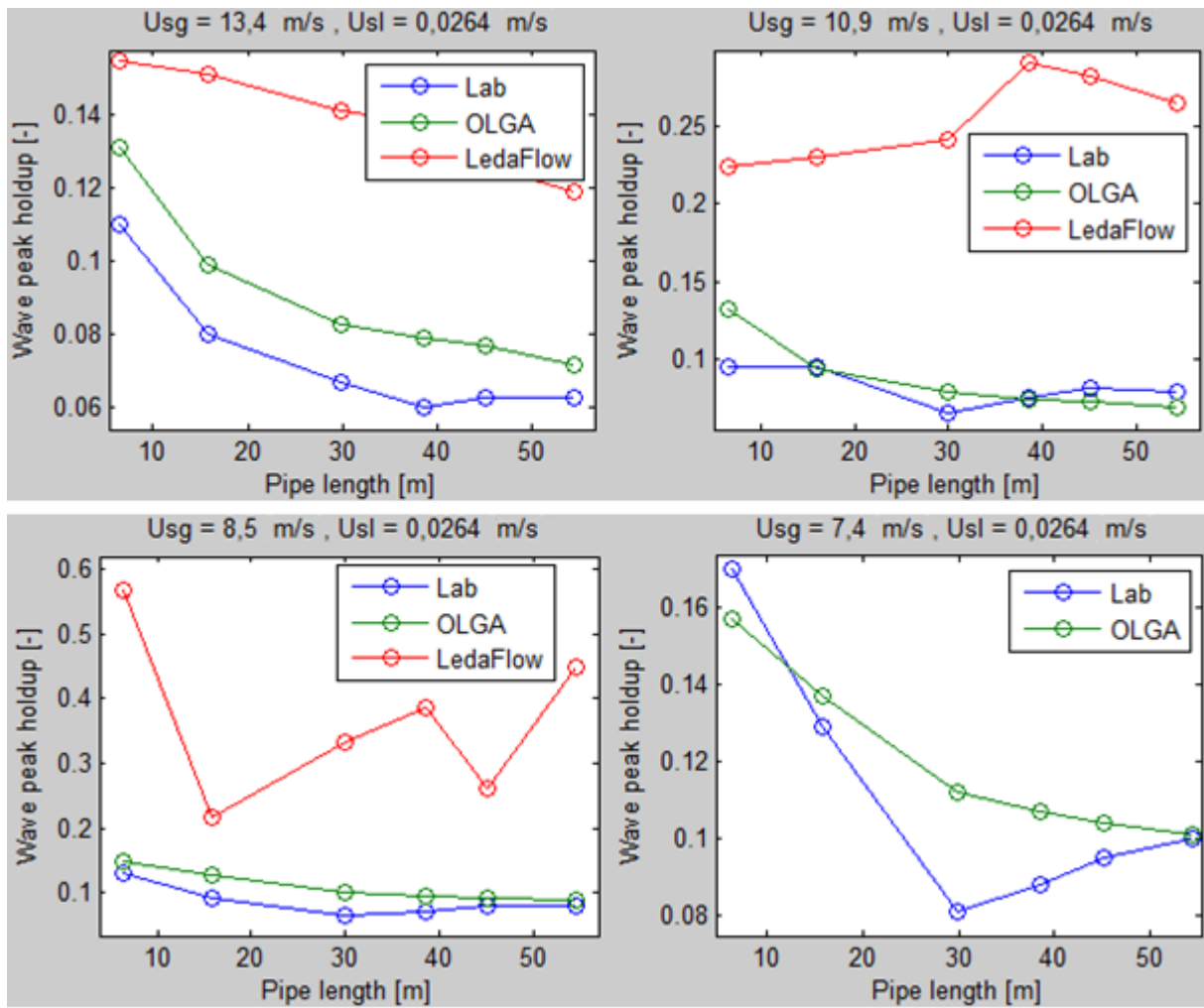


Figure 44: The lab observations of the wave peak holdup compared to the OLGA and LedaFlow simulations for case 5 – 8.

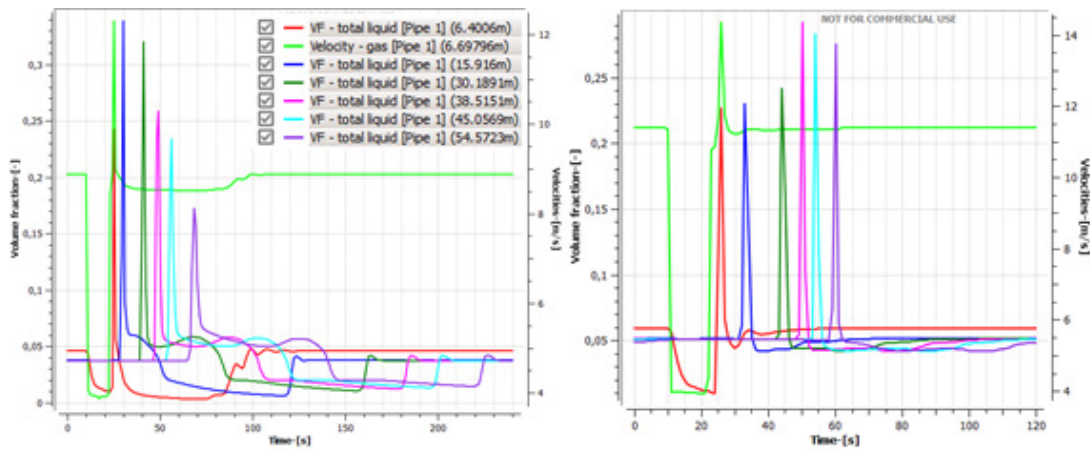


Figure 45: Holdup trend plot of the LedaFlow solution for case 3, $U_{sg} = 8,5$ m/s, $U_{sl} = 0,0113$ m/s, to the left and case 6, $U_{sg} = 10,9$ m/s, $U_{sl} = 0,0264$ m/s, to the right.

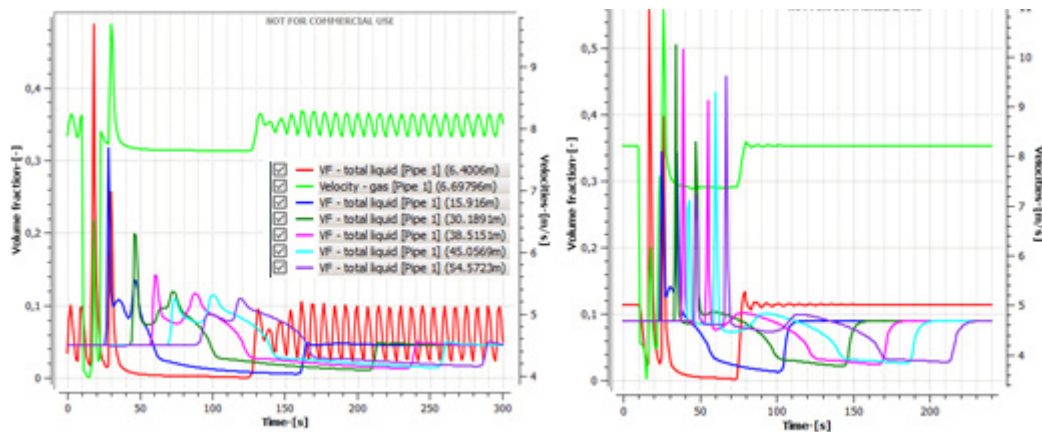


Figure 46: Holdup trend plot of the LedaFlow solution for case 4, $U_{sg} = 7,6$ m/s, $U_{sl} = 0,0113$ m/s, to the left and case 8, $U_{sg} = 7,4$ m/s, $U_{sl} = 0,0264$ m/s, to the right.

There is generally larger deviations between the observed and simulated wave velocity than the wave peak holdup. The figures 47 and 48 below shows the velocity of the waves observed in the lab compared to the OLGA and LedaFlow simulations. The velocity of the observed waves is generally higher than the OLGA simulations, opposite to the holdup that OLGA tended to predict to be slightly higher than observed. It seems like the velocity of the lab observed waves has been more influenced by the turns on the pipeline than the holdup, as the holdup solution predicted by OLGA is closer to the observations than the predicted velocities. The wave velocity predicted by OLGA that is closest to the lab observation is for $U_{sg} = 8,5$ m/s. LedaFlow predicts a slightly lower velocity than OLGA for case 1 and 2, which are the only cases where the OLGA and LedaFlow solutions are almost similar to each other.

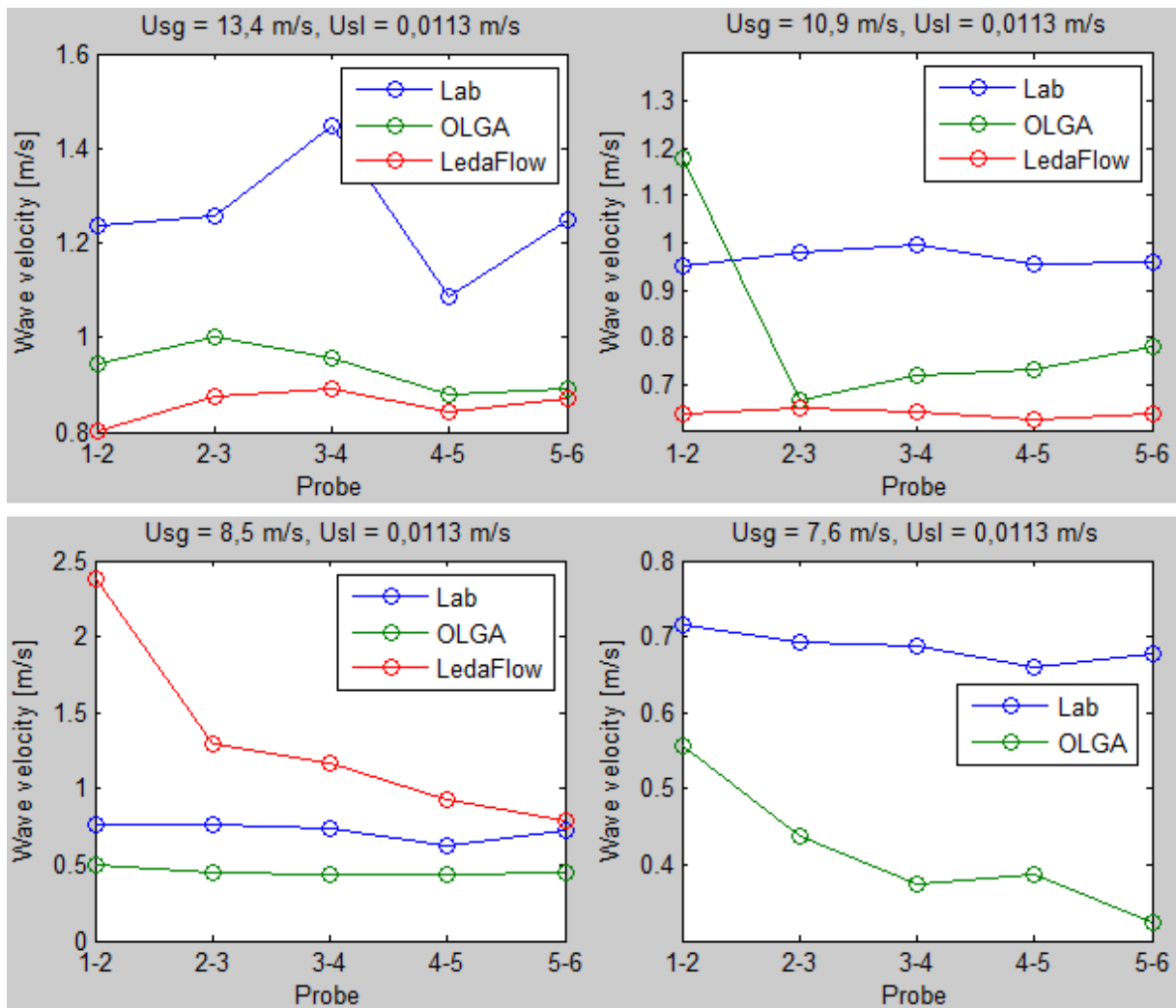


Figure 47: The lab observations of the wave propagation velocity between each probe compared to the OLGA and LedaFlow simulations for case 1 – 4.

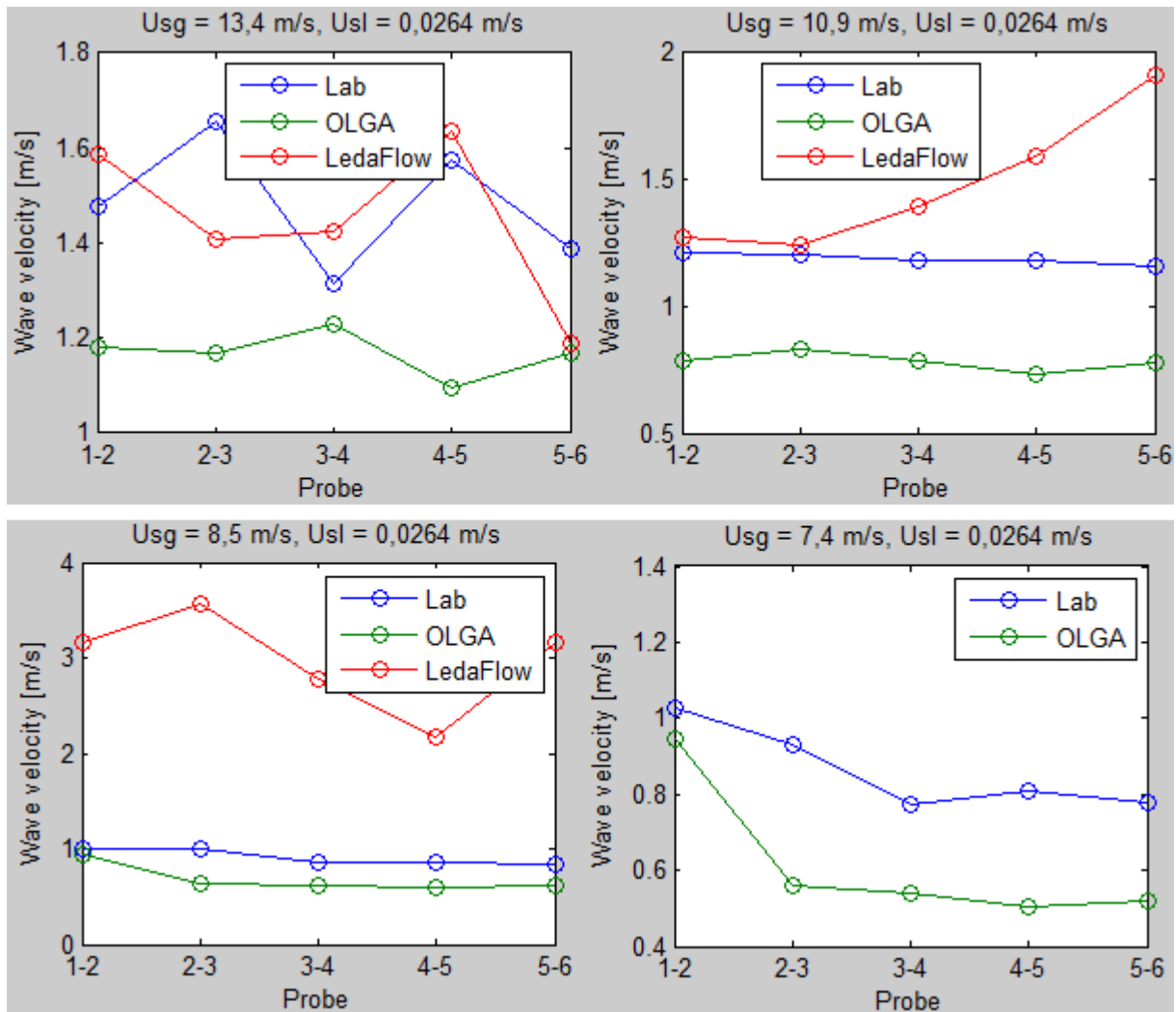


Figure 48: The lab observations of the wave propagation velocity between each probe compared to the OLGA and LedaFlow simulations for case 5 – 8.

Figure 49 below, shows a holdup plot of the OLGA solution for case 8. The wave is not distinct for probe 1, but a wave is propagating all the way downstream the pipeline, and the wave holdup along the pipeline correlates well with the observation, see figure 44. There are continuous fluctuations in both the gas velocity and the holdup at probe 1; and neither smooth stratified flow or constant gas velocity is obtained for probe 1 in this solution. This deviates from the observations, as relatively smooth stratified flow was obtained for probe 1 after the wave had passed, see figure 33. An additional wave is predicted to arrive at probe 2 after 145 seconds. This also deviates from the observations as the second wave was observed to arrive after 15 seconds at probe 2, seen in figure 33.

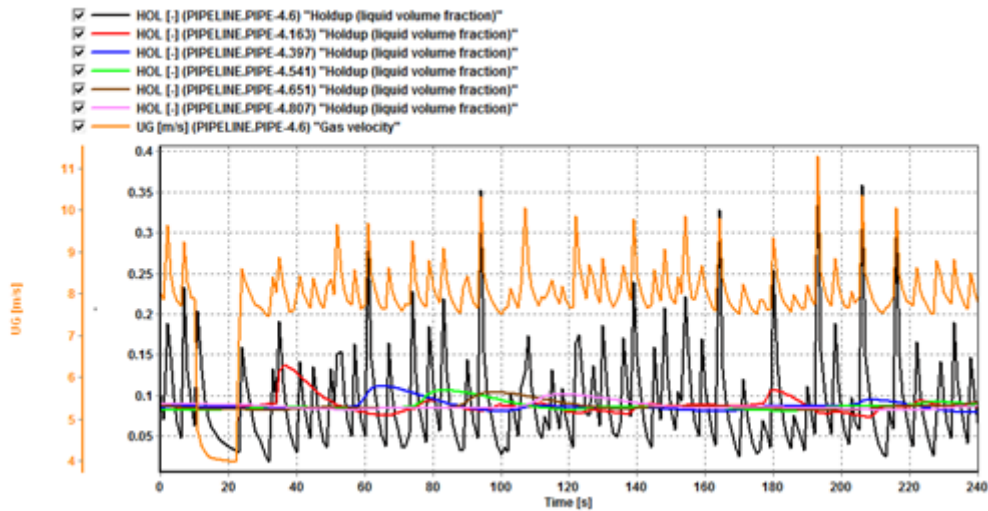


Figure 49: Holdup trend plot of the OLGA solution for case 8, $U_{sg} = 7,4 \text{ m/s}$, $U_{sl} = 0,0264 \text{ m/s}$.

The flow regime ID plot for case 8, $U_{sg} = 7,4 \text{ m/s}$, $U_{sl} = 0,0264 \text{ m/s}$, seen in figure 50 below, shows that OLGA predicts transition into slug flow at 14 occasions. It seems that OLGA starts to run the unit cell model for a short time period, and then returns back to the stratified model. The same trend is also seen in the solution for case 4, presented in figure A 26 in Appendix A. This effect is not seen in any of the ID plots for the LedaFlow simulations, all presented in Appendix A. The flow regime ID in the LedaFlow simulations only vary between smooth stratified flow and wavy stratified flow, which must be expected as the simulated surge wave initiates a wave occurring in the stratified regime. The OLGA flow regime ID trend plots do not distinguish between stratified smooth and stratified wavy flow. It is obviously a weakness in the OLGA model that deviations causing transition into slug flow occurs when trying to simulate a wave with relatively low holdup and occurrence in a stratified flow.

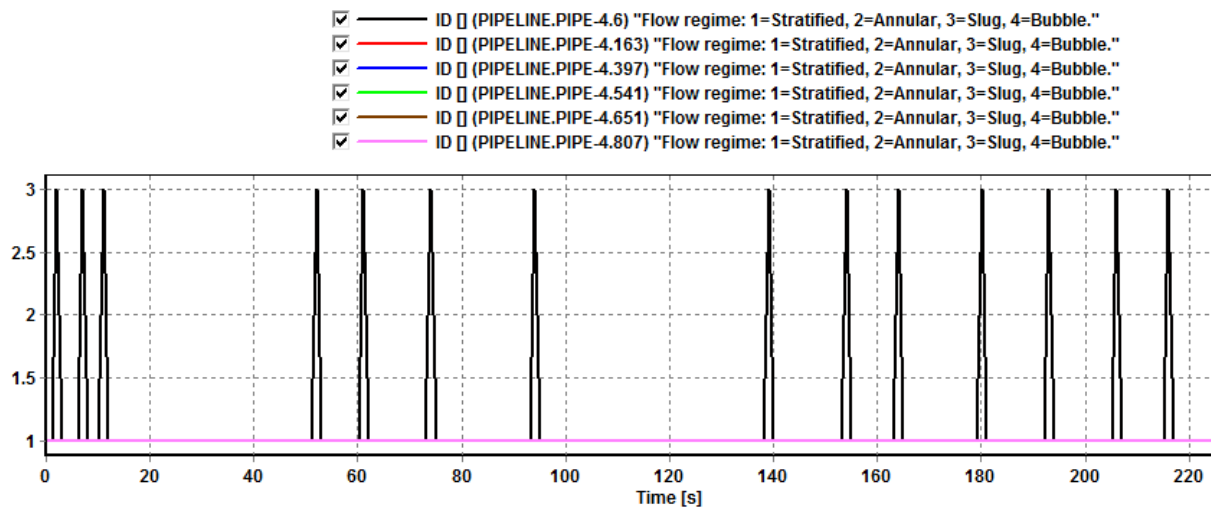


Figure 50: Flow regime ID trend plot for case 8, $U_{sg} = 7,4$ m/s, $U_{sl} = 0,0264$ m/s. Transition into slug flow is predicted for probe 1 at 14 occasions.

The deviations from the observations occurring in the OLGA solutions at the lowest gas flow rates and highest liquid flow rates might be part of the problem of why OLGA has predicted field observed surge waves inaccurately. As surge waves starts to occur in a tail-end production field when the pressure goes down and the drag force from the gas on the liquid no longer is strong enough to maintain a stable stratified flow, and liquid starts to accumulate in low spots. OLGA seems to perform weakest on the lowest gas flow rates, where the interfacial drag from the gas on the liquid is weakest. It seems as OLGA has difficulties to detect the point where the interfacial drag is strong enough to efficiently drag the liquid through the pipeline in a stratified flow.

The simulation programs are designed to simulate realistic oil- and gas pipelines, with a higher inner diameter than the 60 mm pipe applied in the lab. The program has to downscale the calculations by extrapolating out of its optimized design range when they are applied for calculations on the lab pipeline. According to Ivar Brandt, this may promote inaccurate results. Brandt doubted that OLGA was capable of simulating the surge waves observed in the lab because of the relations stated above [29]. Hence this relation likely applies to LedaFlow as well, as LedaFlow is designed to deal with the same type of problems as OLGA. It is therefore interesting that OLGA is able to simulate the lab observations as well as shown above, which is much better than Brandt expected. LedaFlow seems to be more exposed to the relations stated above than OLGA, which might be the reason why LedaFlow shows poor accordance when simulating the cases 3 – 8.

However, it is interesting that OLGA is better than LedaFlow in reproducing the lab observations as the slug capturing applied in the LedaFlow simulations is special designed to be able to capture sharp fronts, while OLGA only was run with first order discretization of the mass equation. It might not be very strange that OLGA is able to describe the lab observations relatively well, even if it is not specially designed to simulate the conditions in the lab pipeline, because the surge waves initiated in the lab pipeline represents much simpler physics than surge waves occurring in three-phase flow in the field. The initiation of real surge waves is much more complicated than the initiation of the surge waves in the lab. The short lab pipeline length allows the use of a finer mesh than what is feasible to use on field pipelines. A very fine mesh is suitable for capturing wave fronts and eliminating numerical diffusion.

6. Conclusion

The waves created in the lab shared several characteristics with surge waves observed in the field: The waves created were characterized by a relatively low peak holdup up to 17 %, a smooth, non breaking front and occurrence in the stratified flow regime. They were initiated as a result of a flow rate ramp up, where liquid accumulated in a low spot in the flowline during a low gas flow rate is expelled through the pipeline when the gas flow rate is ramped up. The way these waves are initiated thus seems to be related to some of the mechanisms that generate surge waves in gas-condensate flowlines. The wave duration was up to 20 seconds at the end of the pipeline. This is 10 times longer than the waves created in the Master Thesis pre-project, only lasting a couple of seconds. The wave duration was still much shorter than one hour, which is normal duration for surge waves observed in the field. The conclusion is therefore that surge waves have been partly reproduced in the lab. The main characteristics of surge waves, except extremely long duration and occurrence in a three-phase flow are satisfied by the waves observed in the lab during this Master Thesis. The shape of the waves changes during the propagation through the pipeline. The rate of change in shape seemed to slow down towards the end of the pipeline and the waves are assumed to be able to travel over a very long distance in a longer test pipeline.

The multiphase flow simulation program OLGA is capable of reproducing the lab observations very well. OLGA predicted waves with very similar behavior as the observations. The general trend was that OLGA predicted a slightly higher wave peak amplitude and a slightly lower wave velocity than what is seen in the lab observations. For the cases with the lowest gas flow rate, OLGA predicted transition into slug flow occasionally. OLGA starts to run the unit cell model for a short time before it returned to the stratified model. This deviates from the observations, as slug flow has not been observed in any of the lab cases.

LedaFlow showed a much more poor performance than OLGA to simulate the lab observations. LedaFlow was only capable of reproducing a solution similar to the observations in two of the eight analyzed cases, which were the cases with highest U_{sg} and lowest U_{sl} . LedaFlow did not predict transition into slug flow in any of the cases. That was expected as LedaFlow was run with slug capturing activated for all the cases. LedaFlow predicted waves with a sharp front, high amplitude and short duration for four of the analyzed cases. LedaFlow did not predict anything that could be compared with the lab observations for the two cases with the lowest U_{sg} .

7. Suggestions for further work

Three-phase experiments with a suitable oil would be interesting to conduct if proper measurement instrumentation can be implemented in the pipeline test section. Then one could study waves, perhaps even more like surge waves in the lab. It would be interesting to find out if the oil and the water phases would separate, resulting in an oil surge followed by a water surge, or if they would come together in one surge wave. OLGA and LedaFlow's capability to reproduce those results would also be interesting to investigate. Such experiments could also be performed in an even longer pipeline, to detect how far the surge waves are able to propagate and to see if even longer and more realistic surge waves can be observed. It would also be advantageous to perform further experiments in a wider pipeline. If the 90 mm pipeline is used instead of the 60 mm, a larger liquid volume would be able to accumulate in the dip, possibly causing even longer surge waves.

References

- [1] M. Langsholt, O. Sendstad and T. Sira, "Surge waves in gas-liquid pipe flow - Experiments and analysis," Kjeller, 2004.
- [2] D. Biberg, H. Holmås, G. Staff, T. Sira, J. Nossen, P. Andersson, C. Lawrence, B. Hu and K. Holmås, "Basic flow modelling for long distance transport of wellstream fluids," *BHR Group 2009 Multiphase Production Technology 14*, 2009.
- [3] H. Torpe, J.-M. Godhavn, S. T. Strand, M. Løkvik, J. Ø. Tengesdal and B. H. Pettersen, "Liquid surge handling at Åsgard by model predictive control," *BHR Group 2009 Multiphase Production Technology 14*, 2009.
- [4] B. H. Pettersen, M. Nordsveen and E. Thomassen, "Liquid inventory and three phase surge wave data from the Midgard gas condensate fields in the North Sea," *BHR Group 2013 Multiphase 16*, 2013.
- [5] K. Holmås, G. G. Lunde, G. Setyadi, P. Angelo and G. Rudrum, "Ormen Lange Flow Assurance System (FAS) - Online Flow Assurance Monitoring and Advice," in *Offshore Technology Conference*, Rio de Janeiro, 2013.
- [6] L. Hagesæther, R. S. Bruvold, W. Postvill and R. Albrechtsen, "Rich gas pipeline operations during tail-end production," in *Pipeline Simulation Interest Group*, Palm Springs, 2004.
- [7] E. Storkaas and J.-M. Godhavn, "Extended slug control for pipeline-riser systems," *BHR Group 2005 Multiphase Production Technology 12*, 2005.
- [8] O. Bratland, *Pipe Flow 2*, 2010.
- [9] G. W. Johnson, J. Nossen and A. F. Bertelsen, "A comparison between experimental and continuous theoretical roll waves in horizontal and slightly inclined pipes at high pressure," in *BHR Group*, 2005.
- [10] O. J. Nydal, Interviewee, *Lecture: Flow Regimes*. [Interview]. 24 January 2013.
]
- [11] K. Holmås, Interviewee, *Phone conversation with Kristian Holmås from FMC*. [Interview]. 15 November 2013.

- [12 L. Hagesæther, K. Lunde, F. Nygård and H. Eidsmoen, "Flow-Assurance Modelling: Reality Check and Aspects of Transient Operations of Gas/Condensate Pipelines," in *Offshore Technology Conference*, Houston, 2006.
- [13 G. G. Lunde, K. Vannes, O. T. McClimans, C. Bums and K. Wittmeyer, "Advanced Flow Assurance System for the Ormen Lange Subsea Gas Development," in *Offshore Technology Conference*, Houston, 2009.
- [14 K. Holmås, G. Gahr Lunde and G. Setyadi, "Prediction of liquid surge waves at Ormen Lange," *BHR Group 2013 Multiphase 16*, 2013.
- [15 G. S. Landsverk, G. Flåten, M. Svenning, D. Pedersen and B. H. Pettersen, "Multiphase flow behaviour at Snøhvit," *BHR Group 2009 Multiphase Production Technology 14*, 2009.
- [16 M. f. p. s. H. Schümann, "holdup calibration," Trondheim, 27 March 2014.
- [17 "Smooth response data," MathWorks, [Online]. Available: <http://www.mathworks.se/help/curvefit/smooth.html>. [Accessed 14 12 2013].
- [18 "The history of OLGA," IFE, [Online]. Available: http://www.ife.no/en/ife/departments/process_and_fluid_flow_tech/historienomolga/view. [Accessed 19 February 2014].
- [19 "Rørene gjorde oljeeventyret mulig," Sintef, [Online]. Available: <http://www.sintef.no/SINTEF-Petroleum-AS/Nyheter/Rorene-gjorde-oljeeventyret-mulig-Aftenposten/>. [Accessed 19 February 2014].
- [20 OLGA _USER MANUAL VERSION 7.0, SPT GROUP.
- [21 K. H. Bendiksen, D. Malnes, R. Moe and S. Nuland, "The Dynamic Two-Fluid Model OLGA: Theory and Application," SPE, 1991.
- [22 Scandpower, "OLGA2000 NTNU April 2001," 2001.
- [23 "LedaFlow history," Kongsberg, [Online]. Available: <http://www.kongsberg.com/en/kogt/offerings/software/ledaflow/ledaflowhistory/>. [Accessed 20 February 2014].
- [24 T. J. Danielson, K. M. Bansal, R. Hansen and E. Leporcher, "LEDA: the next multiphase

-] flow performanse simulator," in *12th International Conference on Multiphase Production Technology*, Barcelona, 2005.
- [25 A. Goldzal, J. I. Monsen, T. J. Danielson, K. M. Bansal, Z. L. Yang, T. Johansen and G. Depay, "LedaFlow 1D: Simulation results with multiphase gas/condensate and oil/gas field data," BHRG, 2007.
- [26 "LedaFlow modelling," Kongsberg Oil & Gas Technologies AS , [Online]. Available: <http://www.kongsberg.com/en/kogt/offerings/software/ledaflow/ledaflowmodeling/>. [Accessed 11 May 2014].
- [27 T. J. Danielson, K. M. Bansal, B. Djoric, D. Larrey, S. T. Johansen, A. D. Leebeeck and J. Kjølås, "Simulation of Slug Flow in Oil and Gas Pipelines Using a New Transient Simulator," in *Offshore Technology Conference*, Houston, 2012.
- [28 I. Brandt, "PVT-luft/vann," 12 December 2013.
-]
- [29 I. Brandt, Interviewee, *Lecture and discussion with Ivar Brandt from Schlumberger*. [Interview]. 12 11 2013.
- [30 K. O. & G. Technologies, "LedaFlow® Flow Assurance for 21 st Century Oil & Gas Production," [Online]. Available: <http://www.kongsberg.com/KOGT/ledaflow/index.html>. [Accessed 19 February 2014].

Appendix A: Lab and simulation results

The results from eight lab cases are presented below. The results are presented as trend plots of the holdup at the six measurement probes seen in figure 25, in order to see the development of the wave along the pipeline. The holdup trend plots have been smoothed with the Matlab moving average function $yy = \text{smooth}(y, 0.01, 'moving')$. Raw holdup plots and a plots of the air flow rate choking are also presented. The OLGA and LedaFlow simulation results are presented with a holdup trend plot and a flow regime ID plot, below the holdup plots of the lab observations for each case. Tables over the flow rates applied to initiate the waves in the simulations are presented, also containing integration time and approximate simulation duration.

Case 1: $U_{sg} = 13,4 \text{ m/s}$, $U_{sl} = 0,0113 \text{ m/s}$

The initial superficial air velocity $U_{sg} = 13,4 \text{ m/s}$, which is the highest U_{sg} that was applied. The superficial water velocity was kept constant at $U_{sl} = 0,0113 \text{ m/s}$. The large air valve was choked from 27 – 17 % of full opening and ramped up to 27 % again to initiate the wave shown in the holdup trend plot in figure A 1 below. Figure A 2 and A 3 shows the OLGA and LedaFlow simulations of the wave. Figures A 4 and A 5 shows the flow regime ID plots predicted by OLGA and LedaFlow. Figure A 6 shows the raw holdup plot from the lab observation. Figure A 7 shows a plot of how the gas flow rate was choked and ramped up again to initiate the wave seen in figure A 1. Table A 1 shows the flow rates applied to initiate the wave in the computational simulations.

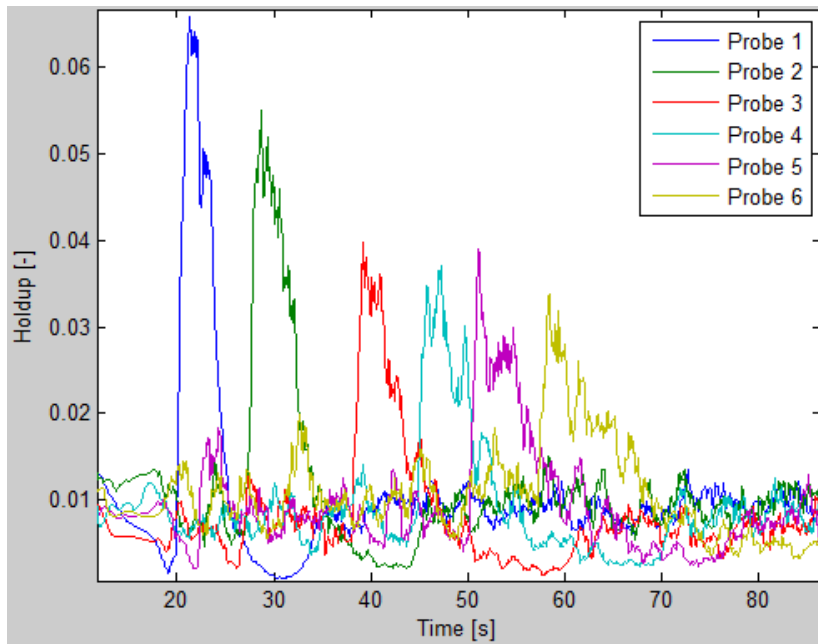


Figure A 1: Holdup trend plot of the surge wave propagation from probe 1 to probe 6.

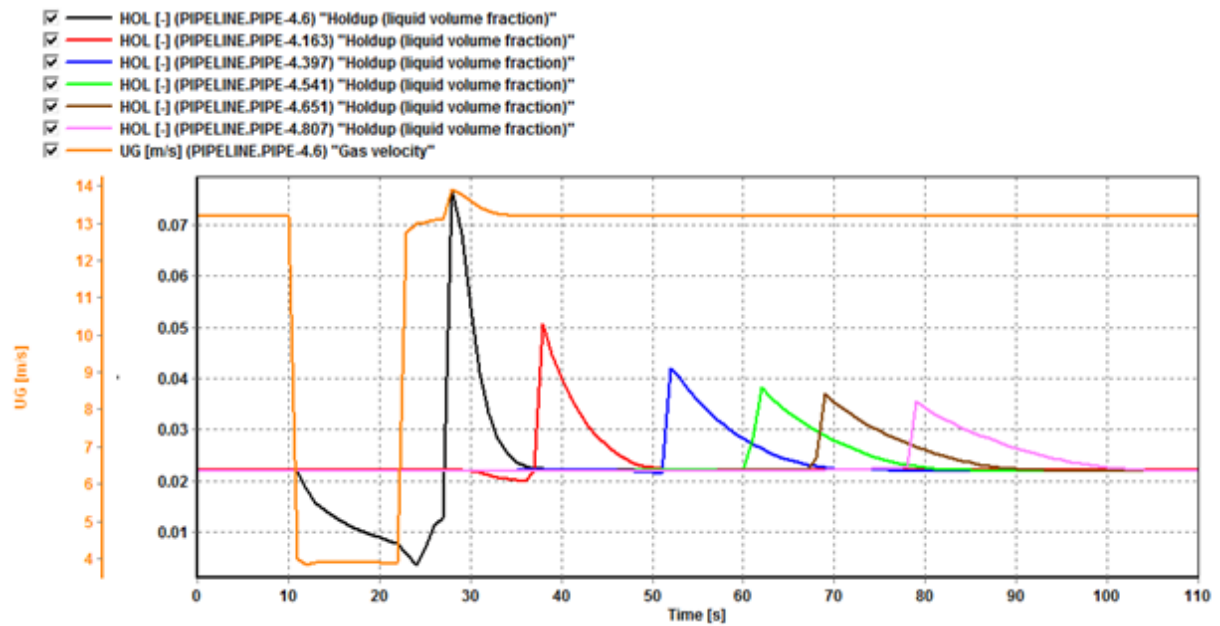


Figure A 2: OLGA simulation holdup trend plot of the wave. The gas velocity is plotted to visualize how the wave was initialized.

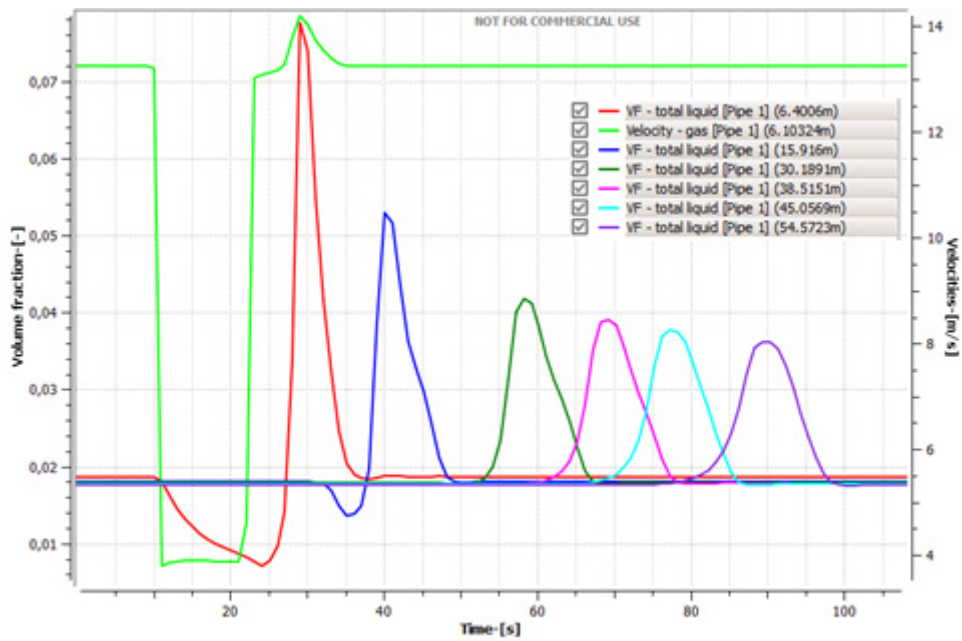


Figure A 3: LedaFlow simulation holdup trend plot of the wave. The gas velocity is plotted to visualize how the wave was initialized.

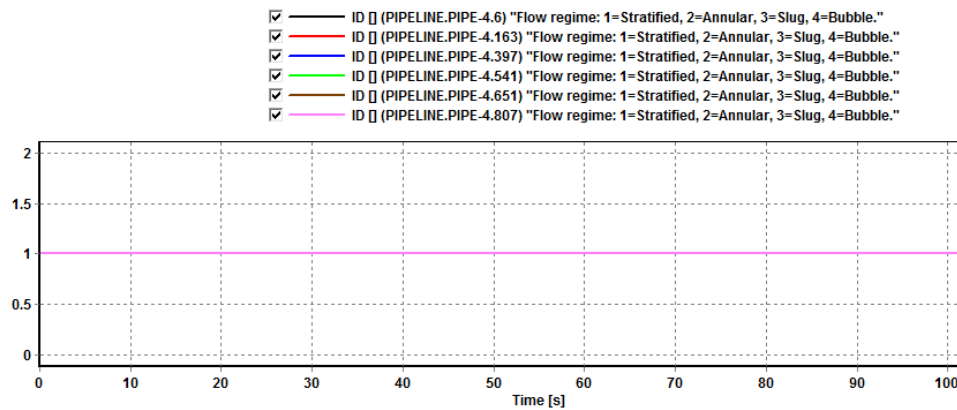


Figure A 4: OLGA flow regime ID trend plot.

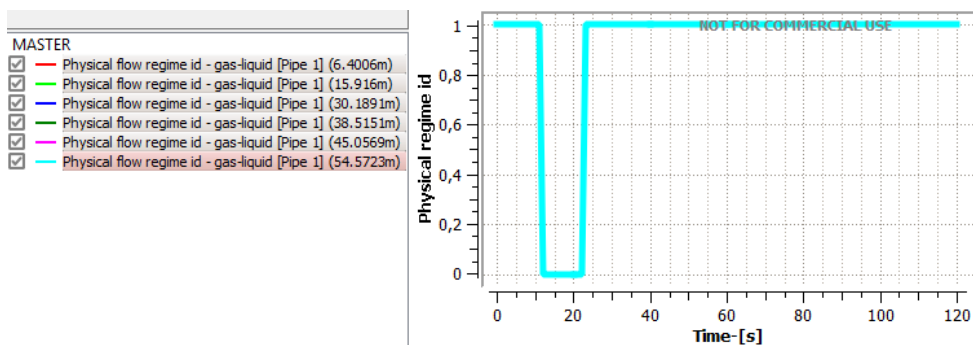


Figure A 5: LedaFlow flow regime ID trend plot. 0 = stratified smooth flow, 1 = stratified wavy flow.

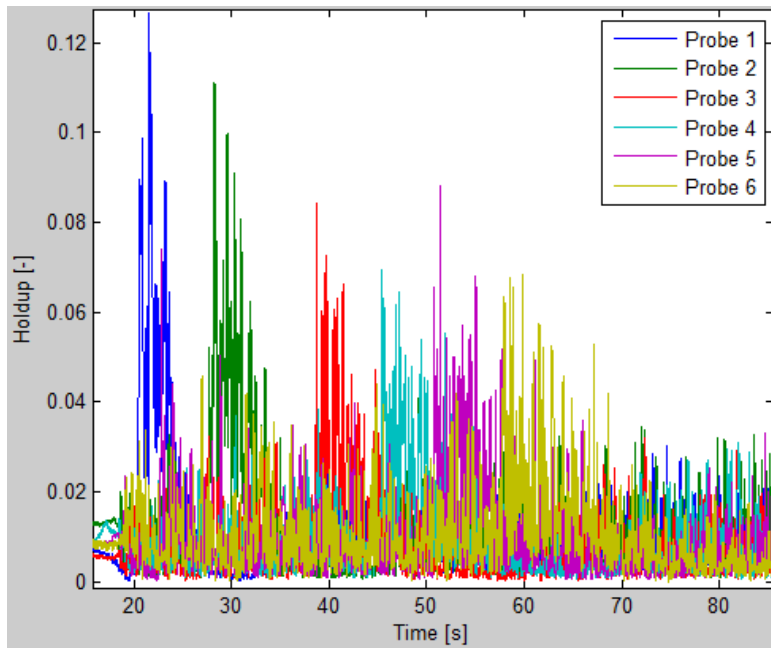


Figure A 6: Raw holdup plot.

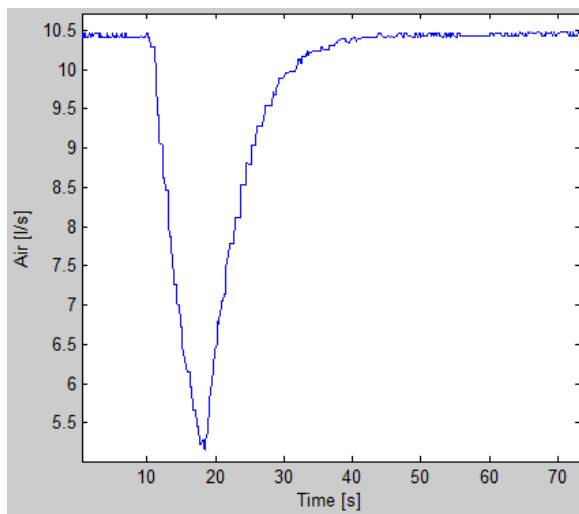


Figure A 7: Air flow rate plot.

Table A 1: The flow rates applied to initiate the wave in the simulations.

	Air source	Water source
Time [s]	Flow rate [kg/s]	Flow rate [kg/s]
0	0,045	0,032
10	0,045	0,032
11	0,013	0,032
22	0,013	0,032
23	0,045	0,032
Integration time:		120 sec
Approximate simulation duration		
OLGA:	2 x 5,5 min	
LedaFlow:	2 x 1 min	

Case 2: $U_{sg} = 10,9 \text{ m/s}$, $U_{sl} = 0,0113 \text{ m/s}$

The initial superficial air velocity $U_{sg} = 10,9 \text{ m/s}$. The superficial water velocity was kept constant at $U_{sl} = 0,0113 \text{ m/s}$. The large air valve was choked from 25 – 17 % of full opening and ramped up to 25 % again to initiate the wave shown in the figure A 8 below. Figure A 9 and A 10 shows the OLGA and LedaFlow simulations of the wave. Figures A 11 and A 12 shows the flow regime ID plots predicted by OLGA and LedaFlow. Figure A 13 shows the raw holdup plot from the lab observation. Figure A 14 shows a plot of how the gas flow rate was choked and ramped up again to initiate the wave seen in figure A 8. Table A 2 shows the flow rates applied to initiate the wave in the simulations.

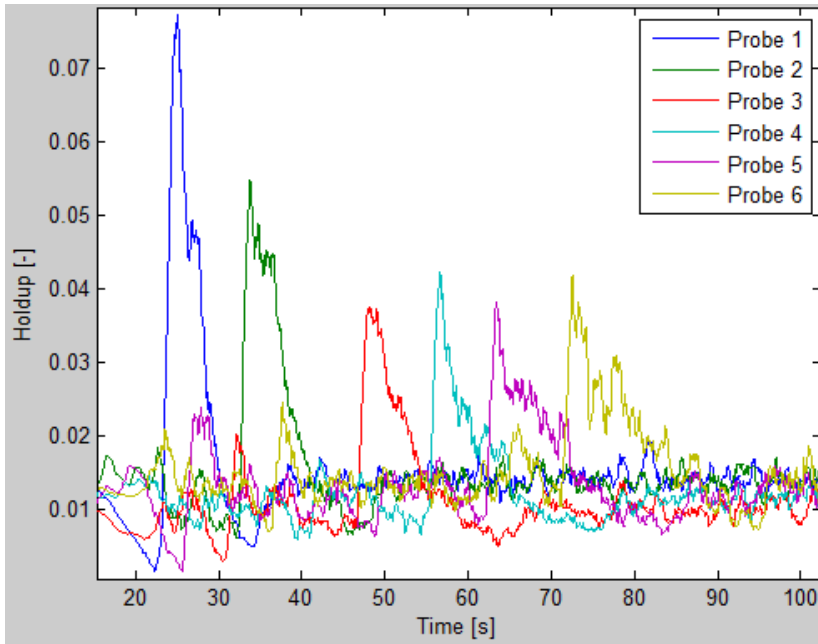


Figure A 8: Holdup trend plot of the surge wave propagation from probe 1 to probe 6.

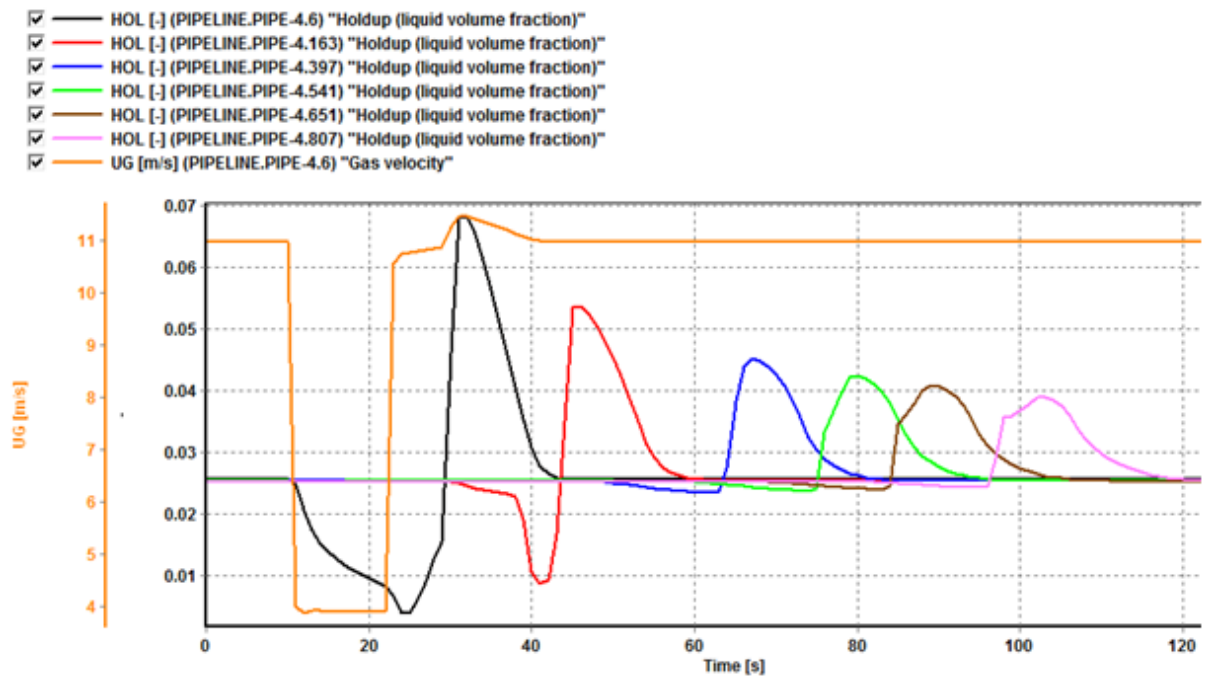


Figure A 9: OLGA simulation holdup trend plot of the wave. The gas velocity is plotted to visualize how the wave was initialized.

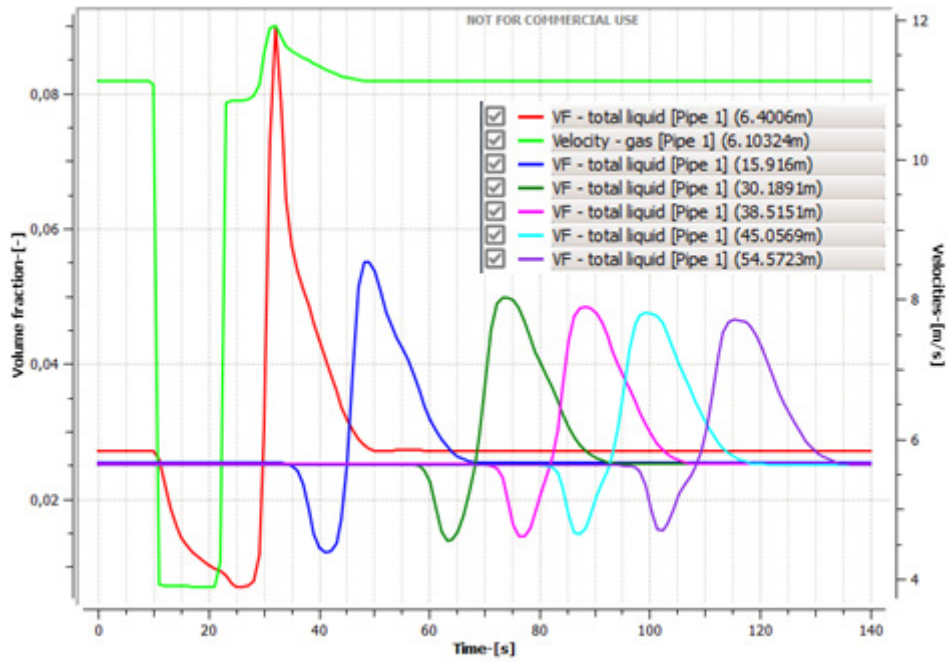


Figure A 10: LedaFlow simulation holdup trend plot of the wave. The gas velocity is plotted to visualize how the wave was initialized.

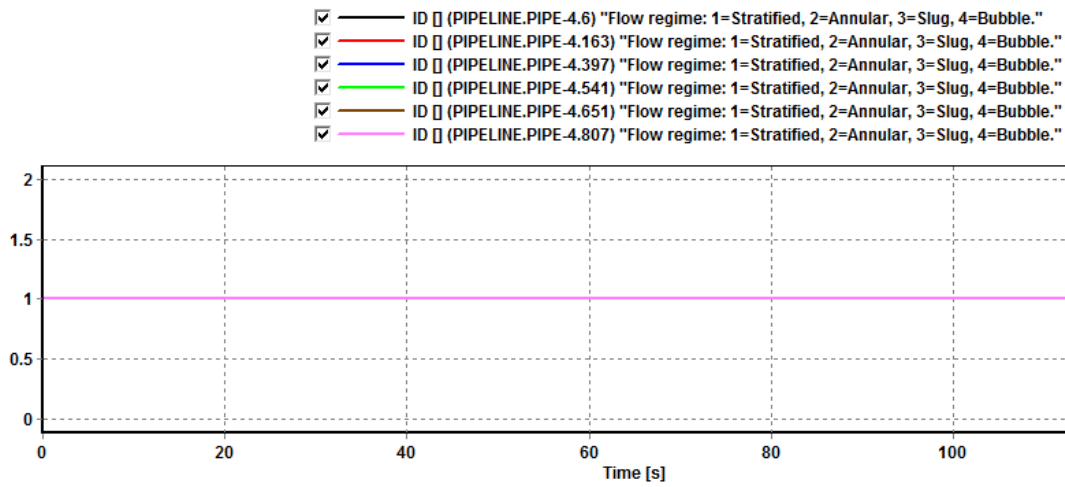


Figure A 11: OLGA flow regime ID trend plot.

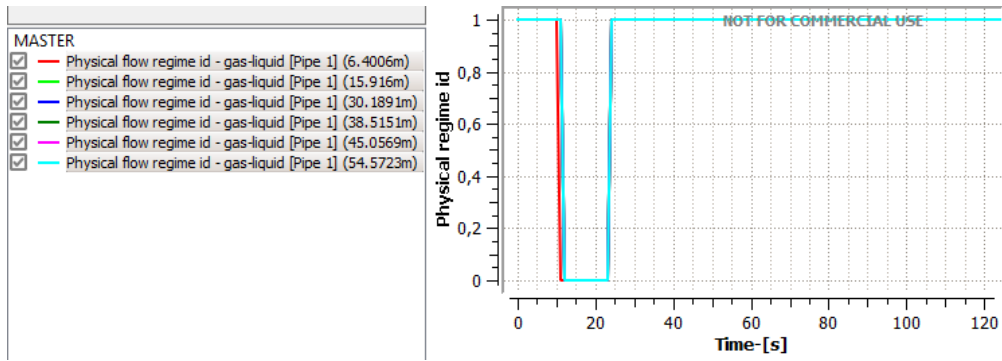


Figure A 12: LedaFlow flow regime ID trend plot. 0 = stratified smooth flow, 1 = stratified wavy flow.

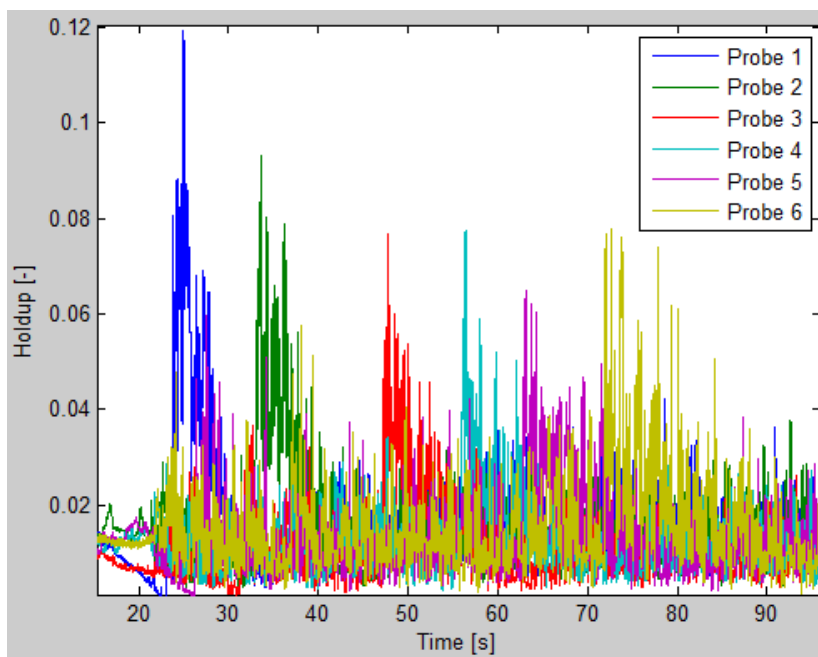


Figure A 13: Raw holdup plot.

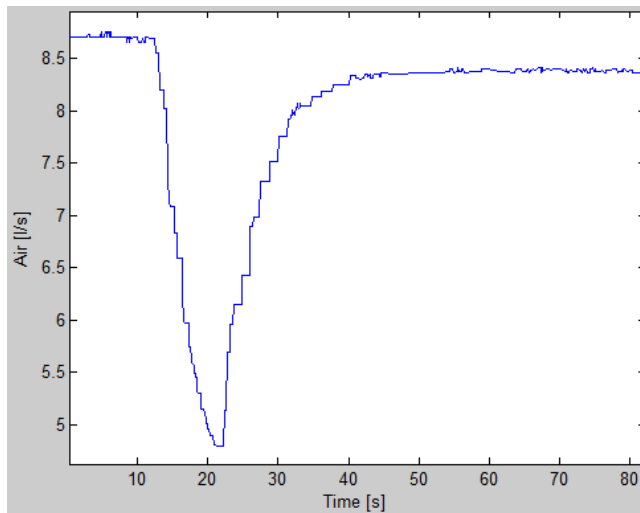


Figure A 14: Air flow rate plot.

Table A 2: The flow rates applied to initiate the wave in the simulations.

	Air source	Water source
Time [s]	Flow rate [kg/s]	Flow rate [kg/s]
0	0,037	0,032
10	0,037	0,032
11	0,013	0,032
22	0,013	0,032
23	0,037	0,032
Integration time:		130 sec
Approximate simulation duration		
OLGA:	2 x 6 min	
LedaFlow:	2 x 1 min	

Case 3: $U_{sg} = 8,5 \text{ m/s}$, $U_{sl} = 0,0113 \text{ m/s}$

The initial superficial air velocity $U_{sg} = 8,5 \text{ m/s}$. The superficial water velocity was kept constant at $U_{sl} = 0,0113 \text{ m/s}$. The large air valve was choked from 23 – 17 % of full opening and ramped up to 23 % again to initiate the wave shown in the figure A 15 below. Figure A 16 and A 17 shows the OLGA and LedaFlow simulations of the wave. Figures A 18 and A 19

shows the flow regime ID plots predicted by OLGA and LedaFlow. Figure A 20 shows the raw holdup plot from the lab observation. Figure A 21 shows a plot of how the gas flow rate was choked and ramped up again to initiate the wave seen in figure A 15. Table A 3 shows the flow rates applied to initiate the wave in the simulations.

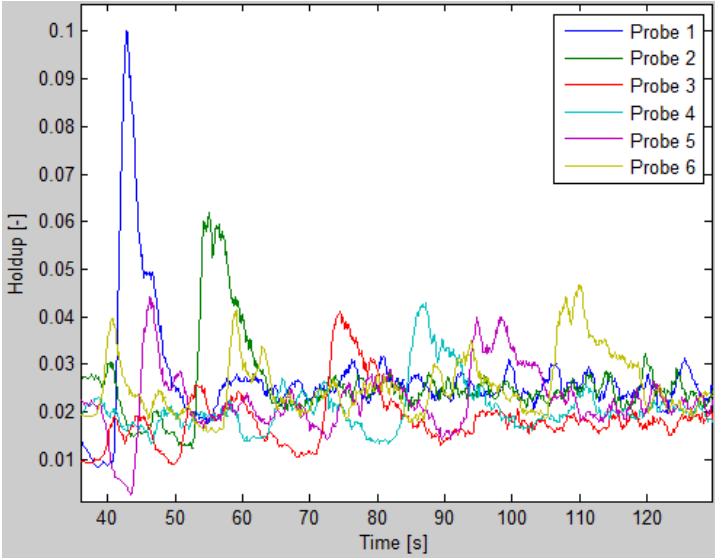


Figure A 15: Holdup trend plot of the surge wave propagation from probe 1 to probe 6.

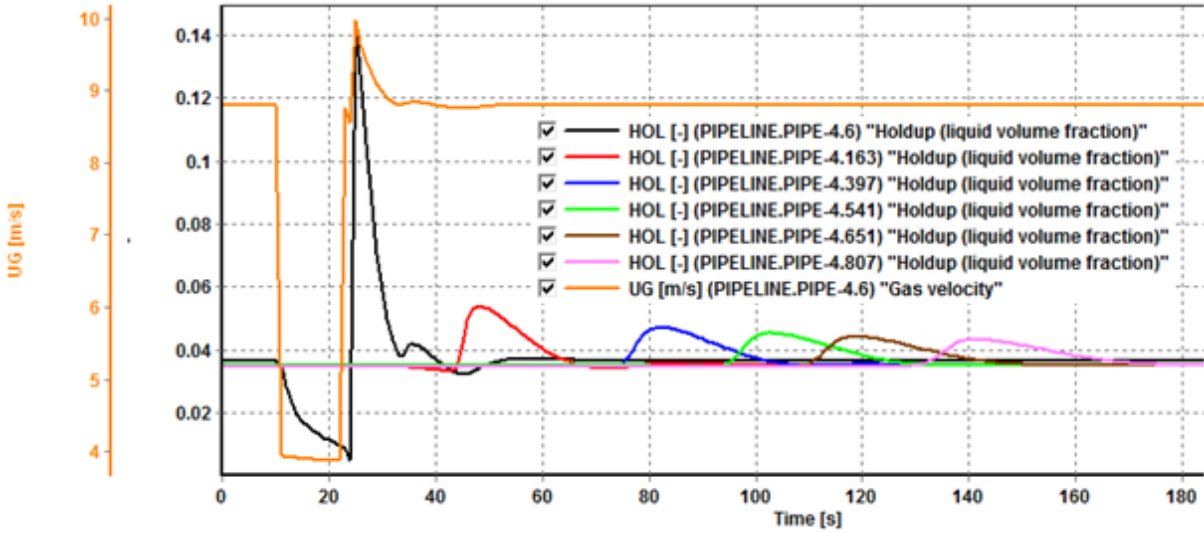


Figure A 16: OLGA simulation holdup trend plot of the wave. The gas velocity is plotted to visualize how the wave was initialized.

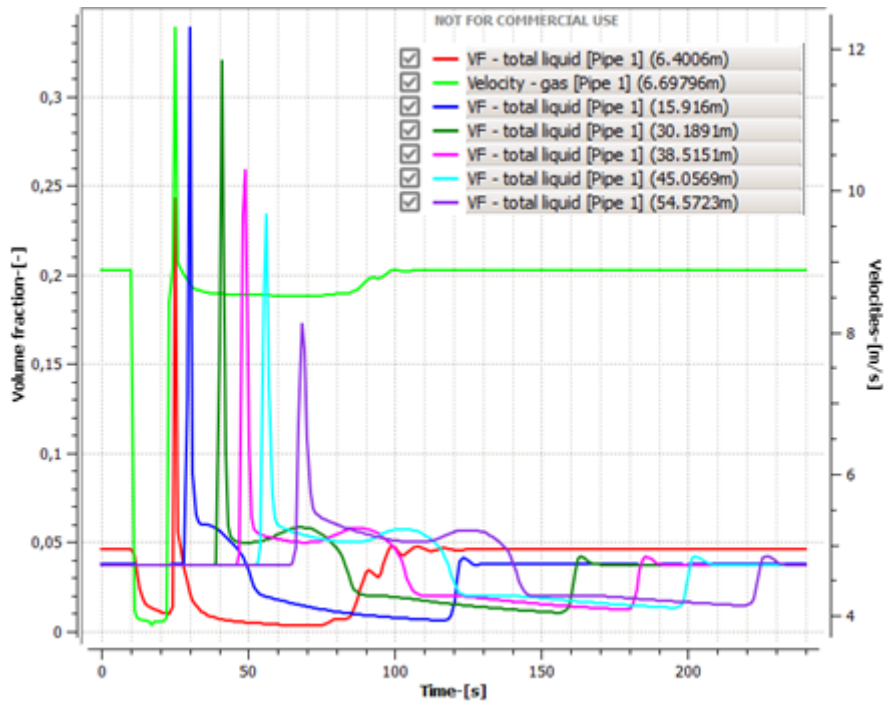


Figure A 17: LedaFlow simulation holdup trend plot of the wave. The gas velocity is plotted to visualize how the wave was initialized.

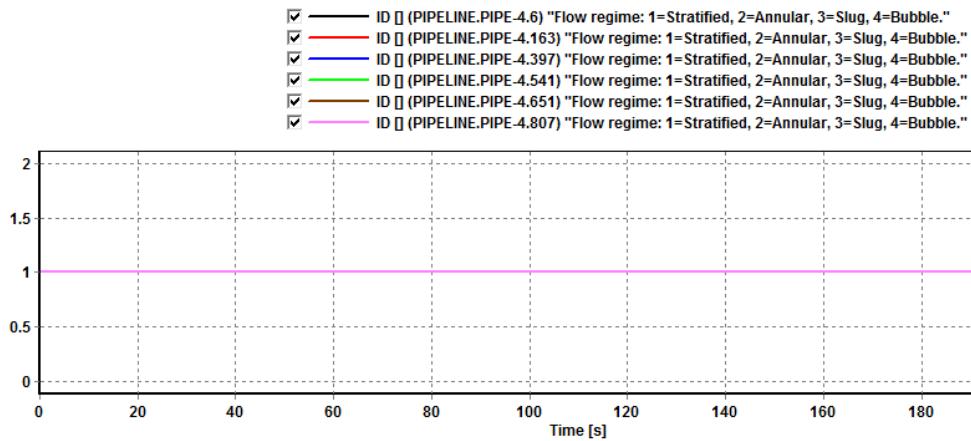


Figure A 18: OLGA flow regime ID trend plot.

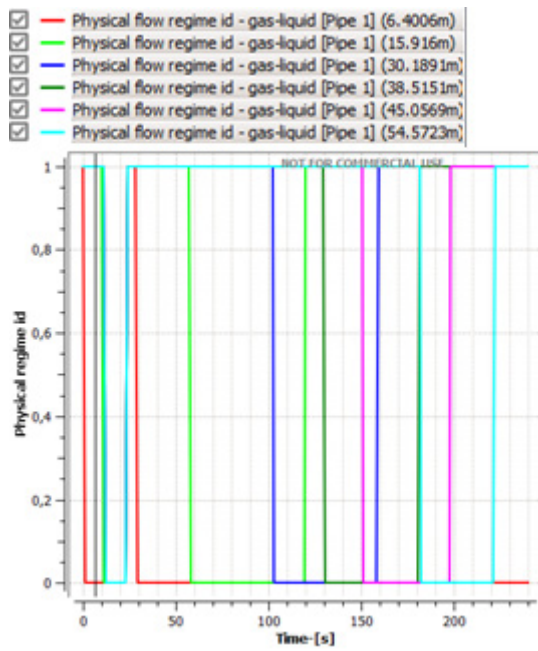


Figure A 19: LedaFlow flow regime ID trend plot. 0 = stratified smooth flow, 1 = stratified wavy flow.

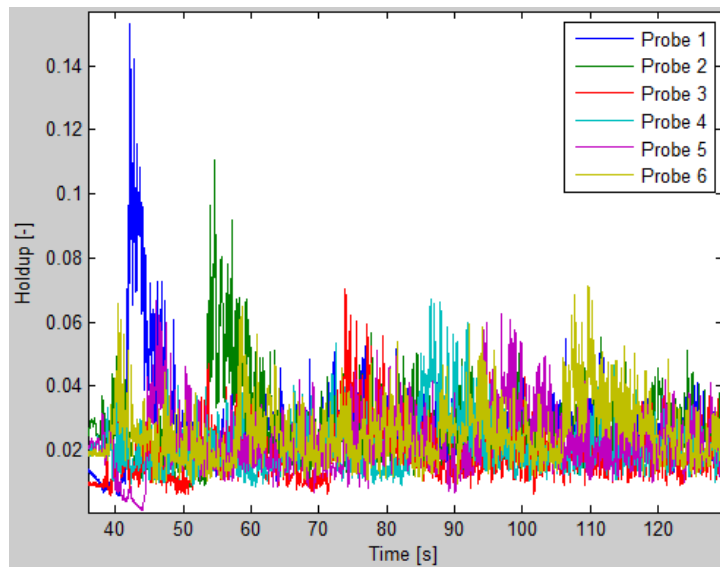


Figure A 20: Raw holdup plot.

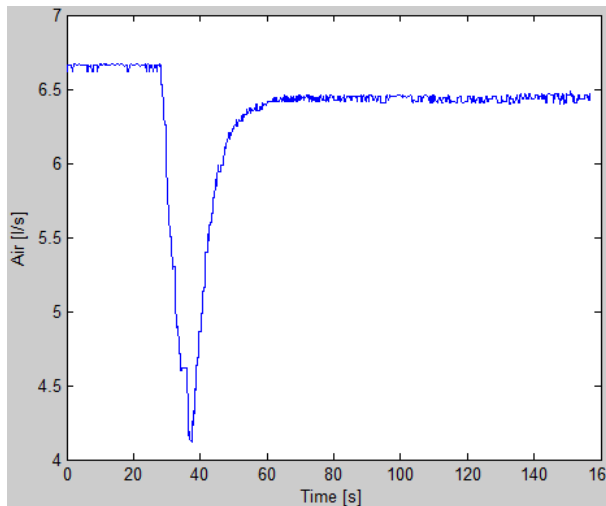


Figure A 21: Air flow rate plot.

Table A 3: The flow rates applied to initiate the wave in the simulations.

	Air source	Water source
Time [s]	Flow rate [kg/s]	Flow rate [kg/s]
0	0,029	0,032
10	0,029	0,032
11	0,013	0,032
22	0,013	0,032
23	0,029	0,032
Integration time:		220 sec
Approximate simulation duration		
OLGA:	2 x 8 min	
LedaFlow:	2 x 2 min	

Case 4: $U_{sg} = 7,6 \text{ m/s}$, $U_{sl} = 0,0113 \text{ m/s}$

The initial superficial air velocity $U_{sg} = 7,6 \text{ m/s}$. The superficial water velocity was kept constant at $U_{sl} = 0,0113 \text{ m/s}$. The large air valve was choked from 22 – 17 % of full opening and ramped up to 22 % again to initiate the wave shown in the figure A 22 below. Figure A 23, A 24 and A 25 shows the OLGA and LedaFlow simulations of the wave. Figures A 26 and

A 27 shows the flow regime ID plots predicted by OLGA and LedaFlow. Figure A 28 shows the raw holdup plot from the lab observation. Figure A 29 shows a plot of how the gas flow rate was choked and ramped up again to initiate the wave seen in figure A 22. Table A 4 shows the flow rates applied to initiate the wave in the simulations.

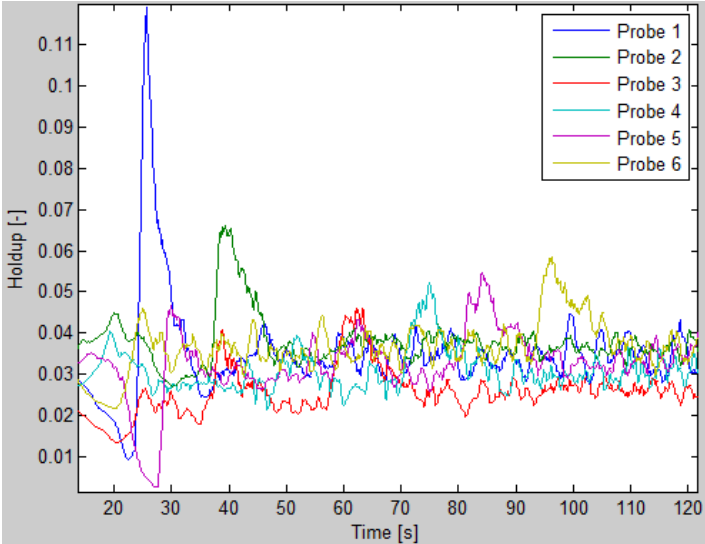


Figure A 22: : Holdup trend plot of the surge wave propagation from probe 1 to probe 6.

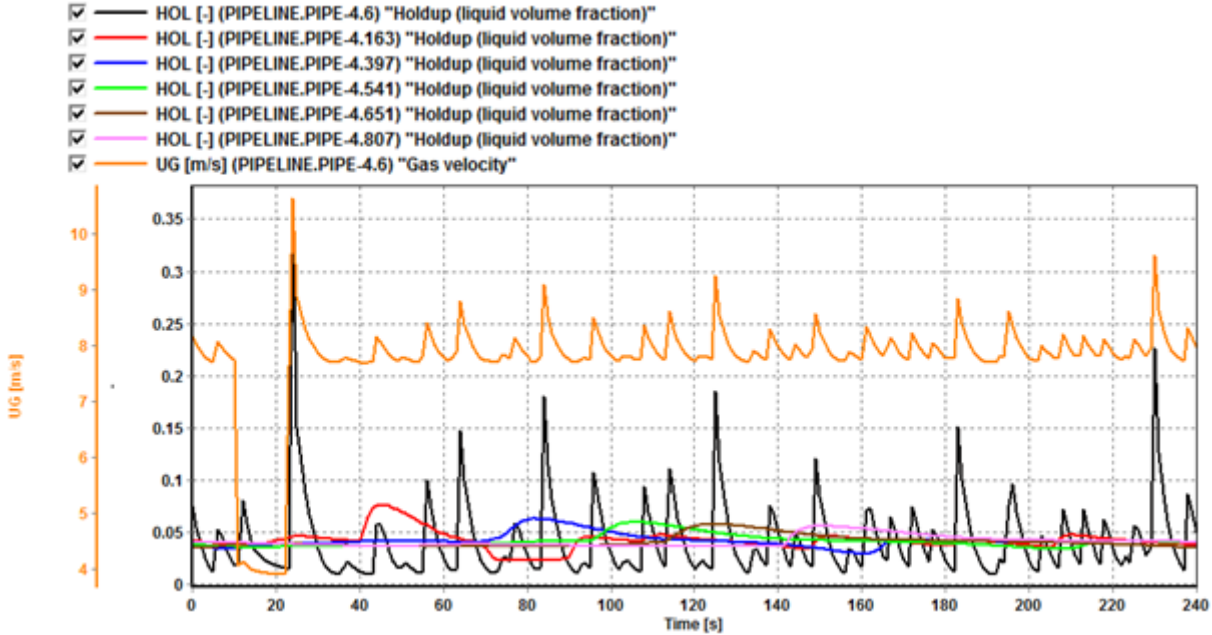


Figure A 23: OLGA simulation holdup trend plot of the wave. The gas velocity is plotted to visualize how the wave was initialized.

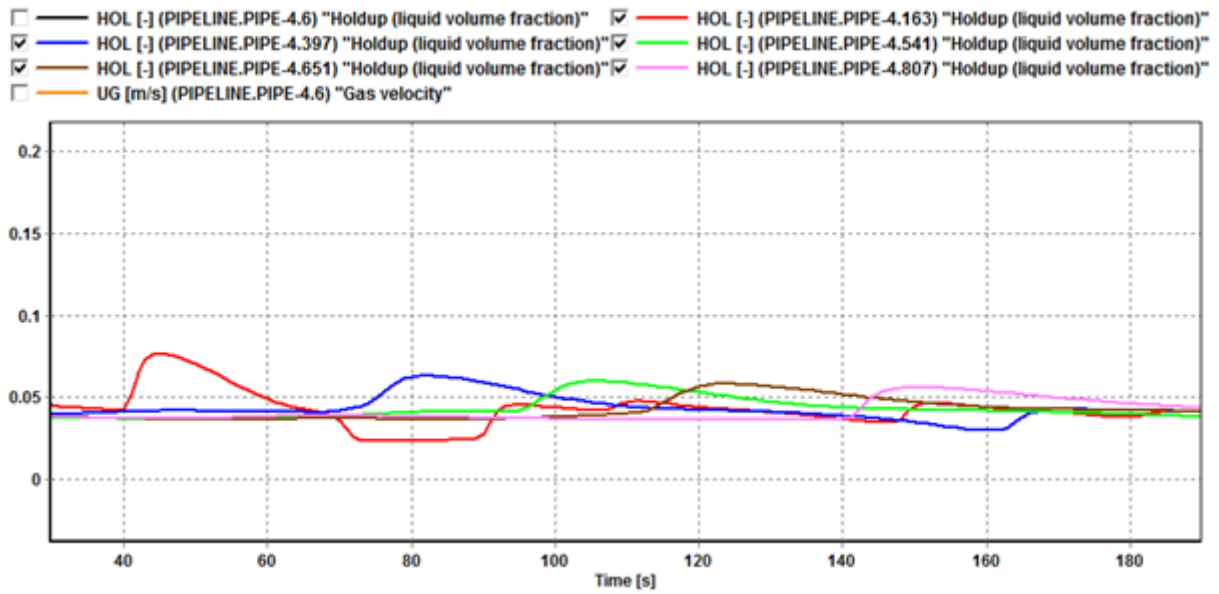


Figure A 24: OLGA simulation holdup trend plot of the wave. The plot for probe 1 and the gas velocity is excluded in order to see the wave for the sequencing probes better.

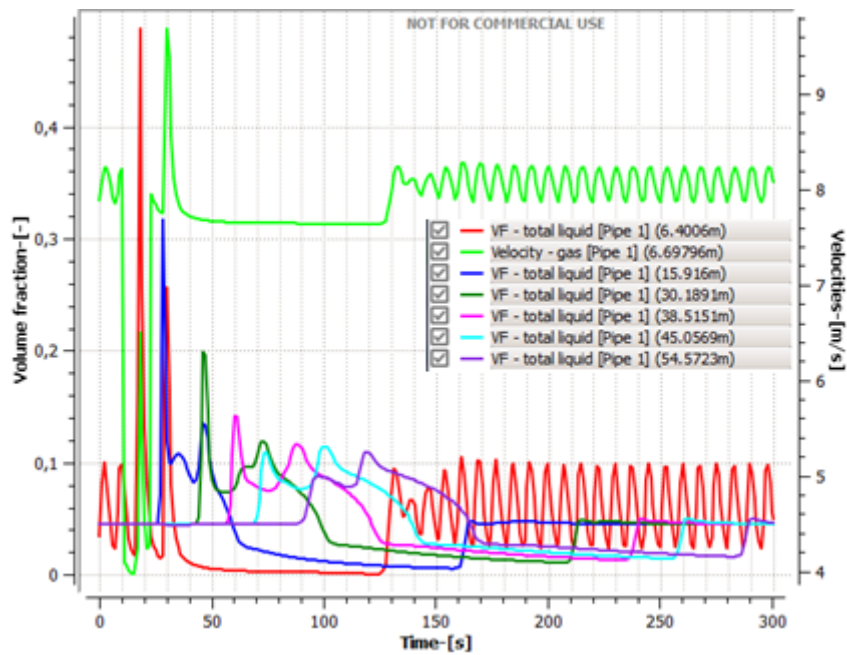


Figure A 25: LedaFlow simulation holdup trend plot of the wave.

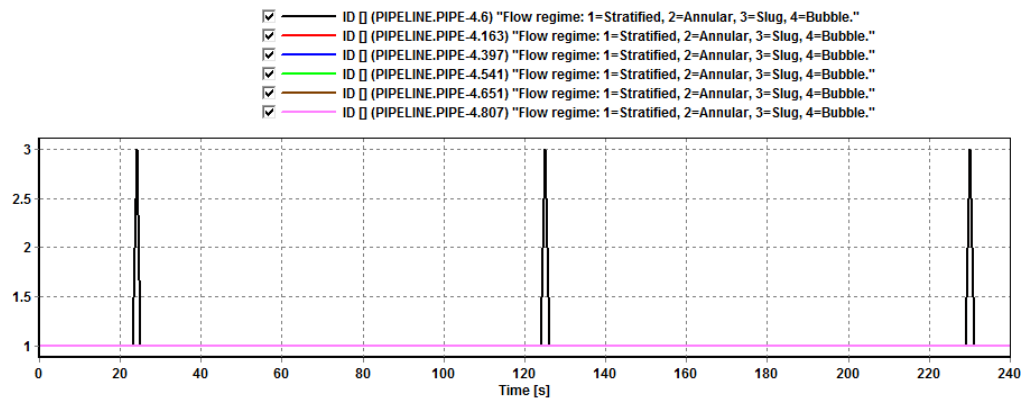


Figure A 26: OLGA flow regime ID trend plot.

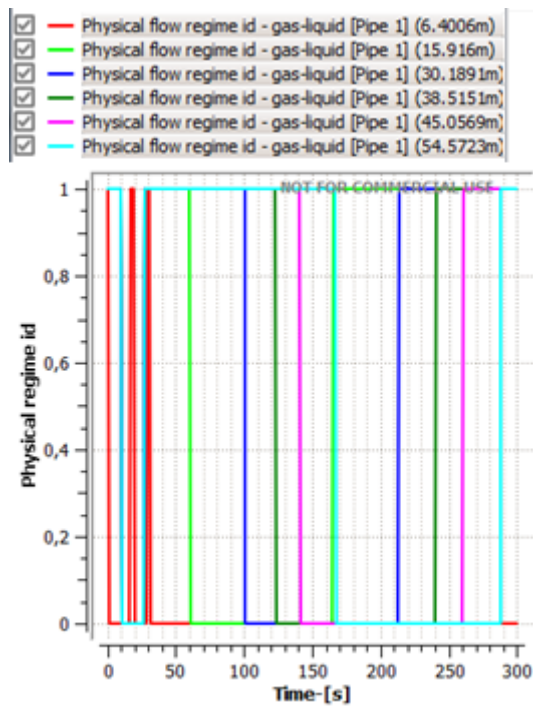


Figure A 27: LedaFlow flow regime ID trend plot. 0 = stratified smooth flow, 1 = stratified wavy flow.

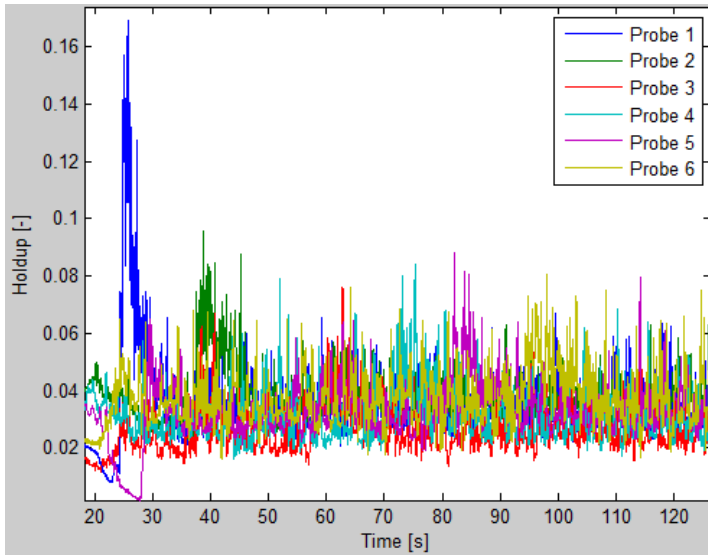


Figure A 28: Raw holdup plot.

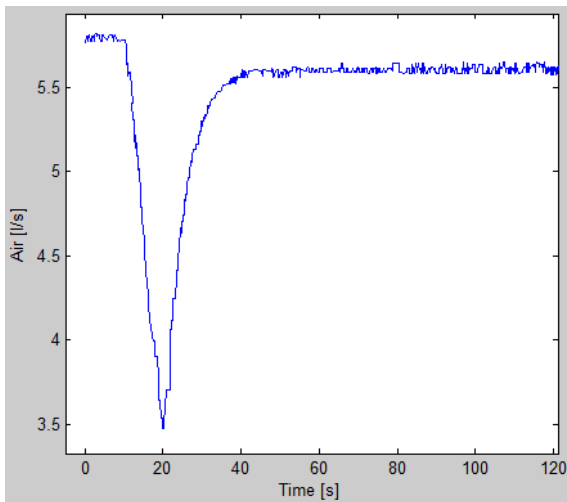


Figure A 29: Air flow rate plot.

Table A 4: The flow rates applied to initiate the wave in the simulations.

	Air source	Water source
Time [s]	Flow rate [kg/s]	Flow rate [kg/s]
0	0,026	0,032
10	0,026	0,032
11	0,013	0,032
22	0,013	0,032
23	0,026	0,032
Integration time:		240 sec
Approximate simulation duration		
OLGA:	2 x 10 min	
LedaFlow:	2 x 2 min	

Case 5: $U_{sg} = 13,4 \text{ m/s}$, $U_{sl} = 0,0264 \text{ m/s}$

The initial superficial air velocity $U_{sg} = 13,4 \text{ m/s}$, which is the highest U_{sg} that was applied. The superficial water velocity was kept constant at $U_{sl} = 0,0246 \text{ m/s}$. The large air valve was choked from 27 – 17 % of full opening and ramped up to 27 % again to initiate the wave shown in the figure A 30 below. Figure A 31 and A 32 shows the OLGA and LedaFlow simulations of the wave. Figures A 33 and A 34 shows the flow regime ID plots predicted by OLGA and LedaFlow. Figure A 35 shows the raw holdup plot from the lab observation. Figure A 36 shows a plot of how the gas flow rate was choked and ramped up again to initiate the wave seen in figure A 30. Table A 5 shows the flow rates applied to initiate the wave in the simulations.

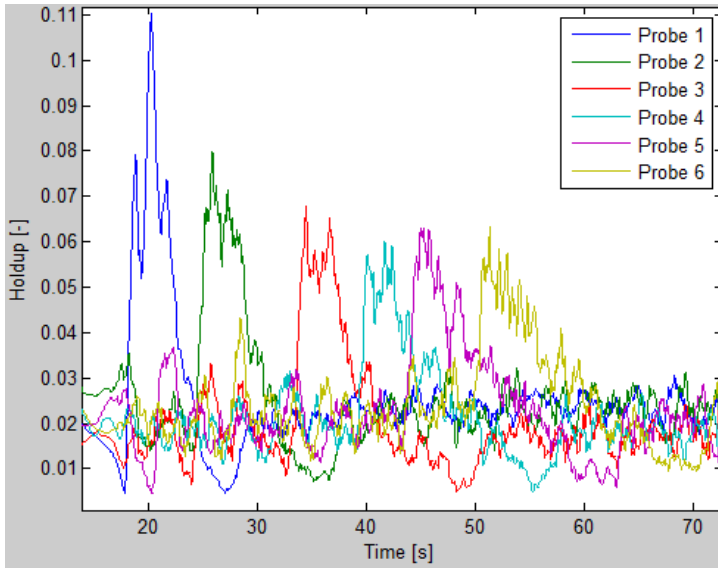


Figure A 30: Holdup trend plot of the surge wave propagation from probe 1 to probe 6.

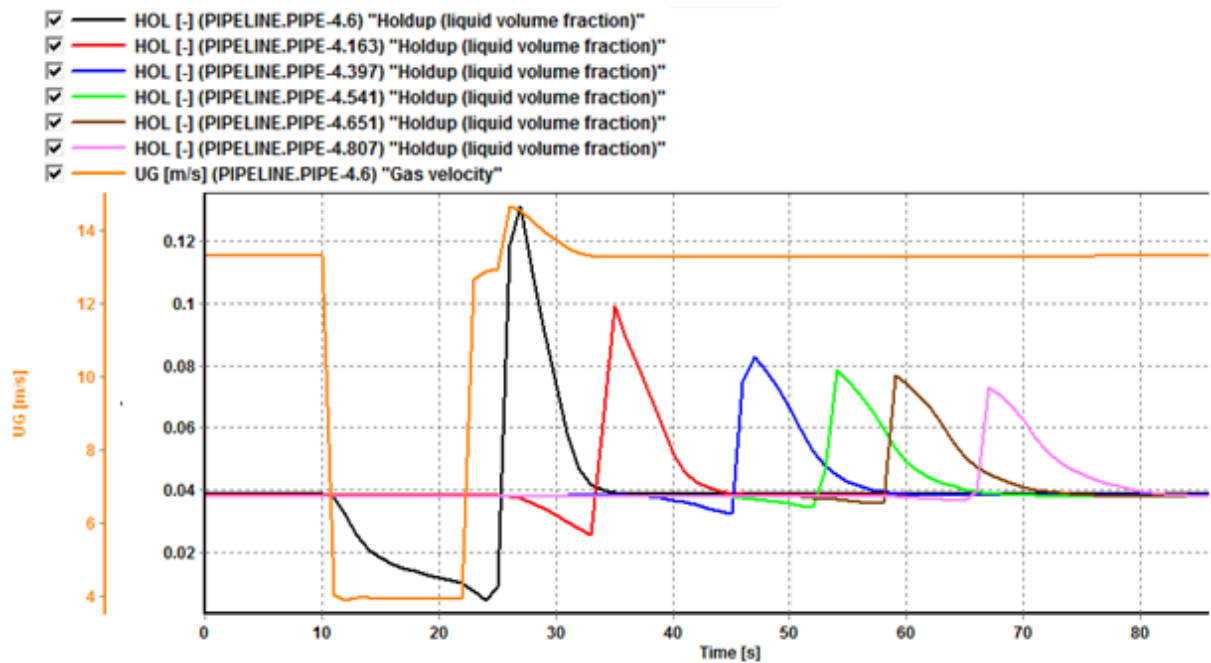


Figure A 31: OLGA simulation holdup trend plot of the wave. The gas velocity is plotted to visualize how the wave was initialized.

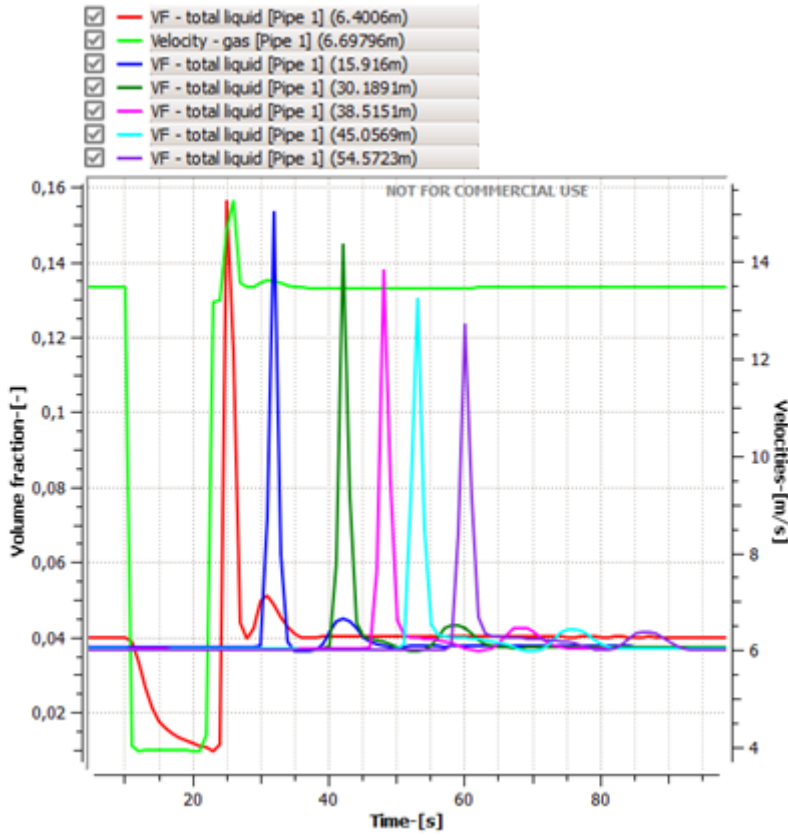


Figure A 32: LedaFlow simulation holdup trend plot of the wave. The gas velocity is plotted to visualize how the wave was initialized.

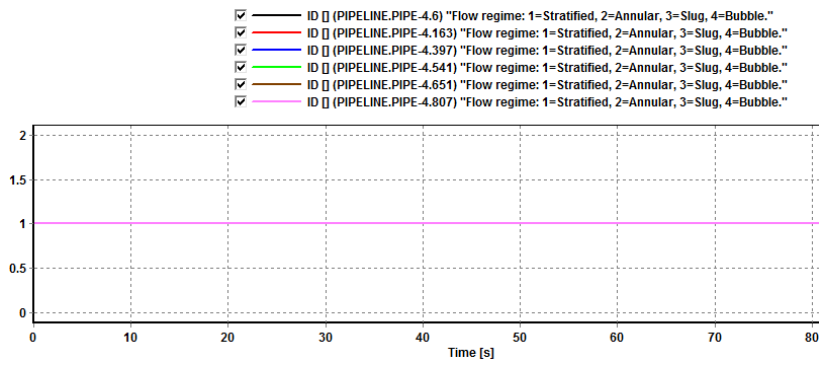


Figure A 33: OLGA flow regime ID trend plot.

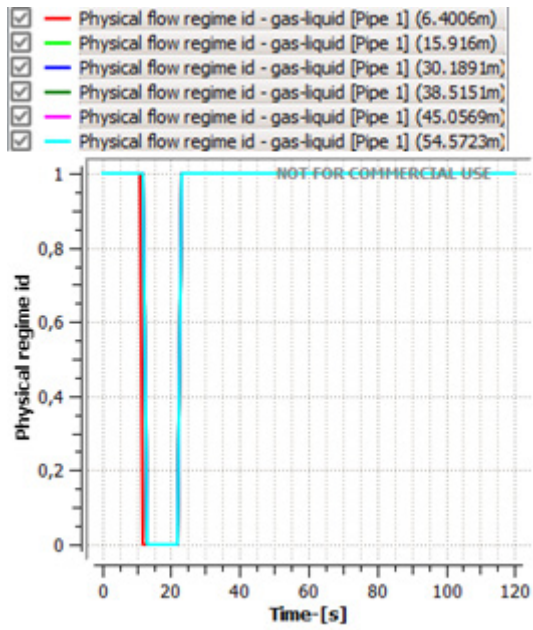


Figure A 34: LedaFlow flow regime ID trend plot. 0 = stratified smooth flow, 1 = stratified wavy flow.

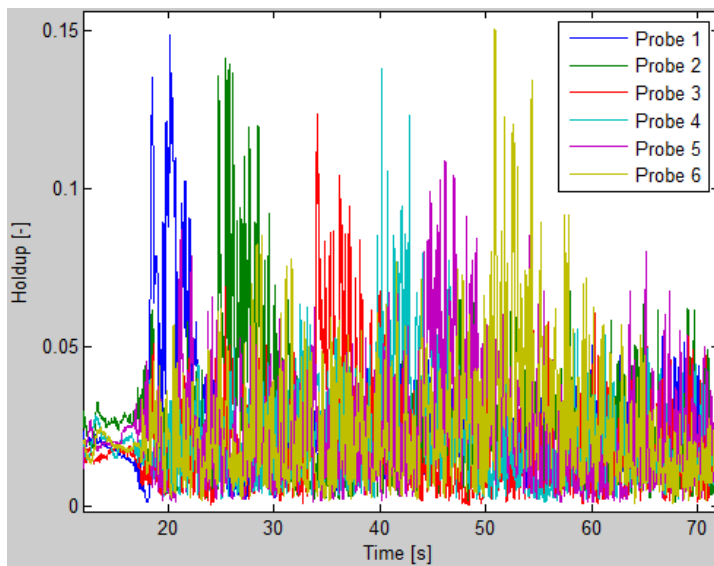


Figure A 35: Raw holdup plot.

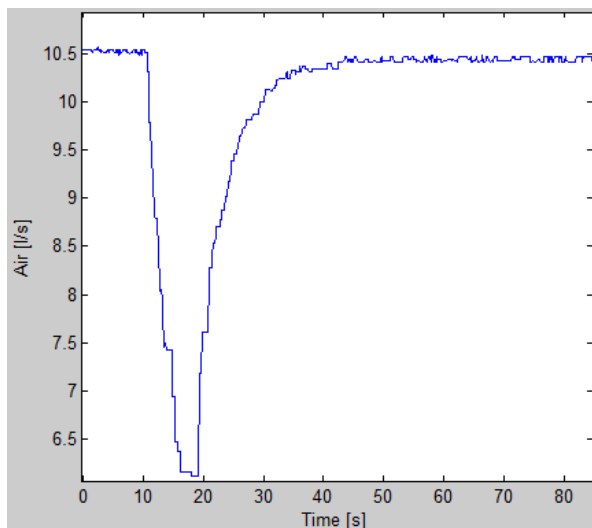


Figure A 36: Air flow rate plot.

Table A 5: The flow rates applied to initiate the wave in the simulations.

	Air source	Water source
Time [s]	Flow rate [kg/s]	Flow rate [kg/s]
0	0,045	0,075
10	0,045	0,075
11	0,013	0,075
22	0,013	0,075
23	0,045	0,075
Integration time:		100 sec
Approximate simulation duration		
OLGA:	2 x 4,5 min	
LedaFlow:	2 x 1 min	

Case 6: $U_{sg} = 10,9 \text{ m/s}$, $U_{sl} = 0,0264 \text{ m/s}$

The initial superficial air velocity $U_{sg} = 10,9 \text{ m/s}$. The superficial water velocity was kept constant at $U_{sl} = 0,0264 \text{ m/s}$. The large air valve was choked from 25 – 17 % of full opening and ramped up to 25 % again to initiate the wave shown in the figure A 37 below. Figure A 38 and A 39 shows the OLGA and LedaFlow simulations of the wave. Figures A 40 and A 41 shows the flow regime ID plots predicted by OLGA and LedaFlow. Figure A 42 shows the raw holdup plot from the lab observation. Figure A 43 shows a plot of how the gas flow rate was choked and ramped up again to initiate the wave seen in figure A 37. Table A 6 shows the flow rates applied to initiate the wave in the simulations.

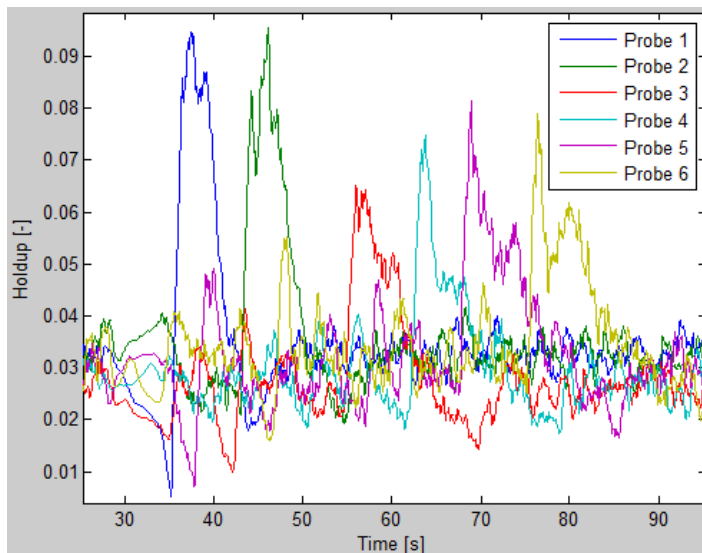


Figure A 37: Holdup trend plot of the surge wave propagation from probe 1 to probe 6.

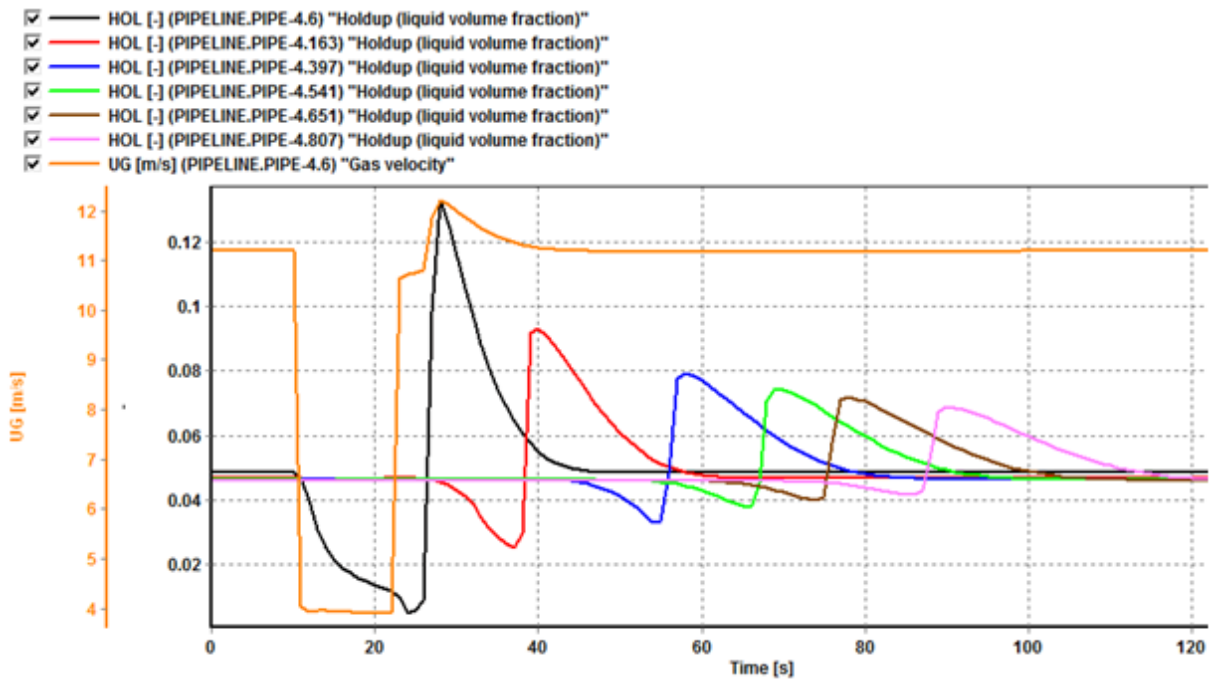


Figure A 38: OLGA simulation holdup trend plot of the wave. The gas velocity is plotted to visualize how the wave was initialized.

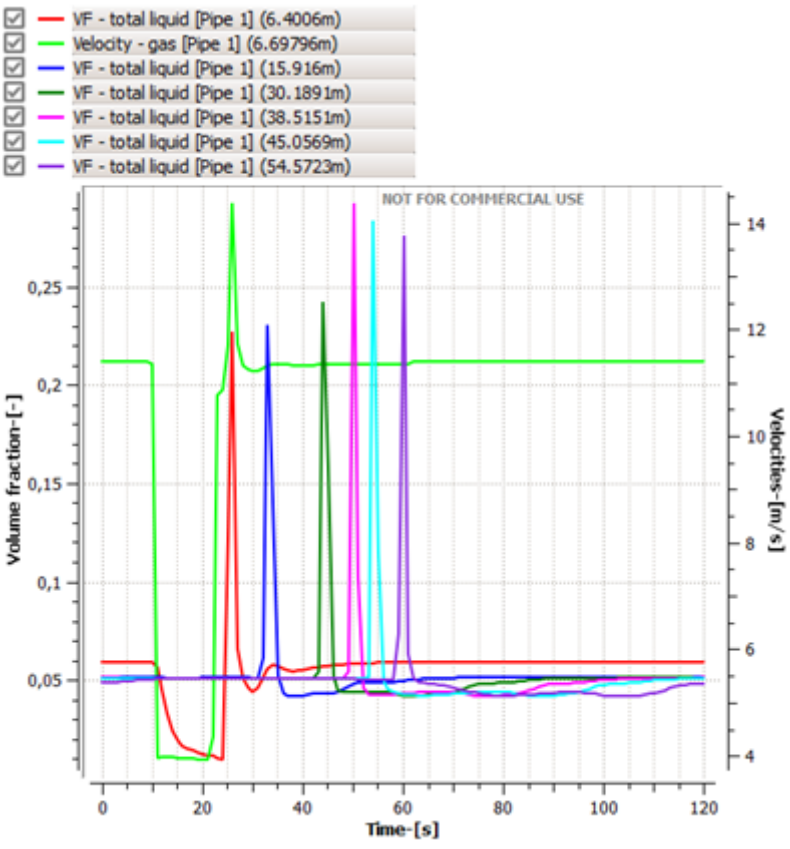


Figure A 39: LedaFlow simulation holdup trend plot of the wave. The gas velocity is plotted to visualize how the wave was initialized.

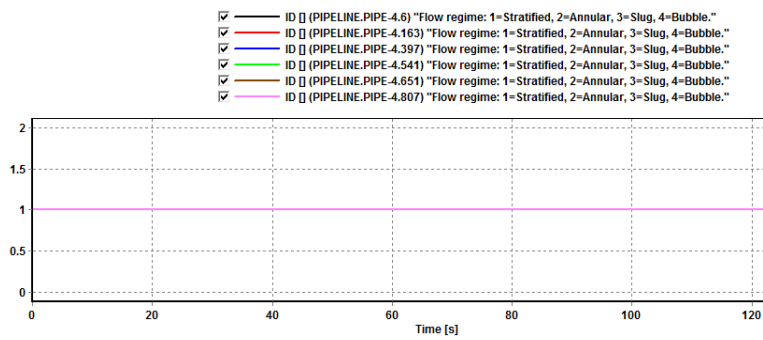


Figure A 40: OLGA flow regime ID trend plot.

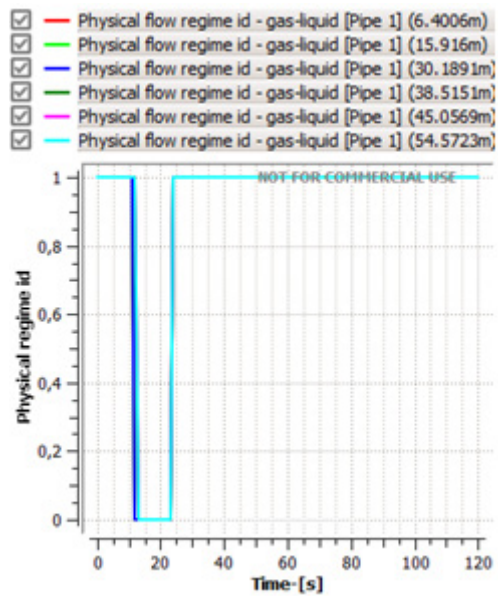


Figure A 41: LedaFlow flow regime ID trend plot. 0 = stratified smooth flow, 1 = stratified wavy flow.

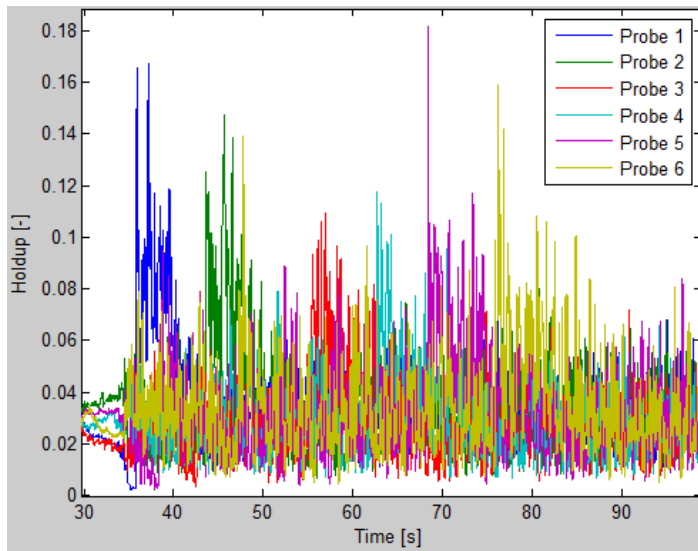


Figure A 42: Raw holdup plot.

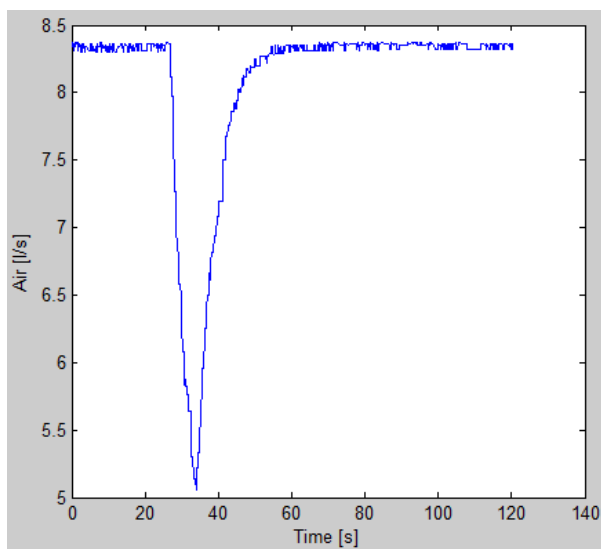


Figure A 43: Air flow rate plot.

Table A 6: The flow rates applied to initiate the wave in the simulations.

	Air source	Water source
Time [s]	Flow rate [kg/s]	Flow rate [kg/s]
0	0,037	0,075
10	0,037	0,075
11	0,013	0,075
22	0,013	0,075
23	0,037	0,075
Integration time:		135 sec
Approximate simulation duration		
OLGA:	2 x 6 min	
LedaFlow:	2 x 1 min	

Case 7: $U_{sg} = 8,5$ m/s, $U_{sl} = 0,0264$ m/s

The initial superficial air velocity $U_{sg} = 8,5$ m/s. The superficial water velocity was kept constant at $U_{sl} = 0,0264$ m/s. The large air valve was choked from 23 – 17 % of full opening and ramped up to 23 % again to initiate the wave shown in the figure A 44 below. Figure A 45 and A 46 shows the OLGA and LedaFlow simulations of the wave. Figures A 47 and A 48 shows the flow regime ID plots predicted by OLGA and LedaFlow. Figure A 49 shows the raw holdup plot from the lab observation. Figure A 50 shows a plot of how the gas flow rate was choked and ramped up again to initiate the wave seen in figure A 44. Table A 7 shows the flow rates applied to initiate the wave in the simulations.

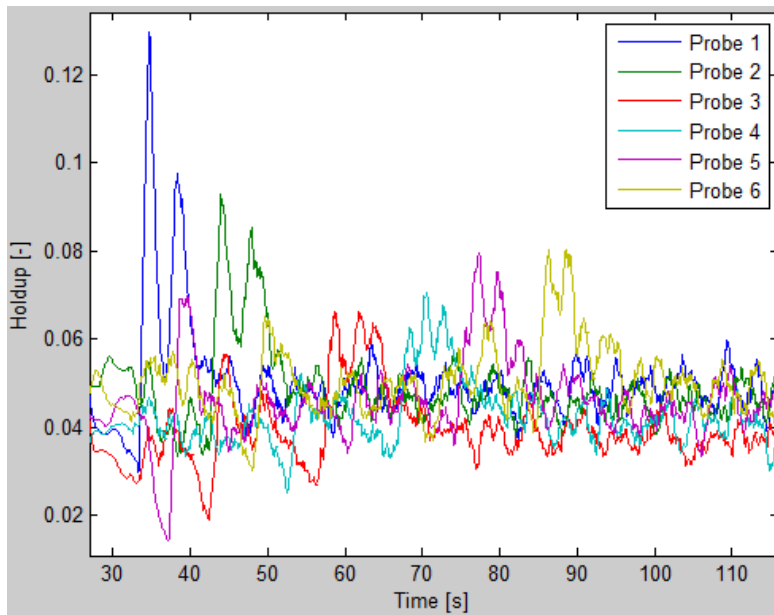


Figure A 44: Holdup trend plot of the surge wave propagation from probe 1 to probe 6.

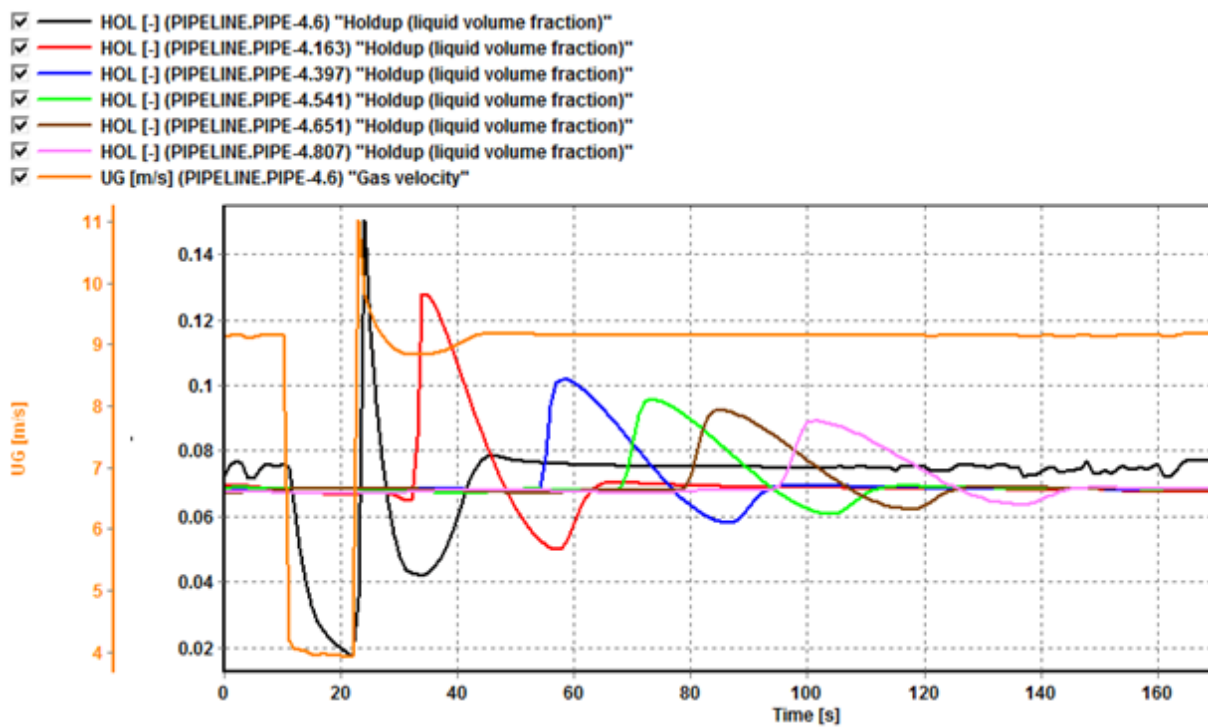


Figure A 45: OLGA simulation holdup trend plot of the wave. The gas velocity is plotted to visualize how the wave was initialized.

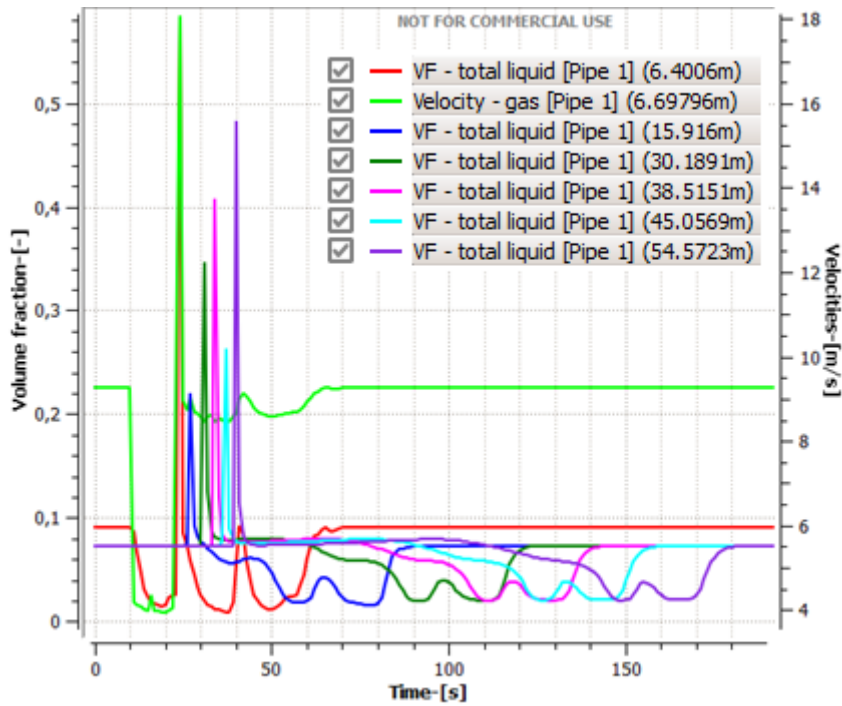


Figure A 46: LedaFlow simulation holdup trend plot of the wave. The gas velocity is plotted to visualize how the wave was initialized.

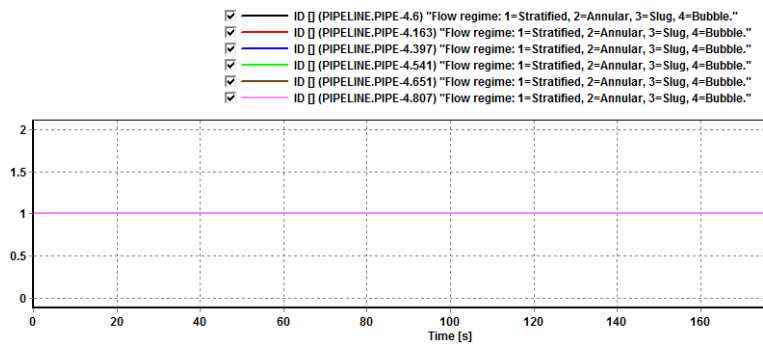


Figure A 47: OLGA flow regime ID trend plot.

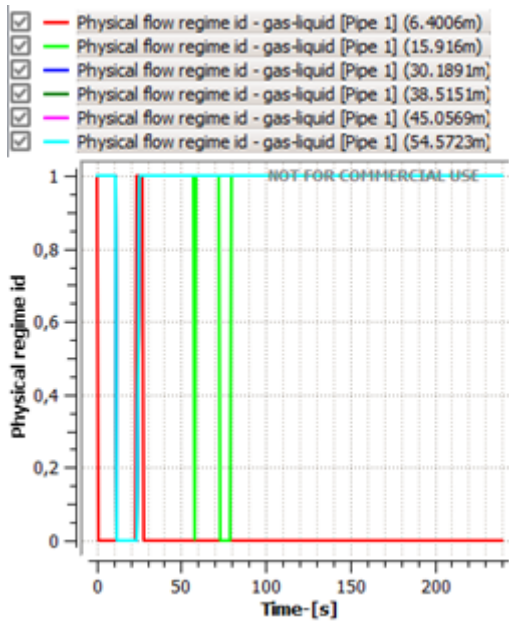


Figure A 48: LedaFlow flow regime ID trend plot. 0 = stratified smooth flow, 1 = stratified wavy flow.

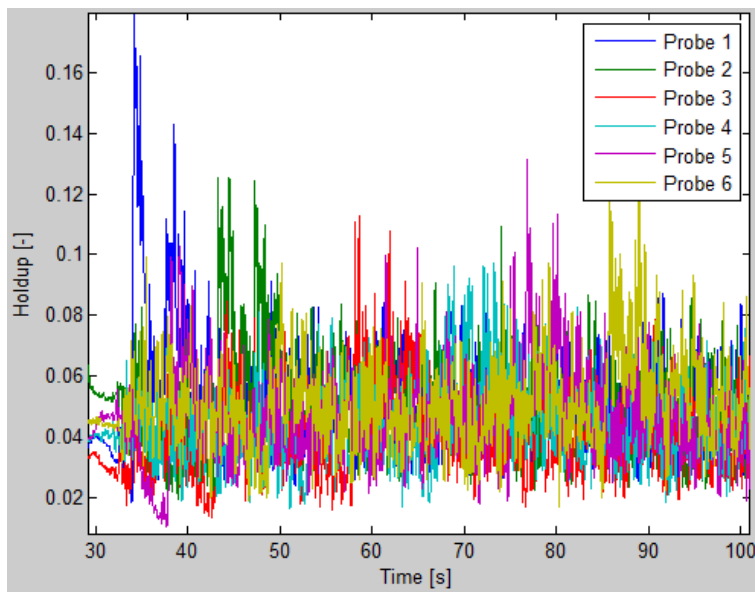


Figure A 49: Raw holdup plot.

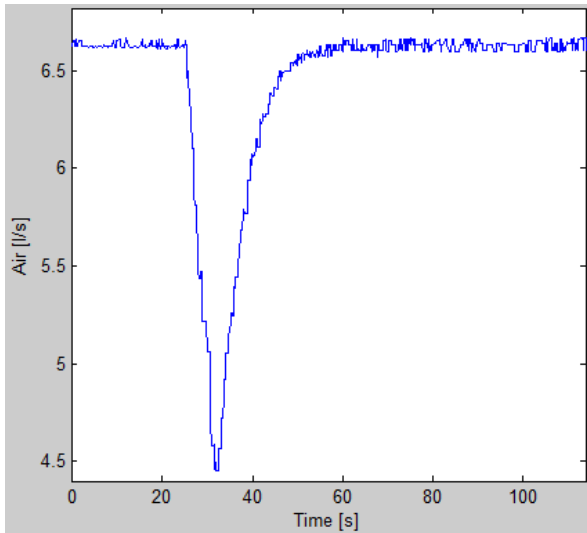


Figure A 50: Air flow rate plot.

Table A 7: The flow rates applied to initiate the wave in the simulations.

	Air source	Water source
Time [s]	Flow rate [kg/s]	Flow rate [kg/s]
0	0,029	0,075
10	0,029	0,075
11	0,013	0,075
22	0,013	0,075
23	0,029	0,075
Integration time:		200 sec
Approximate simulation duration		
OLGA:	2 x 8 min	
LedaFlow:	2 x 2 min	

Case 8: $U_{sg} = 7,4 \text{ m/s}$, $U_{sl} = 0,0264 \text{ m/s}$

The initial superficial air velocity $U_{sg} = 7,4 \text{ m/s}$, which is the lowest U_{sg} applied. The superficial water velocity was kept constant at $U_{sl} = 0,0264 \text{ m/s}$. The large air valve was choked from 22 – 17 % of full opening and ramped up to 22 % again to initiate the wave shown in the figure A 51 below. Figure A 52, A 53 and A 54 shows the OLGA and LedaFlow simulations of the wave. Figures A 55 and A 56 shows the flow regime ID plots predicted by OLGA and LedaFlow. Figure A 57 shows the raw holdup plot from the lab observation. Figure A 58 shows a plot of how the gas flow rate was choked and ramped up again to initiate the wave seen in figure A 51. Table A 8 shows the flow rates applied to initiate the wave in the simulations.

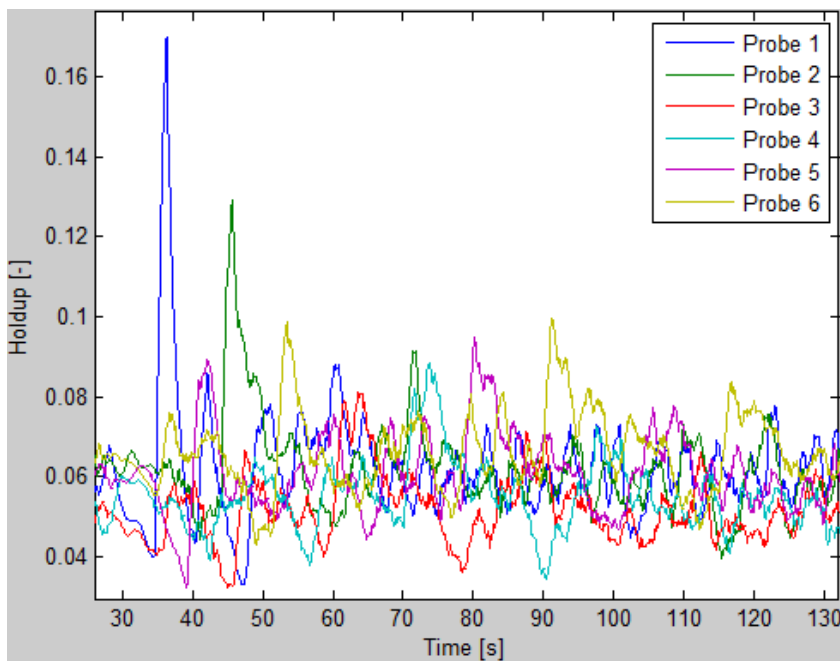


Figure A 51: Holdup trend plot of the surge wave propagation from probe 1 to probe 6.

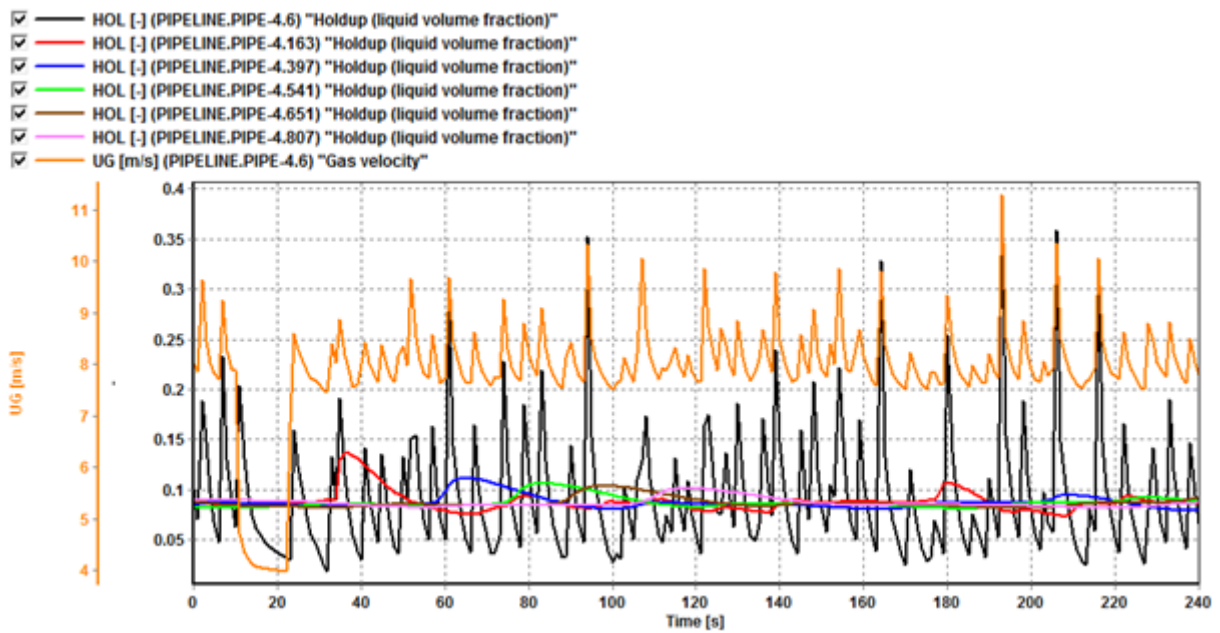


Figure A 52: OLGA simulation holdup trend plot of the wave. The gas velocity is plotted to visualize how the wave was initialized.

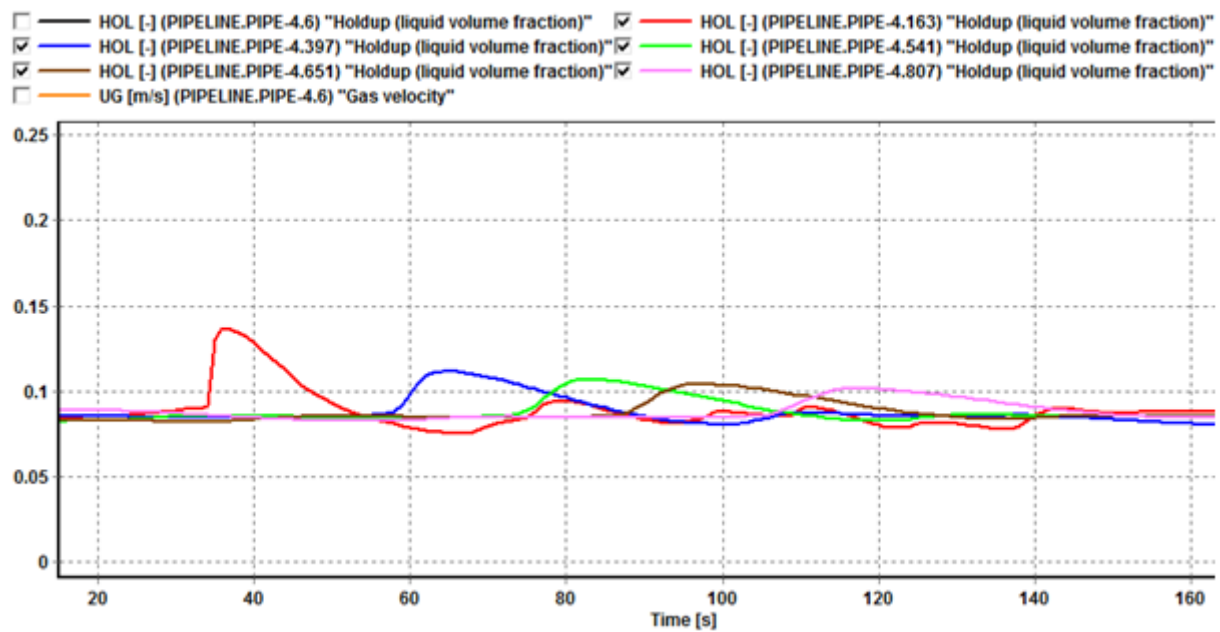


Figure A 53: OLGA simulation holdup trend plot of the wave. The plot for probe 1 and the gas velocity is excluded in order to see the wave for the sequencing probes better.

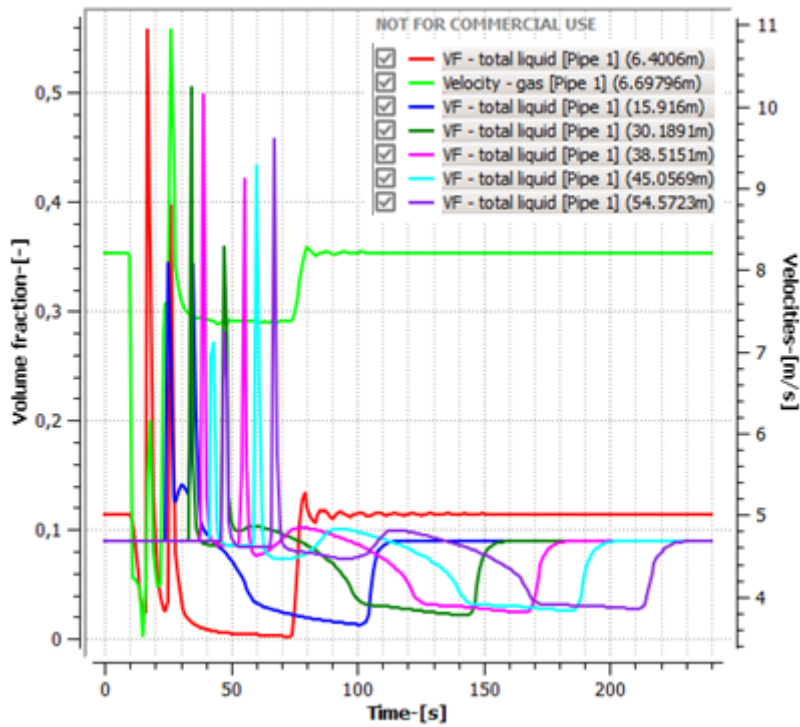


Figure A 54: LedaFlow simulation holdup trend plot of the wave. The gas velocity is plotted to visualize how the wave was initialized.

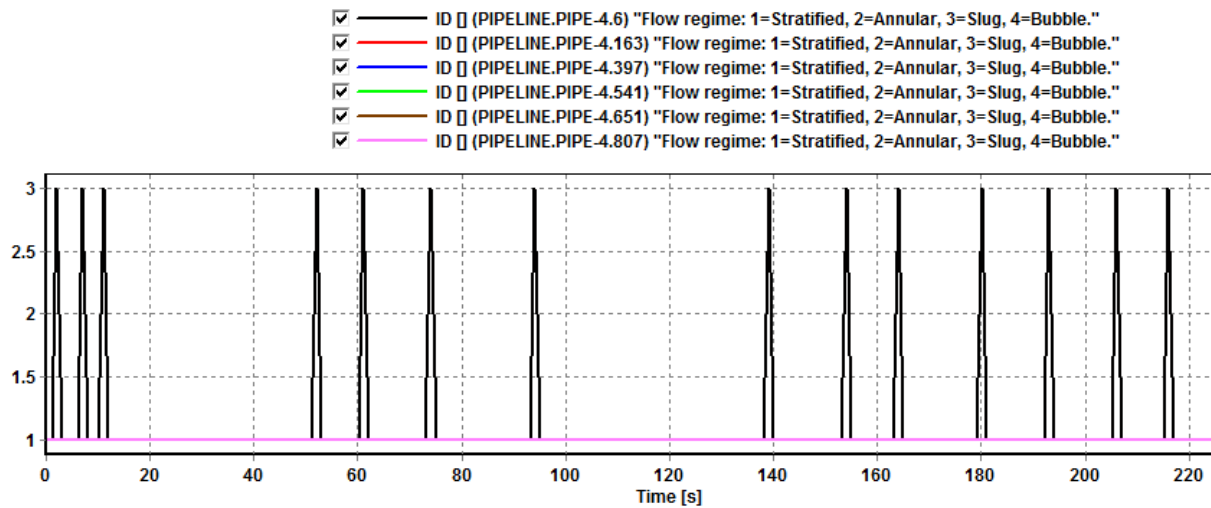


Figure A 55: OLGA flow regime ID trend plot.

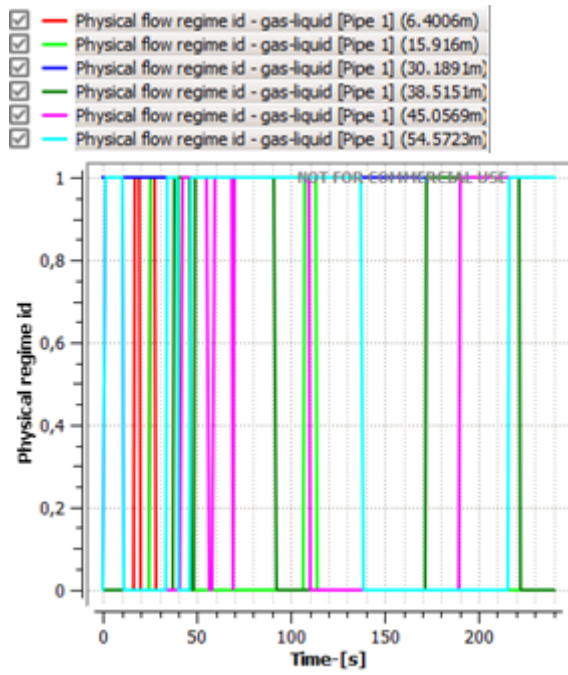


Figure A 56: LedaFlow flow regime ID trend plot. 0 = stratified smooth flow, 1 = stratified wavy flow.

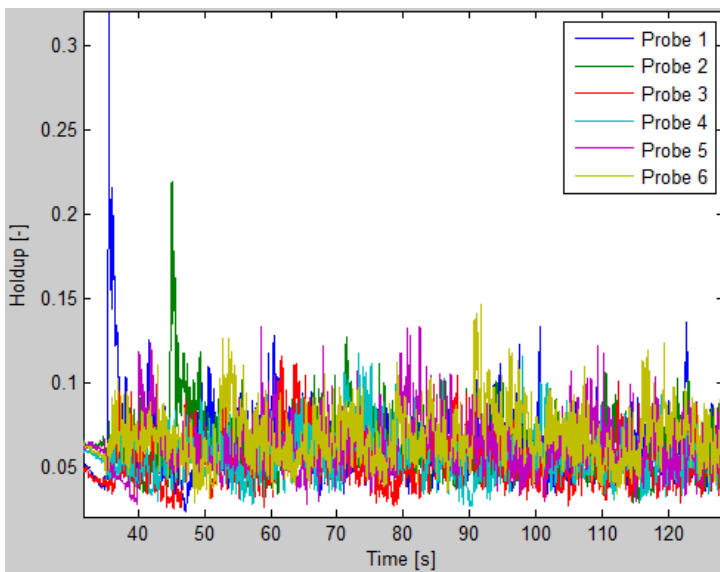


Figure A 57: Raw holdup plot.

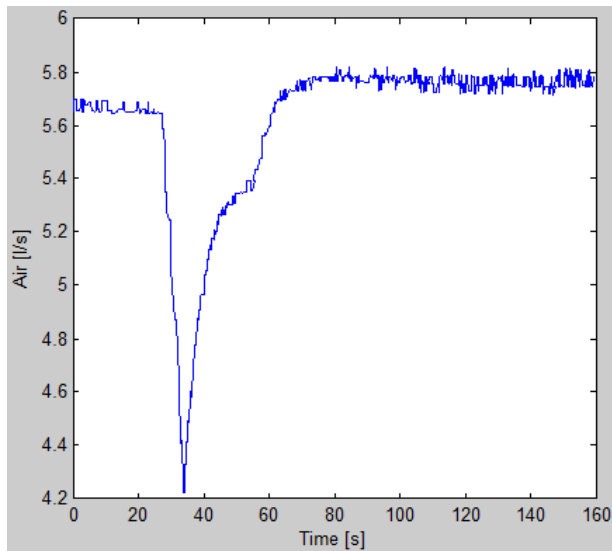


Figure A 58: Air flow rate plot.

Table A 8: The flow rates applied to initiate the wave in the simulations.

	Air source	Water source
Time [s]	Flow rate [kg/s]	Flow rate [kg/s]
0	0,025	0,075
10	0,025	0,075
11	0,013	0,075
22	0,013	0,075
23	0,025	0,075
Integration time:		240 sec
Approximate simulation duration		
OLGA:	2 x 10 min	
LedaFlow:	2 x 2 min	

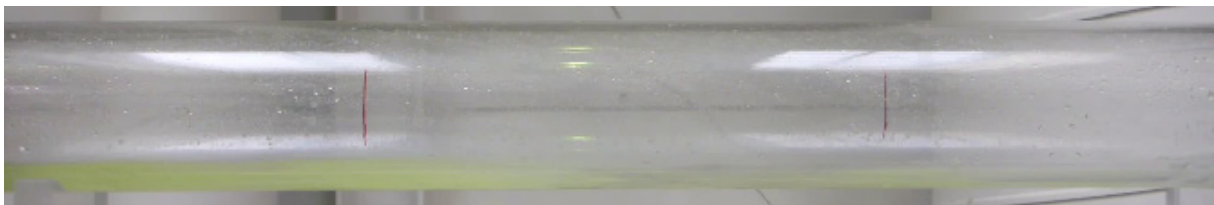
Appendix B: Camera screenshots

Three cameras were positioned along the pipeline, at 6,85 m, 30,54 m and 55,02 m behind the inlet nozzle respectively, see figure 25. All the waves were recorded and screenshots of the waves for all the eight cases presented in Appendix A are presented below.

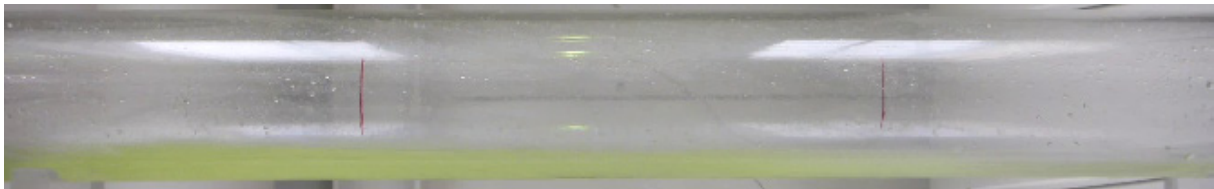
Case 1: $U_{sg} = 13,4 \text{ m/s}$, $U_{sl} = 0,0113 \text{ m/s}$

Camera 1:

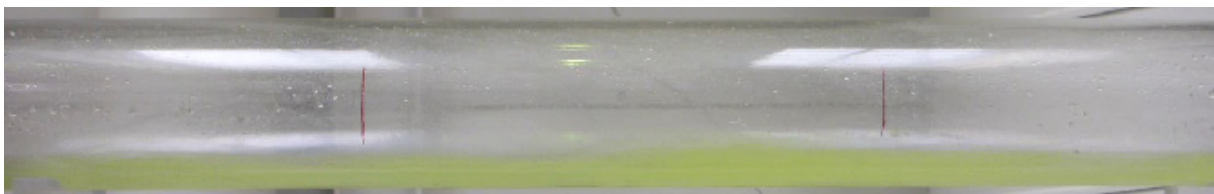
The wave moves from the left to the right in the images.



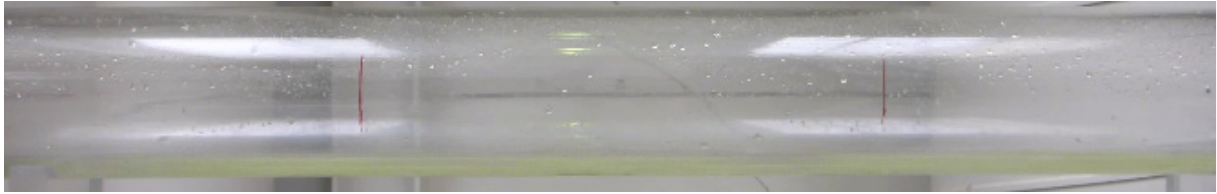
The wave front is coming.



The wave front is passing.



The wave peak is passing.



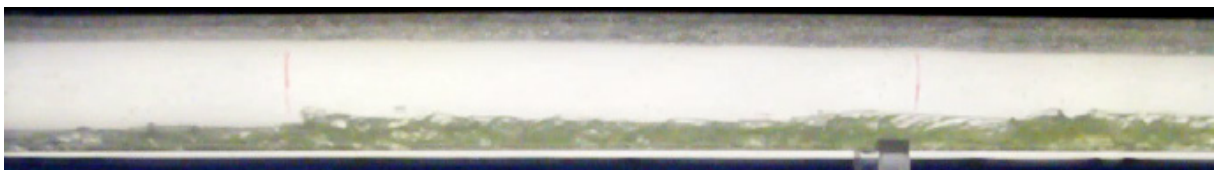
The wave has passed and steady state stratified flow is reestablished.

Camera 2:

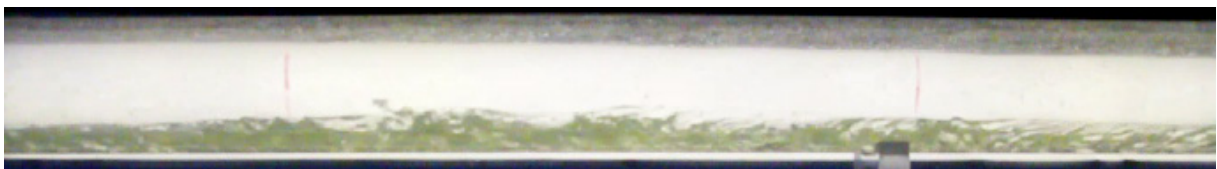
The wave moves from the right to the left in the images.



The wave front is coming.



The wave front is passing.



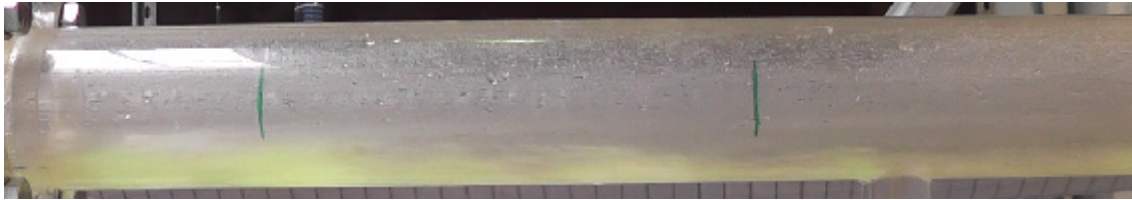
The wave peak is passing.



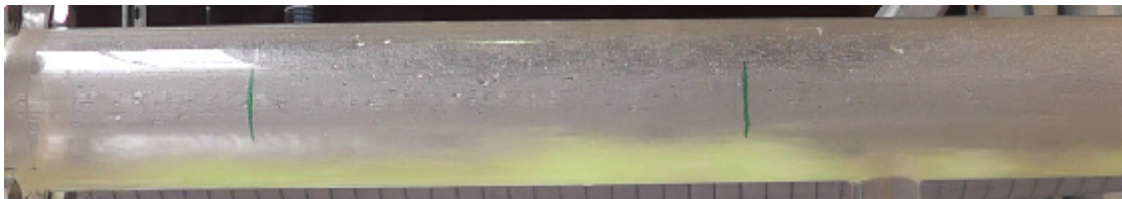
The wave has passed and steady state stratified flow is reestablished.

Camera 3:

The wave moves from the left to the right in the images.



The wave front is coming.



The wave front and peak is passing.



The wave has passed and steady state stratified flow is reestablished.

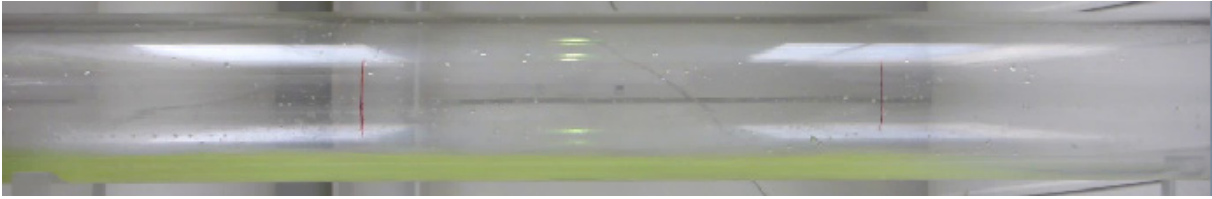
Case 2: $U_{sg} = 10,9 \text{ m/s}$, $U_{sl} = 0,0113 \text{ m/s}$

Camera 1:

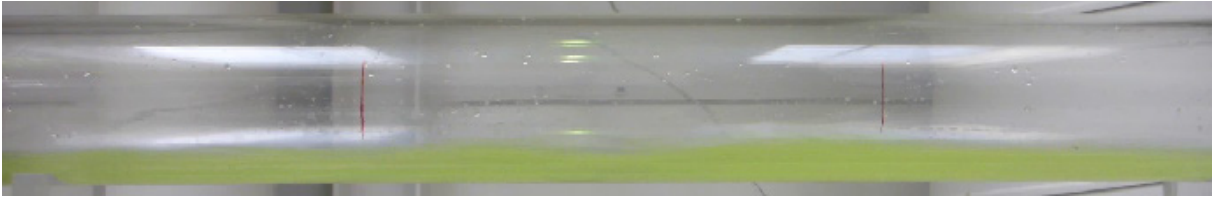
The wave moves from the left to the right in the images.



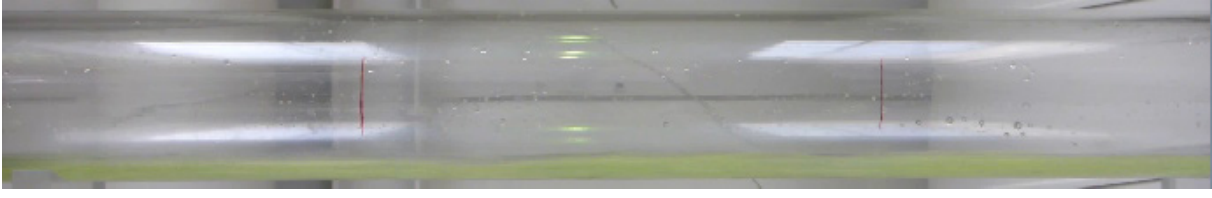
The wave front is coming.



The wave front is passing.



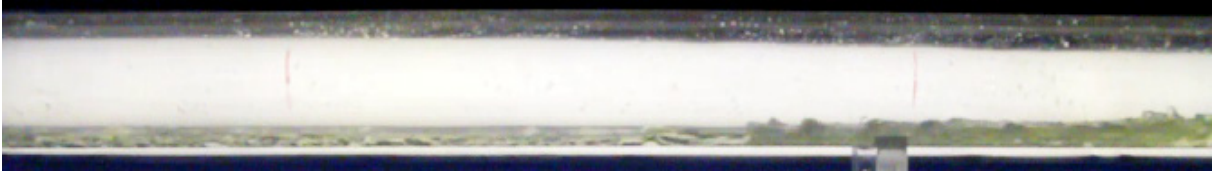
The wave peak is passing.



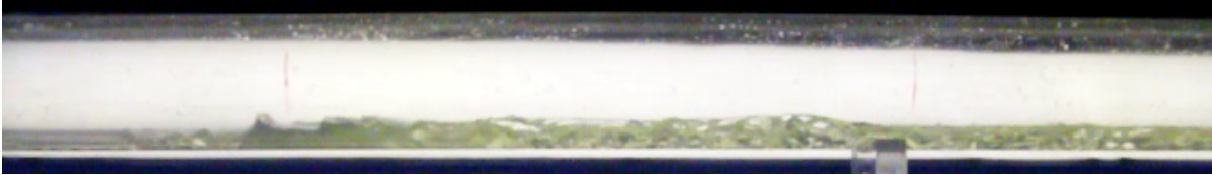
The wave has passed and steady state stratified flow is reestablished.

Camera 2:

The wave moves from the right to the left in the images.



The wave front is coming.



The wave front is passing.



The wave peak is passing.



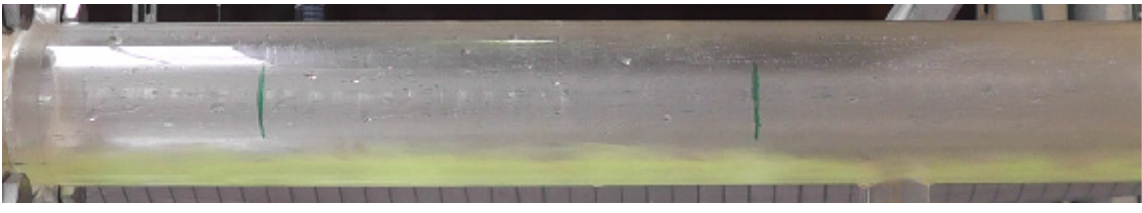
The wave has passed and steady state stratified flow is reestablished.

Camera 3:

The wave moves from the left to the right in the images.



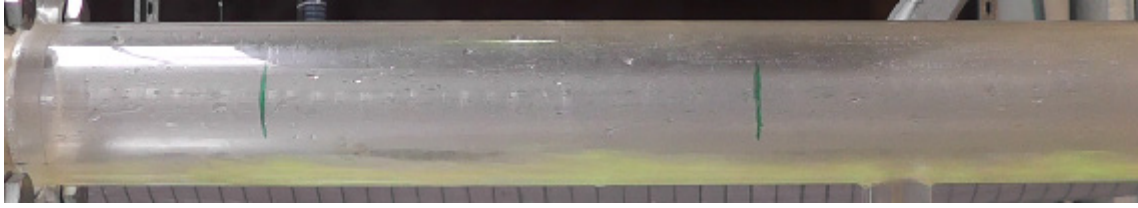
The wave front is coming.



The wave front is passing.



The wave peak is passing.



The wave has passed and steady state stratified flow is reestablished.

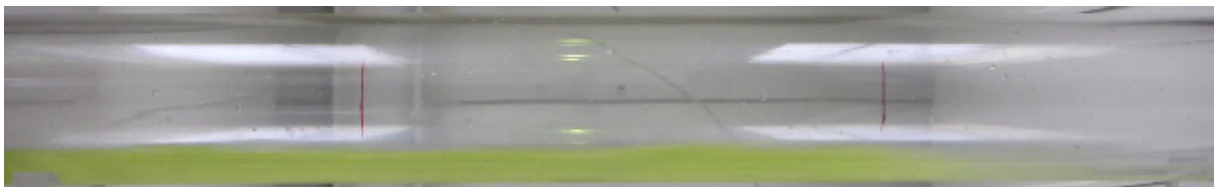
Case 3: $U_{sg} = 8,5 \text{ m/s}$, $U_{sl} = 0,0113 \text{ m/s}$

Camera 1:

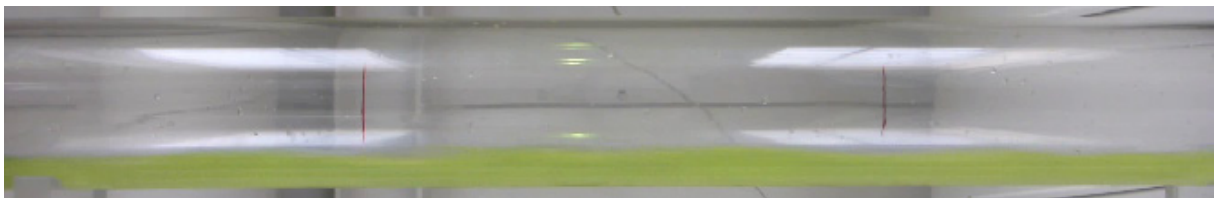
The wave moves from the left to the right in the images.



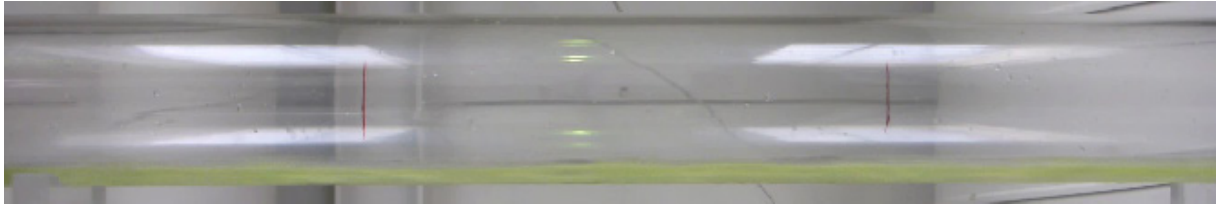
The wave front is coming.



The wave front is passing.



The wave peak is passing.



The wave has passed and steady state stratified flow is reestablished.

Camera 2:

The wave moves from the right to the left in the images.



The wave front is coming.



The wave front is passing.



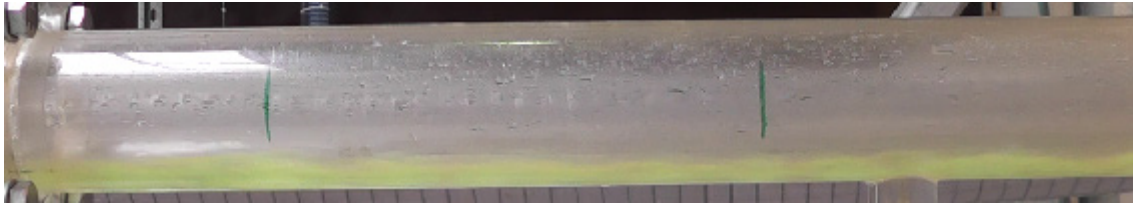
The wave peak is passing.



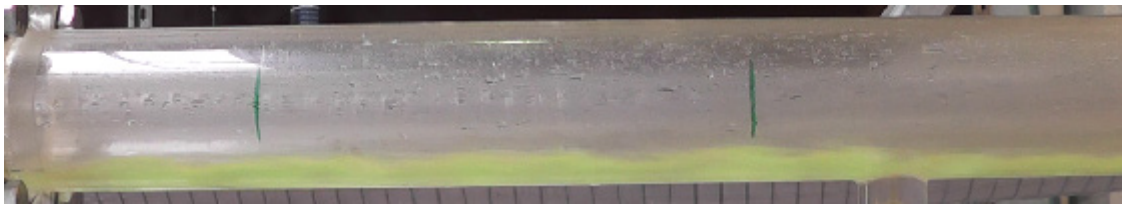
The wave has passed and steady state stratified flow is reestablished.

Camera 3:

The wave moves from the left to the right in the images.



The wave front is coming.



The wave front and peak is passing.

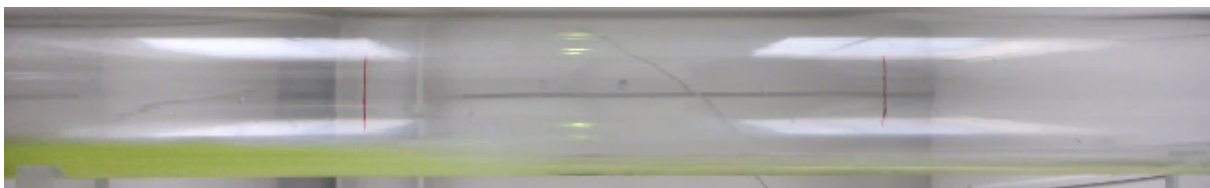


The wave has passed and steady state stratified flow is reestablished.

Case 4: $U_{sg} = 7,6 \text{ m/s}$, $U_{sl} = 0,0113 \text{ m/s}$

Camera 1:

The wave moves from the left to the right in the images.



The wave front is coming.



The wave front is passing.



The wave peak is passing.



The wave has passed and steady state stratified flow is reestablished.

Camera 2:

The wave moves from the right to the left in the images.



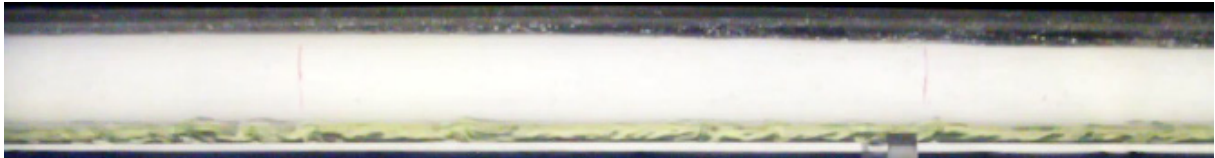
The wave front is coming.



The wave front is passing.



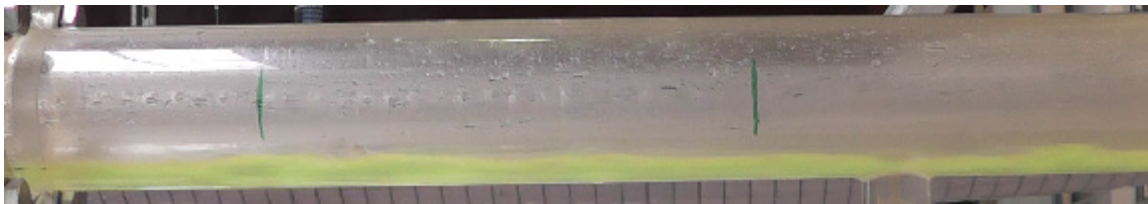
The wave peak is passing.



The wave has passed and steady state stratified flow is reestablished.

Camera 3:

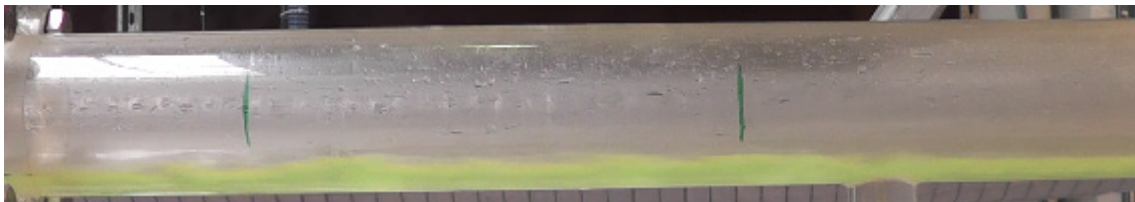
The wave moves from the left to the right in the images.



The wave front is coming.



The wave front is passing.



The wave peak is passing.



The wave has passed and steady state stratified flow is reestablished.

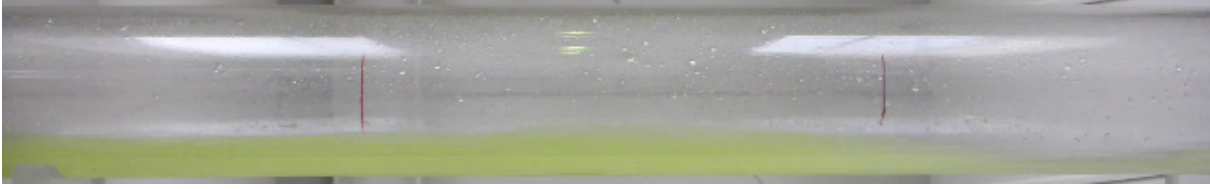
Case 5: $U_{sg} = 13,4 \text{ m/s}$, $U_{sl} = 0,0264 \text{ m/s}$

Camera 1:

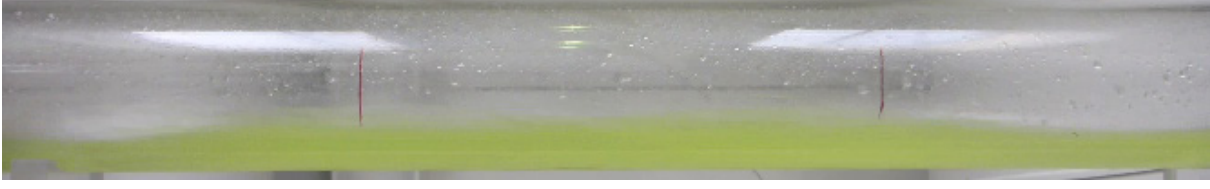
The wave moves from the left to the right in the images.



The wave front is coming.



The wave front is passing.



The wave peak is passing.



The wave has passed and steady state stratified flow is reestablished.

Camera 2:

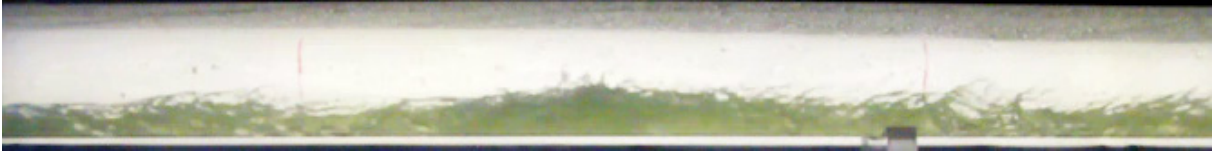
The wave moves from right to left in the images.



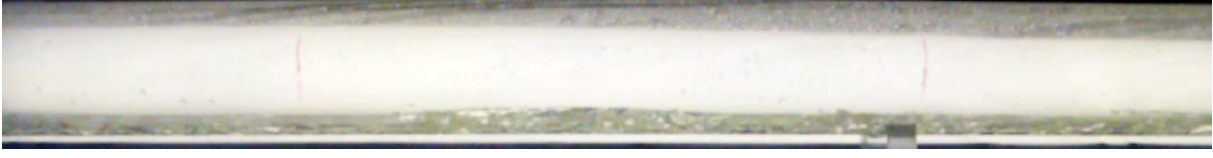
The wave front is coming.



The wave front is passing.



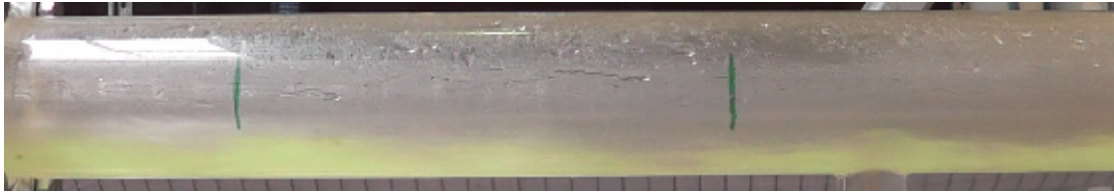
The wave peak is passing.



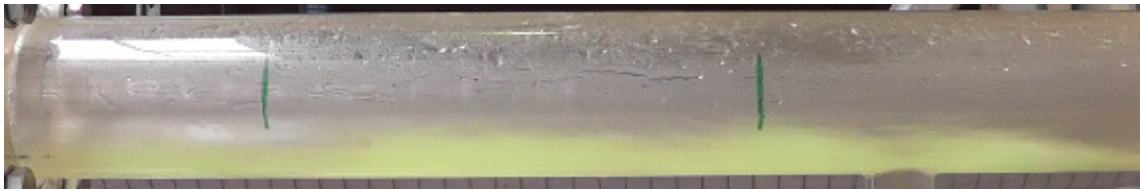
The wave has passed and steady state stratified flow is reestablished.

Camera 3:

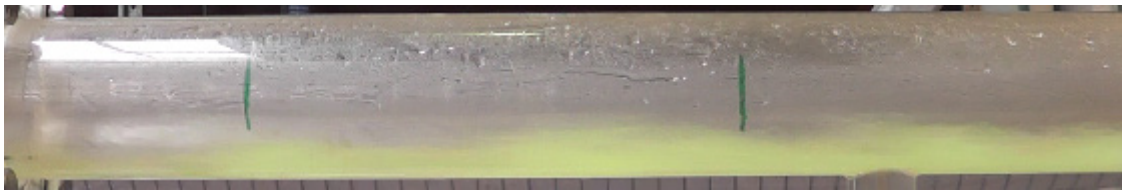
The wave moves from the left to the right in the images.



The wave front is coming.



The wave front is passing.



The wave peak is passing.

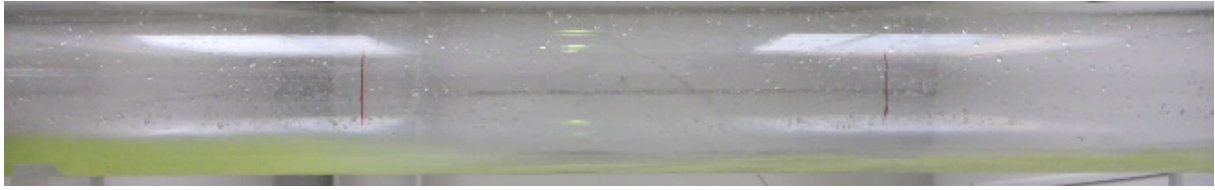


The wave has passed and steady state stratified flow is reestablished.

Case 6: $U_{sg} = 10,9 \text{ m/s}$, $U_{sl} = 0,0264 \text{ m/s}$

Camera 1:

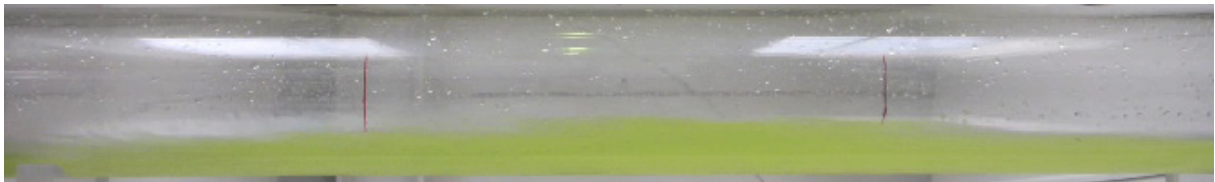
The wave moves from the left to the right in the images.



The wave front is coming.



The wave front is passing.



The wave peak is passing.



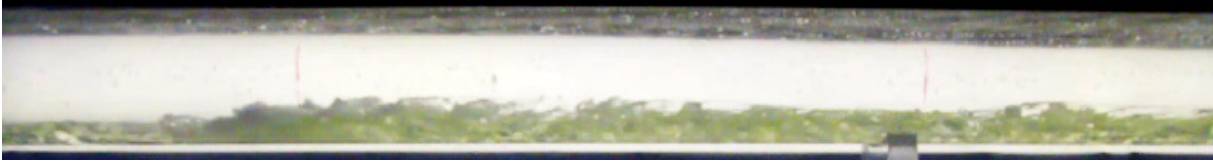
The wave has passed and steady state stratified flow is reestablished.

Camera 2:

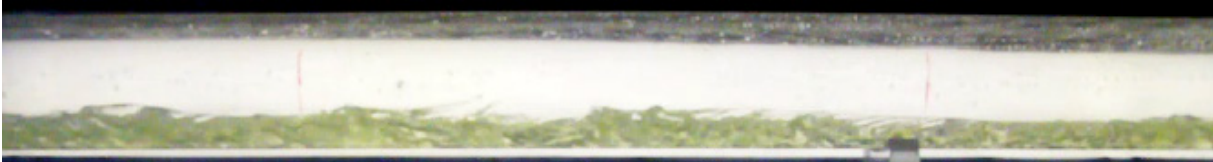
The wave moves from the right to the left in the images.



The wave front is coming.



The wave front is passing.



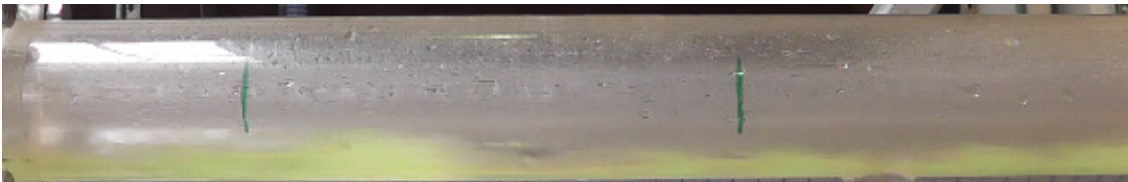
The wave peak is passing.



The wave has passed and steady state stratified flow is reestablished.

Camera 3:

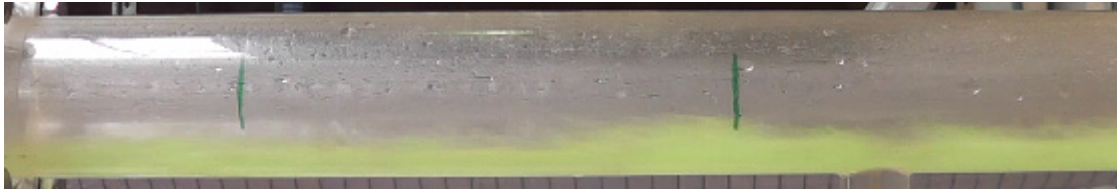
The wave moves from the left to the right in the images.



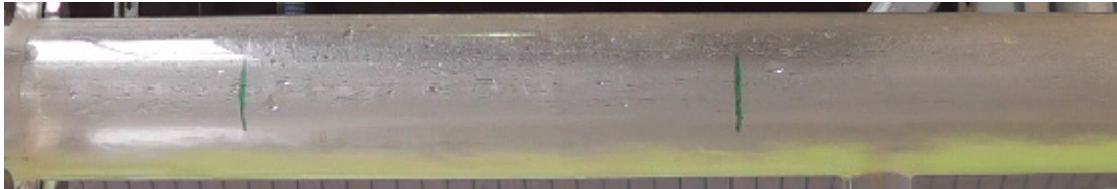
The wave front is coming.



The wave front is passing.



The wave peak is passing.



The wave has passed and steady state stratified flow is reestablished.

Case 7: $U_{sg} = 8,5 \text{ m/s}$, $U_{sl} = 0,0264 \text{ m/s}$

Camera 1:

The wave moves from the left to the right in the images.



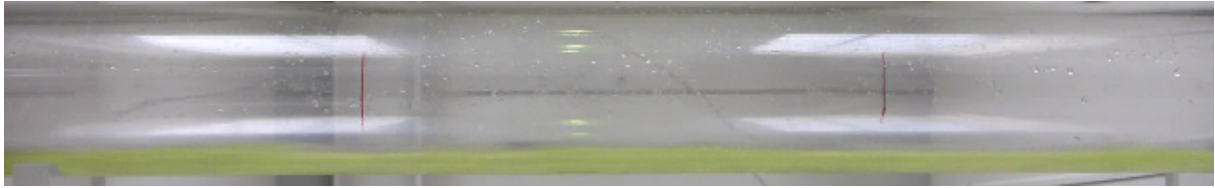
The wave front is coming.



The wave front is passing.



The wave peak is passing.



The wave has passed and steady state stratified flow is reestablished.

Camera 2:

The wave moves from the right to the left in the images.



The wave front is coming.



The wave front is passing.



The wave peak is passing.



The wave has passed and steady state stratified flow is reestablished.

Camera 3:

The wave moves from the left to the right in the images.



The wave front is coming.



The wave front and peak is passing.



The wave has passed and steady state stratified flow is reestablished.

Case 8: $U_{sg} = 7,4 \text{ m/s}$, $U_{sl} = 0,0264 \text{ m/s}$

Camera 1:

The wave moves from the left to the right in the images.



The wave front is coming.



The wave front and peak is passing.



The wave has passed and steady state stratified flow is reestablished.

Camera 2:

The wave moves from the right to the left in the images.



The wave front is coming.



The wave front is passing.



The wave peak is passing.



The wave has passed and steady state stratified flow is reestablished.

Camera 3:

The wave moves from the left to the right in the images.



The wave front is coming.



The wave front is passing.



The wave peak is passing.



The wave has passed and steady state stratified flow is reestablished.


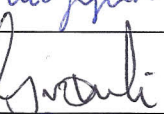
Risk Assessment Report

Multiphase Flow - Horizontal Loop

Prosjektnavn	Multiphase Flow - Horizontal Loop
Apparatur	Multiphase Flow - Horizontal Loop
Enhet	NTNU-EPT
Apparaturansvarlig	Ole Jørgen Nydal
Prosjektleder	Ole Jørgen Nydal
HMS-koordinator	Morten Grønli
HMS-ansvarlig (linjeleder)	Olav Bolland
Plassering	FlerfaseLaben
Romnummer	C164
Risikovurdering utført av	Erik Langørgen, Seid Ehsan Marashi, Mariana Jose De La Coromoto Diaz Arias, Morten Grønli

Approval:

Apparatur kort (UNIT CARD) valid for:	12 months
Forsøk pågår kort (EXPERIMENT IN PROGRESS) valid for:	12 months

Rolle	Navn	Dato	Signatur
Prosjektleder	Ole Jørgen Nydal	19/11/13	
HMS koordinator	Morten Grønli	14/11-2013	
HMS ansvarlig (linjeleder)	Olav Bolland	27/11 2013	